

# **Work in progress**

by

Alfred Alocias Mariadason

THESIS

for the degree of

MASTER OF SCIENCE



Faculty of Mathematics and Natural Sciences  
University of Oslo

May 2018

TODO: write creative commons licence

# **Abstract**

Work in progress

# Acknowledgements

Work in progress

# CONTENTS

|   |           |
|---|-----------|
| <b>Contents</b>   | <b>5</b>  |
| <b>1 Introduction</b>   | <b>11</b> |
| 1.1 Structure and Goals . . . . .   | 12        |
| <b>2 Many-Body Quantum Theory</b>   | <b>15</b> |
| 2.1 The Hamiltonian and the Born-Oppenheimer Approximation . . . . .      | 16        |
| 2.2 Slater Determinant and Permanent . . . . .                            | 17        |
| 2.3 Variational Principle . . . . .                                       | 18        |
| 2.4 Energy Functional . . . . .   | 18        |
| 2.5 Hartree-Fock Theory . . . . .   | 19        |
| 2.5.5 Assumptions . . . . .   | 19        |
| 2.5.5 The $\mathcal{J}$ and $\mathcal{K}$ Operators . . . . .             | 20        |
| 2.5.5 Hartree-Fock Equations . . . . .                                    | 20        |
| 2.6 Restricted Hartree-Fock and Roothan-Hall-Equations . . . . .          | 22        |
| 2.7 Unrestricted Hartree-Fock and Poople-Nesbet-Equations . . . . .       | 23        |
| 2.8 Convergence and Mixing . . . . .                                      | 23        |
| 2.9 Quantum Monte Carlo . . . . .   | 25        |
| 2.9.9 The Variational Principle and Expectation Value of Energy . . . . . | 25        |
| 2.9.9 Metropolis-Hastings Algorithm . . . . .                             | 26        |
| 2.9.9 Diffusion Theory and the PDF . . . . .                              | 27        |
| 2.9.9 Importance Sampling . . . . .                                       | 28        |
| 2.9.9 The Trial Wavefunction: One-Body . . . . .                          | 29        |
| 2.9.9 The Trial Wavefunction: Splitting the Slater Determinant . . . . .  | 30        |
| 2.9.9 The Trial Wavefunction: Jastrow Factor . . . . .                    | 31        |
| 2.9.9 Connect the Jastrows . . . . .                                      | 33        |
| 2.10 Density Matrices . . . . .   | 34        |
| <b>3 Basis Functions</b>  | <b>37</b> |

|          |   |           |
|----------|---|-----------|
| 3.1      | Hermite Functions . . . . .                       | 38        |
| 3.2      | Gaussian Type Orbitals . . . . .                  | 38        |
| 3.2.2    | Hermite-Gaussian Functions . . . . .              | 39        |
| 3.3      | Integral Elements . . . . .                       | 40        |
| 3.3.3    | Overlap Distribution . . . . .                    | 41        |
| 3.3.3    | Overlap Integral . . . . .                        | 43        |
| 3.3.3    | Potential Integral . . . . .                      | 44        |
| 3.3.3    | Laplacian Integral . . . . .                      | 44        |
| 3.3.3    | Coulomb Potential Integral . . . . .              | 45        |
| 3.3.3    | Coulomb Interaction Integral . . . . .            | 47        |
| 3.3.3    | Recurrence Relation . . . . .                     | 49        |
| 3.3.3    | Coulomb Distribution Integral . . . . .           | 50        |
| 3.4      | Double-Well Functions . . . . .                   | 51        |
| 3.4.4    | The Eigenvalue problem . . . . .                  | 51        |
| 3.4.4    | Choosing the Basis Functions . . . . .            | 52        |
| 3.4.4    | Degeneracy . . . . .                              | 52        |
| 3.5      | Summary . . . . .                                 | 53        |
| 3.6      | Further Work . . . . .                            | 55        |
| <b>4</b> | <b>Numerical Optimization</b>                     | <b>57</b> |
| 4.1      | The Optimization Problem . . . . .                | 57        |
| 4.2      | Gradient Descent . . . . .                        | 58        |
| 4.3      | Adaptive Stochastic Gradient Descent . . . . .    | 62        |
| 4.4      | Newtons-Method and Quasi-Newton Methods . . . . . | 62        |
| 4.5      | BFGS Method . . . . .                             | 65        |
| 4.6      | Line search methods . . . . .                     | 66        |
| 4.7      | Stochastic-Adaptive-BFGS . . . . .                | 67        |
| 4.8      | Simulated Annealing . . . . .                     | 68        |
| <b>5</b> | <b>Implementation</b>                             | <b>73</b> |
| 5.1      | Cartesian Basis . . . . .                         | 76        |
| 5.2      | Hartree-Fock . . . . .                            | 76        |
| 5.2.2    | Parallelization of Two-Body Matrix . . . . .      | 77        |
| 5.2.2    | Tabulation of Two-Body Matrix . . . . .           | 79        |
| 5.3      | Variational Monte Carlo . . . . .                 | 80        |
| 5.3.3    | Slater Optimizations . . . . .                    | 81        |
| 5.3.3    | Jastrow Optimizations . . . . .                   | 82        |

|          |  |           |
|----------|--|-----------|
| 5.3.3    | Optimization For Tabulation . . . . .          | 83        |
| 5.3.3    | Tabulating Hermite Polynomials . . . . .       | 84        |
| 5.4      | Minimization . . . . .                         | 84        |
| 5.5      | Auto-Generation . . . . .                      | 85        |
| 5.5.5    | Hermes . . . . .                               | 85        |
| 5.5.5    | Double-Well Basis . . . . .                    | 86        |
| 5.6      | Verification . . . . .                         | 86        |
| 5.6.6    | Hartree-Fock . . . . .                         | 86        |
| 5.6.6    | Variational Monte-Carlo . . . . .              | 86        |
| <b>6</b> | <b>Results</b>                                 | <b>89</b> |
| 6.1      | Tweaks and Experimentation . . . . .           | 89        |
| 6.1.1    | Simulated Annealing . . . . .                  | 89        |
| 6.2      | Hartree-Fock . . . . .                         | 90        |
| 6.3      | VMC . . . . .                                  | 91        |
| <b>A</b> |  | <b>93</b> |
| A.1      | Lagrange Multiplier Method . . . . .           | 93        |
| A.2      | Interaction-Term in Fock-Operator . . . . .    | 93        |
| A.3      | Multi-Index Notation . . . . .                 | 94        |
| <b>B</b> |  | <b>97</b> |
| B.1      | Derivatives of Hermite Functions . . . . .     | 97        |
| B.2      | Derivatives of Padé-Jastrow Function . . . . . | 98        |
| B.3      | Derivatives of NQS-Wavefunction . . . . .      | 98        |

# Symbols List

Work in progress

| Symbol           | Meaning   |
|------------------|---|
| $\psi$           | Spin-orbital  |
| $\phi$           | Spacial part of spin-orbital  |
| $\chi$           | Basis functions used in basis-expansion                             |
| $\Psi$           | Trial wavefunction  |
| $\Phi$           | Slater determinant  |
| $g$              | Hermite-Gaussian  |
| $G$              | Gaussian-Type-Orbital (GTO)   |
| $\Omega$         | Overlap Distribution  |
| $\xi$            | Recurrence relation for Coulomb integral                            |
| $\boldsymbol{x}$ | Bold lower case symbol is a <i>vector</i> .                         |
| $\boldsymbol{X}$ | Bold upper case symbol is a <i>matrix</i> .                         |
| $\nabla_x$       | Gradient with derivatives of components in $\boldsymbol{x}$         |
| $\nabla_x$       | Laplacian with second derivatives of components in $\boldsymbol{x}$ |
| $\mathcal{H}$    | Caligraphed symbol is an operator.                                  |
| $\{X\}_{k=0}^N$  | A set with elements $X_0, \dots, X_N$                               |

Table 0.1: List of symbols used with explanation.



# Source Code

Work in progress



## INTRODUCTION

At present time we live in an era of flourishing technological advances and groundbreaking scientific discoveries. A time in which discoveries are made across fields with large cooperative work. With the scale of the problems, so to does the demand for computations in science grow.

The modern computer was introduced to the world somewhere in the middle of the last century and has become a staple tool in scientific work ever since. Within all big breakthroughs in science in the modern days, some kind of computer simulations were made, a numerical experiment was made prior to the actual physical experiments. The reason for this? As problems get larger in scale, the possible closed-form solution with the good-old pen-and-paper approach dwindles. The only possibility is then to resort to numerical solutions and the modern computer, although a beast to be tamed, is the best candidate tool.

Some of the earliest simulations made were indeed in the field of quantum many-body physics, the (in)famous Manhattan Project and ever since then the field of many-body quantum theory and quantum chemistry has grown rapidly and given promising results in relation to reality. It has been used to simulate atoms, bond-energies of atomic systems, studies of condensed matter physics and many more.

In this thesis we go into detail on the popular Hartree-Fock method and the Variational Monte-Carlo method with the quantum-dot single- and double-well potentials as primary systems of study with this chapter being a brief introduction to the structure and goals of the thesis.

## 1.1 Structure and Goals

The main goal(at least at some point into the semester) was to make a code-base for large-scale quantum many-body calculations from scratch. Of course there exists many such code-bases and competing with those in terms of scalability and computational efficiency is beyond the scope of this thesis, the choice for a from-scratch approach was made in order to gain some insight into the methods and a better understanding for the programming aspects which would follow. With this in mind, we did however get much inspiration from previous theses and implementations from other sources as well.

The main goals for the thesis was

- Make a general C++ code for the *Hartree-Fock method* and the *Variational Monte Carlo method* which could take any basis into play with minimal effort.
- Use the C++ code on different *quantum mechanical many-body systems* and use this as validation of the code and benchmark the code.
- Build an optimal one-body basis with the Hartree-Fock method and make improvements on this basis with the variational Monte-Carlo method with a *Slater-Jastrow* wavefunction.

With this in mind a general open-source code for the restricted Hartree-Fock method was developed and is open for use in <https://github.com/Oo1Insane1oO/HartreeFock>. The variational Monte-Carlo method is also open-source and for use in <https://github.com/Oo1Insane1oO/VMC>. Both repositories each have a directory with tests implemented, see section 5.6 for more information on these tests.

Extending the code to other systems is made easier with python scripts given in the mentioned repositories. A better description of these are given in the repositories themselves and involve auto-generation of abstract wavefunction classes which only need to be filled in with analytical expressions and are otherwise already integrated with the existing code.

The thesis itself is built in three parts

- Quantum Theory: Theory for the implementation.
- Choice of Basis: The form of the wavefunction.
- Implementation: The code with optimizations.
- Results: The resulting data from the simulations.

We basically start off with the background in quantum many-body theory, make a specialization into a set of basis functions, implement these in a general C++ -code with auto-generation of

expressions and template classes in Python and present the results from the simulations run with the implementation.



## MANY-BODY QUANTUM THEORY

Ever since the dawn of Quantum-Mechanics, with Boltzmanns model for the  $I_2$  molecule in 1877 to the photoelectric by Einstein in 1905, Bohrs model for the hydrogen atom in 1913 and - of course - the discovery of the Schrödinger equation, physicists have been curious as to if the theory could be applied to larger systems. The first milestone however can be traced back to the 1927 paper by Walter Heitler and Fritz London which studied the stability of the hydrogen molecule and of course the well-known Pauli-principle. Still it wasn't before later when increased computational power came into play that many-body quantum mechanics and many-body quantum chemistry skyrocketed and started to become as natural a part of the science laboratory as physical experiments since the former is far less expensive<sup>1</sup>. The challenge thus became to tackle the ever-increasing computational cost of actually solving Schrödingers equation for a many-body system.

Many methods have been devised and the basis in quantum chemistry is the *Hartree-Fock method* while it being a good first approximation, it is known to be poor at modeling correlations and is only useful for building a basis set to be used in other methods like *coupled-cluster* or *configuration interaction*. The quantum mechanical properties as a whole is also approximated with the *Born-Oppenheimer approximation* and individual electrons are not assigned to a single atomic core, but rather spread out across the molecule.

We will in this chapter take forth the theory regarding the basics of identical particles and *many-body quantum mechanics*. The reader is referred to [16] for an introductory text on quantum mechanics(for single particles) and also the so-called *Dirac-notation* used throughout the entire chapter. We will address methods regarding computational quantum mechanics and further deepen into Hartree-Fock methods and Variational Monte Carlo method.

---

<sup>1</sup>Economically

## 2.1 The Hamiltonian and the Born-Oppenheimer Approximation

The task at hand is to solve the many-body system described by *Schrödinger's* equation

$$\mathcal{H} |\Psi_i\rangle = E_i |\Psi_i\rangle \quad (2.1)$$

for some state  $|\Psi_i\rangle$  with energy  $E_i$ . Usually the desired state is the ground-state energy  $E_0$  of the system meaning we are primarily interested in the *ground-state*  $|\Psi_0\rangle$ .

With the goal determined we can define the system to consist of  $N$  identical particles<sup>2</sup> with positions  $\{\mathbf{r}_i\}_{i=0}^{N-1}$  and  $A$  nuclei with positions  $\{\mathbf{R}_k\}_{k=0}^{A-1}$ . The Hamiltonian  $H$  is then

$$\mathcal{H} = -\frac{1}{2} \sum_i \nabla_i^2 + \sum_{i<j} f(\mathbf{r}_i, \mathbf{r}_j) - \frac{1}{2} \sum_k \frac{\nabla_k^2}{M_k} + \sum_{k<l} g(\mathbf{R}_k, \mathbf{R}_l) + V(\mathbf{R}, \mathbf{r}) \quad (2.2)$$

The first and second terms represent the kinetic- and inter-particle interaction terms<sup>3</sup> for the  $N$  identical particles while the latter three represent kinetic- and interaction terms for the nuclei (with the last one being the nuclei-particle interaction). The constant  $M_k$  is the mass of nucleon  $k$  and  $Z_k$  is the corresponding atomic number.

We assume the nuclei to be much heavier than the identical particles, meaning they move much slower, at which the system can be viewed as electrons moving around the vicinity of stationary nuclei. This means the kinetic term for the nuclei vanish and the nuclei-nuclei interaction becomes a constant<sup>4</sup>. The approximation we end up with is the so-called *Born-Oppenheimer approximation* and the Hamiltonian is now

$$\mathcal{H} = \mathcal{H}_0 + \mathcal{H}_I \quad (2.3)$$

where we have split the Hamiltonian in a *one-body* part and a *two-body* or *interaction* parts defined as

$$\mathcal{H}_0 \equiv -\frac{1}{2} \sum_i \nabla_i^2 + V(\mathbf{R}, \mathbf{r}) \quad (2.4)$$

and

$$\mathcal{H}_I \equiv \sum_{i<j} f(\mathbf{r}_i, \mathbf{r}_j) \quad (2.5)$$

---

<sup>2</sup>These are in both atomic physics and in the quantum dot case always fermions or bosons.

<sup>3</sup>This is usually the well-known Coulomb interaction.

<sup>4</sup>Adding a constant to an operator does not alter the eigenvector, only the eigenvalues by the constant factor[28].



## 2.2 Slater Determinant and Permanent

Throughout section 2.1 we only referred to the wavefunction  $\Psi$  as a state, a function closely connected to the probabilistic nature of the quantum particles. However, we have not given it a form. One possible solution is the *Hartree product*  $\Psi_H$  defined as

$$\Psi_H = \prod_i \psi_i(\mathbf{r}_i) \quad (2.6)$$

with  $\{\psi\}_{i=0}^N$  being the orbitals which solve the single-particle Schrödinger equation for  $H_0$ . The Hartree-product is unfortunately a poor choice since it does not solve the  $H_I$  part meaning it is not a physically valid solution. This comes from the fact that the Hartree-product does not take into account the fact that the particles in question are *identical particles*. Since the particles are identical, switching the labels on the particles shouldn't change the expectation value of some observable. If we run this remark through we end up with the conclusion that the state  $|\Psi\rangle$  must be either symmetric or antisymmetric with the symmetric part being the *bosonic state* and antisymmetric being the *fermionic state*. The connection between antisymmetric states and fermions is called the *Pauli exclusion principle*.

The problem with the Hartree-product is, with the above sentiment, that it is not symmetric nor antisymmetric. However we can transform it with an operator

$$\mathcal{B} \equiv \frac{1}{N!} \sum_p \sigma_b \mathcal{P} \quad (2.7)$$

where  $\sigma_b$  is defined as

$$\sigma_b \equiv \begin{cases} 1 & b \text{ represents bosonic system} \\ (-1)^p & b \text{ represents fermionic system} \end{cases} \quad (2.8)$$

$\mathcal{P}$  is a permutation operator that switches the labels on particles<sup>5</sup> and  $p$  is the parity of permutations. The operator  $\mathcal{B}$  has the following properties

- Applying  $\mathcal{B}$  to itself doesn't change the operator meaning  $\mathcal{B}^2 = \mathcal{B}$ .
- The Hamiltonian  $\mathcal{H}$  and  $\mathcal{B}$  commute, that is  $[\mathcal{B}, \mathcal{H}] = [\mathcal{H}, \mathcal{B}]$ .
- $\mathcal{B}$  is *unitary*, which means  $\mathcal{B}^\dagger \mathcal{B} = \mathcal{I}$ .

The solution  $\Psi_T$  to the Schrödinger equation can now be written as

$$\Psi_T(\mathbf{r}) = \sqrt{N!} \mathcal{B} \Psi_H(\mathbf{r}) \quad (2.9)$$

---

<sup>5</sup> $P_{ij}\Psi(\mathbf{r}_1, \dots, \mathbf{r}_i, \dots, \mathbf{r}_j, \dots, \mathbf{r}_N) = \Psi(\mathbf{r}_1, \dots, \mathbf{r}_j, \dots, \mathbf{r}_i, \dots, \mathbf{r}_N)$  [47].

The antisymmetric case of  $\mathcal{B}$  results in a *Slater determinant*

$$\Psi_T^{\text{AS}} = \frac{1}{\sqrt{N!}} \sum_P (-1)^P \mathcal{P}_P \prod_i \psi_i \quad (2.10)$$

while the symmetric case gives the so-called *permanent*<sup>6</sup>.

$$\Psi_T^{\text{S}} = \sqrt{\frac{\prod_{i=1}^N n_i!}{N!}} \sum_P \mathcal{P}_P \prod_i \psi_i \quad (2.11)$$

Notice that the coordinated  $\mathbf{r}_{i=0}^N$  is a bit of a sloppy notation as it also implicitly includes the spin orbitals. The extra factor in the symmetric case is to preserve the normalization due to number of particles, the  $n_i$  factor is determined by the the quantum-number for state  $i$ .

## 2.3 Variational Principle

One important remark is that the Slater determinant and the permanent do not solve the interaction part, but only serves as a so-called *ansatz* or guess on the true ground-state wavefunction. This is quite useful due to the *variational principle*.

The Variational principle states that for any normalized function  $\Psi$  in Hilbert Space[16] with a Hermitian operator  $\mathcal{H}$  the minimum eigenvalue  $E_0$  for  $\mathbf{H}$  has an upper-bound given by the expectation value of  $\mathcal{H}$  in the function  $\Psi$ . That is

$$E_0 \leq \langle \mathcal{H} \rangle = \frac{\langle \Psi | \mathcal{H} | \Psi \rangle}{\langle \Psi | \Psi \rangle} \quad (2.12)$$

See [16] for proof and more.

The mentioned ansatz is thereby guaranteed to give energies larger than or equal the true ground state energy meaning a minimization method is sufficient in order to get closer to this minimum.

## 2.4 Energy Functional

We can find a more convenient expression for this energy by using equation 2.9 and equation 2.12. This gives us

$$E[\Psi] = N! \langle \Psi_{\text{H}} | \mathcal{H} \mathcal{B} | \Psi_{\text{H}} \rangle \quad (2.13)$$

where the hermitian and unitary property of  $\mathcal{B}$  as well as the fact that  $\mathcal{B}$  and  $H$  commute have been used. This energy functional(functional in the sense that it is dependant on the wave

---

<sup>6</sup>The permanent is basically just a determinant with all the negative signs replaced by positive ones.

function). Applying the  $\mathcal{B}$  operator to the Hartree-product, pulling the sum out of the integrals and relabeling with the following definitions

$$\begin{aligned}\langle p|h|q\rangle &\equiv \langle \psi_p(\mathbf{r})|h(\mathbf{r})|\psi_q(\mathbf{r})\rangle = \int \psi_p^*(x)h(\mathbf{r})\psi_q(\mathbf{r})d\mathbf{r} \\ \langle pq|f|rs\rangle &\equiv \langle \psi_p(\mathbf{r}_1)\psi_q(\mathbf{r}_2)|f(\mathbf{r}_1,\mathbf{r}_2)|\psi_r(\mathbf{r}_1)\psi_s(\mathbf{r}_2)\rangle \\ &= \int \psi_p(\mathbf{r}_1)\psi_q(\mathbf{r}_2)f(\mathbf{r}_1,\mathbf{r}_2)\psi_r(\mathbf{r}_1)\psi_s(\mathbf{r}_2)d\mathbf{r}\end{aligned}$$

yields in<sup>7</sup>

$$E[\Psi] = \langle p|H_0|p\rangle + \frac{1}{2} \sum_{p,q} [\langle pq|f_{12}|pq\rangle \pm \langle pq|f_{12}|qp\rangle] \quad (2.14)$$

The first part is written with the assumption that the single-particle wave functions  $\{\psi\}$  are orthogonal and the 1/2 factor in front of the so-called *direct* and *exchange* terms<sup>8</sup> is due to the fact that we count the permutations twice in the sum when applying the  $\mathcal{B}$  operator. The sign in the interaction term are chosen as positive for bosonic systems and negative for fermionic systems.

The expression given in equation 2.14 is the functional form we will use to derive the Hartree-fock equations in the following section.

## 2.5 Hartree-Fock Theory

Hartree-Fock method is a many-body method for approximating the wavefunction of a stationary many-body quantum state and thereby also obtain an estimate for the energy in this state.

The main idea is to represent the system as a *closed-shell* system and then variationally optimize the Slater determinant [46] and then iteratively solve the arising non-linear eigenvalue problem. This approach is not generally feasible as the size of the system increases, however for a closed-shell system in the quantum dot case it should be enough to build a basis, which is the goal here. For more details around the motivation and usages of the Hartree-Fock method see[46].

In this section we will derive the Hartree-Fock equations, following closely the literature by J.M Thijssen[47].

### 2.5.5 Assumptions

Hartree-Fock method makes the following assumptions of the system

<sup>7</sup>Notice also that  $f_{12}$  is to imply integrals over two labels  $r_1$  and  $r_2$ .

<sup>8</sup>The direct term is just due to inherent behaviour of the charge of the particles (known as the Coulomb repulsion). The exchange term is a direct consequence of the probabilistic nature of the identical particles.

- The *Born-Oppenheimer approximation* holds.
- All relativistic effects are negligible.
- The wavefunction can be described by a single *Slater determinant*.
- The *Mean Field Approximation* holds.

With these inherent approximations the last one is the most important to take into account as it can cause large deviations from test solutions (analytic solutions, experimental data etc.) since the electron correlations is in reality, for many cases, not negligible. There exists many methods that try to fix this problem, but the *Variational Monte Carlo* (or VMC) is the method for deeper explorations in this Thesis, see section 2.9 for more details.

### 2.5.5 The $\mathcal{J}$ and $\mathcal{K}$ Operators

Before we begin with the Hartree-Fock equations it is desirable to rewrite the energy function obtained in section 2.4 (form given in equation 2.14) with two operators  $\mathcal{J}$  and  $\mathcal{K}$  defined as

$$\begin{aligned}\mathcal{J} &\equiv \sum_k \langle \psi_k^* | f_{12} | \psi_k \rangle = \int \psi_k^*(\mathbf{r}) f_{12} \psi_k(\mathbf{r}) d\mathbf{r} \\ \mathcal{K} &\equiv \sum_k \langle \psi_k^* | f_{12} | \psi \rangle = \int \psi_k^*(\mathbf{r}) f_{12} \psi(\mathbf{r}) d\mathbf{r}\end{aligned}\tag{2.15}$$

The  $\mathcal{J}$  operator just gives the simple interaction-term while the  $\mathcal{K}$  operator gives the exchange term with the arbitrary (notice no index)  $\psi(\mathbf{r})$ . The energy functional is thus rewritten to

$$E[\Psi] = \sum_i \left\langle \psi_i \left| h + \frac{1}{2}(\mathcal{J} \pm \mathcal{K}) \right| \psi_i \right\rangle\tag{2.16}$$

where the one-body Hamiltonian is split into a sum of single particle functions as  $H_0 = \sum_i h(\mathbf{r}_i)$ .

### 2.5.5 Hartree-Fock Equations

As a reminder. The wavefunctions  $\{\psi\}$  in equation 2.16 are spin-orbitals with both a spacial part and a spin part. In order to obtain the Hartree-Fock equations we try to minimize the energy functional in order to obtain the ground-state energy for a many-body system. This is done by a variational method.

The first observation to notice is the fact that variations in the spin-orbitals  $\{\psi\}$  need to respect the spin-orthogonality relation

$$\langle \psi_i | \psi_j \rangle = \delta_{ij}\tag{2.17}$$

with  $\delta_{ij}$  being the well-known Kronecker-delta. This property is essentially a constraint to the minimization problem and the method to be used is the *Lagrange multiplier method*[28], with the following *Lagrangian*

$$\mathcal{L} = \delta E[\Psi] - \sum_{ij} \Lambda_{ij} [\langle \psi_i | \psi_j \rangle - \delta_{ij}] \quad (2.18)$$

We know then that the minimum is reached when a displacement on the spin-orbitals  $\psi_i \rightarrow \psi_i + \delta \psi_i$  results in an energy variation of zero meaning  $\delta E[\Psi] = 0$  in the minimum. Which gives the variational problem

$$\sum_i \langle \delta \psi_i | h + \mathcal{J} \pm \mathcal{K} | \psi_i \rangle - \sum_{ij} \Lambda_{ij} \langle \delta \psi_i | \psi_j \rangle + \text{c.c} = 0 \quad (2.19)$$

where c.c is a notation for the complex conjugate of the inner-products on its left-hand side.

The shift in the spin orbitals  $\{\delta \psi\}$  is arbitrary and the constraints are symmetric<sup>9</sup> meaning we can with the *Fock-operator*

$$\mathcal{F} \equiv h + \mathcal{J} \pm \mathcal{K} \quad (2.20)$$

define the following eigenvalue problem

$$\mathcal{F} \psi_i = \sum_j \Lambda_{ij} \psi_j \quad (2.21)$$

Choosing the Lagrange parameter  $\Lambda_{ij}$  such that  $\{\psi\}_{k=1}^N$  forms an orthonormal set for  $\mathcal{F}$  with eigenvalues  $\{\epsilon\}_{k=1}^N$ . This reduces the eigenvalue equation to

$$\mathcal{F} |\psi\rangle = \epsilon |\psi\rangle \quad (2.22)$$

with  $\epsilon = (\epsilon_0, \dots, \epsilon_N)$  being the set of eigenvalues of  $\mathcal{F}$  meaning we have  $N + 1$  equations to be solved.

If we only take the  $N$  lowest eigenfunctions into the Slater the corresponding eigenenergy is referred to as the *Hartree-Fock energy* and is the estimated ground-state energy which the Hartree-Fock method gives. We can rewrite the energy functional with the eigenenergies to

$$E[\Psi] = \sum_i \left\langle \psi_i \left| \epsilon_i - \frac{1}{2}(\mathcal{J} \pm \mathcal{K}) \right| \psi_i \right\rangle \quad (2.23)$$

In the derivation of the Hartree-Fock equations we only worked with spin-orbital functions  $\{\psi\}$ . However it is much more convenient to rewrite these in terms of spatial orbitals  $\{\phi\}$  and integrate the spin-dependant part out. There are two ways of doing this and the two different approaches give the so-called *restricted Hartree-Fock* and *unrestricted Hartree-Fock* methods.

---

<sup>9</sup> $\langle \psi_i | \psi_j \rangle = \langle \psi_j | \psi_i \rangle^* \Rightarrow \Lambda_{ij} = \Lambda_{ji}^*$

## 2.6 Restricted Hartree-Fock and Roothan-Hall-Equations

The restricted spin-orbitals are paired as<sup>10</sup>

$$\{\psi_{2l-1}, \psi_{2l}\} = \{\phi_l(\mathbf{r})\alpha(s), \phi_l(\mathbf{r})\beta(s)\} \quad (2.24)$$

with  $\alpha(s)$  and  $\beta(s)$  being different spin-states (up and down). This pairing of spin-states with same and same spacial-orbitals means we can pull the spin degrees of freedom out from the  $\mathcal{J}$  and  $\mathcal{K}$  operators, reduce the sum to only run over half the states and multiply the entire sum by 2. The result is that the restricted energy-functional reads

$$E[\Psi] = \sum_{i=1}^N \varepsilon_i - \sum_{i=1}^{\frac{N}{2}} \langle i | 2\mathcal{J} \pm \mathcal{K} | i \rangle \quad (2.25)$$

Notice that the  $\mathcal{K}$  operators sum only runs up to half the number of states.

As the title suggests we are going to end up with a set of equations referred to as the *Roothan-Hall-equations*. We start by first expanding the spacial part  $\{\phi\}$  of the spin orbitals  $\{\psi\}$  in some known orthonormal basis  $\{\chi\}_{i=1}^L$

$$\phi_i(\mathbf{r}) = \sum_{p=1}^L C_{pi} \chi_p(\mathbf{r}) \quad (2.26)$$

and introduce the *Fock-matrix*  $F$  (associated with the Fock-operator) with elements

$$F_{pq} = h_{pq} + \sum_{pq} \rho_{pq} (2D_{prqs} \pm D_{prsq}) \quad (2.27)$$

We have here introduced a one-body matrix defined as

$$h_{pq} \equiv \langle p | h | q \rangle \quad (2.28)$$

a *density matrix* defined as<sup>11</sup>

$$\rho_{pq} \equiv \sum_{i=1}^{\frac{N}{2}} C_{pi} C_{qi}^* \quad (2.30)$$

and an interaction-matrix  $D$  with elements

$$D_{pqrs} \equiv \langle pq | f_{12} | rs \rangle \quad (2.31)$$

---

<sup>10</sup>This is specialised for a two-spin system. For a system with more spin-states one needs to either choose different spacial-orbitals or add more such orbitals which effectively changes the energy-levels.

<sup>11</sup>This is just the matrix formed by

$$\sum_i |\phi_i\rangle \langle \psi_i| \quad (2.29)$$

which is in quantum mechanics defined as the so-called *density matrix*.

for convenience. The implicit relabeling of  $\chi_p(\mathbf{r}) \rightarrow p$  is also present in the above expression for the Fock-matrix. The Hartree-Fock equations (equation 2.22) are then for the restricted case written as

$$\mathbf{F}\mathbf{C}_i = \epsilon \mathbf{S}\mathbf{C}_i \quad (2.32)$$

with  $\mathbf{S}$  being the overlap matrix with elements

$$S_{pq} \equiv \langle p | q \rangle \quad (2.33)$$

This concludes the essential parts of the derivations of the Hartree-Fock equations. We also present the unrestricted case in section 2.7 below.

## 2.7 Unrestricted Hartree-Fock and Poople-Nesbet-Equations

In the spirit of completion we also write out the equations for the unrestricted case. The equations are in this case called the *Poople-Nesbet equations*. The derivations are exactly the same as for the restricted case, but without the spin-pairing in equation 2.24. We get two equations, one for the spin-up states and one for the spin-down[47]. The equations are<sup>12</sup>

$$\begin{aligned} \mathbf{F}^+ \mathbf{C}^+ &= \epsilon \mathbf{S} \mathbf{C}^+ \\ \mathbf{F}^- \mathbf{C}^- &= \epsilon \mathbf{S} \mathbf{C}^- \end{aligned} \quad (2.34)$$

The elements of the Fock-matrices for spin-up and spin-down are

$$F_{pq}^{\pm} = h_{pq} + \sum_{k_{\pm}} \sum_{rs} C_{rk_{\pm}}^{\pm\dagger} C_{sk_{\pm}}^{\pm\dagger} [D_{prqs} - D_{prsq}] + \sum_{k_{\mp}} \sum_{rs} C_{rk_{\mp}}^{\mp\dagger} C_{sk_{\mp}}^{\mp\dagger} D_{prqs} \quad (2.35)$$

The Hartree-Fock algorithm thus involves two eigenvalue problems at each iteration. Notice also that the summation index  $k_{\pm}$  runs over the spin-up or spin-down states respectively and the  $r$  and  $s$  runs over all the spacial basis functions.

## 2.8 Convergence and Mixing

The Hartree-Fock equations themselves are what we call a system of non-linear equations meaning that they need to be solved iteratively<sup>13</sup>. A simple brute-force way of setting a convergence threshold is to say

$$|\epsilon_{\text{new}}^{\text{HF}} - \epsilon_{\text{old}}^{\text{HF}}| < \text{threshold} \quad (2.36)$$

<sup>12</sup>These are just two Roothan-Hall equations.

<sup>13</sup>and pray for convergence...

The factors determining the achievement that is correct convergence to a ground-state is the basis set of choice, but even with a good set the notorious divergence can occur. There are two methods in particular which are made to account for this. The first one is a simple *mixing*[47] of the current density matrix and the one obtained at previous iteration

$$\rho_{\text{new}} = \alpha \rho_{\text{new}} + (1 - \alpha) \rho_{\text{old}}, \quad 0 < \alpha \leq 1 \quad (2.37)$$

This method stems from the observation that for some systems the Hartree-Fock energies start to oscillate and the above mixing seems to be quite efficient at reducing the oscillations.

The more popular approach however is the DIIS procedure, also known as Pulay mixing[40, 41].

We use the simple mixing in this thesis.

Here is also a figure describing the algorithm.

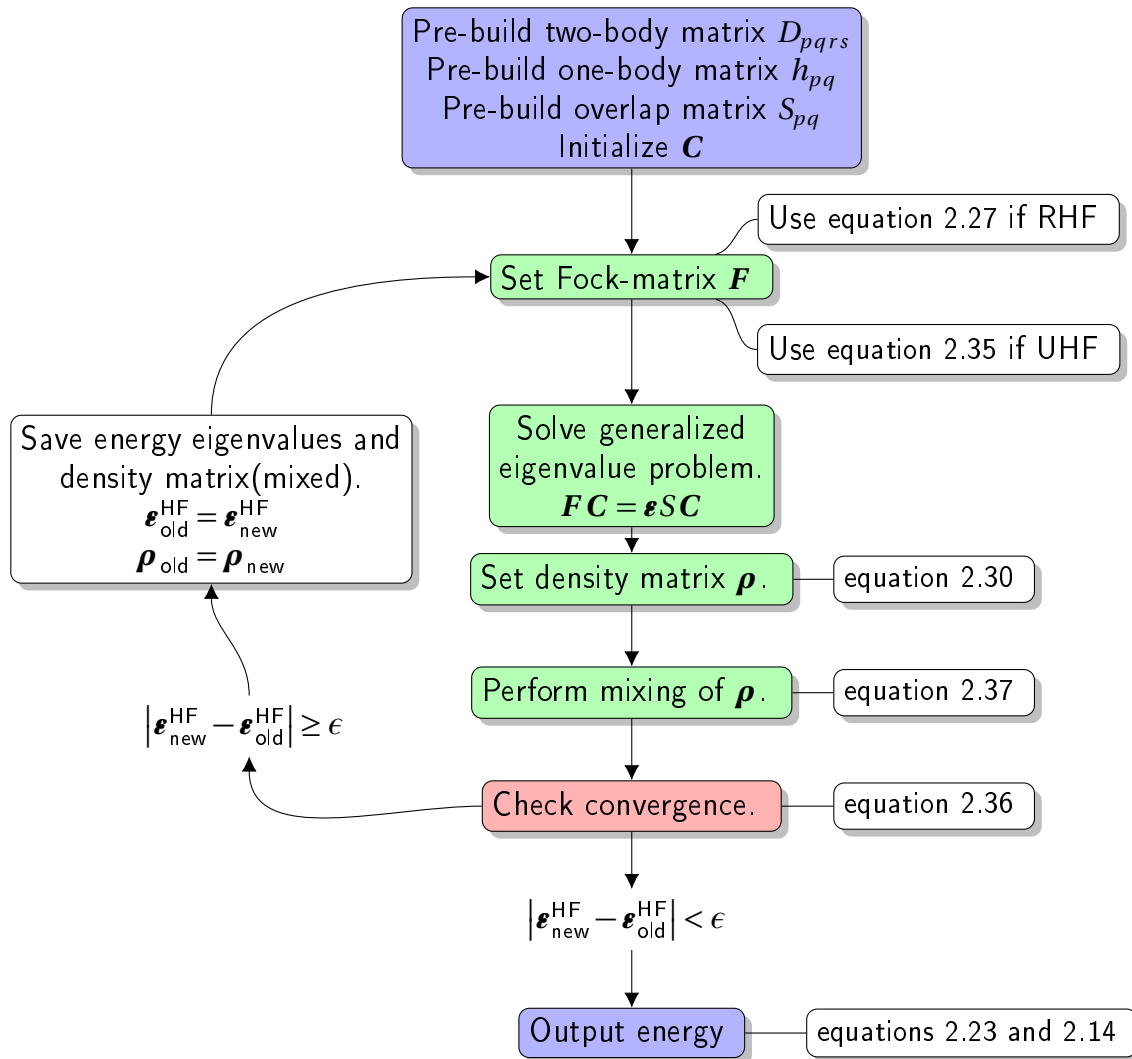


Figure 2.1: Hartree-Fock Algorithm.



## 2.9 Quantum Monte Carlo

Quantum Monte Carlo, or QMC is a method for solving Schrödinger's equation by a statistical approach using so-called *Markov Chain* simulations (also called random walk). The nature of the wave function at hand is fundamentally a statistical model defined on a large configuration space with small areas of densities. The Monte Carlo method is perfect for solving such a system because of the non-homogeneous distribution of calculation across the space. An standard approach with equal distribution of calculation would then be a waste of computation time.

We will in this chapter address the Metropolis algorithm which is used to create a Markov chain and derive the equations used in the variational method.

The chapter will use *Dirac Notation* [16] and all equations stated assume atomic units ( $\hbar = m_e = e = 4\pi\epsilon_0$ ) » REF HERE ATOMIC UNITS «.

### 2.9.9 The Variational Principle and Expectation Value of Energy

Given a Hamiltonian  $\hat{H}$  and a trial wave function  $\Psi_T(\mathbf{R}; \boldsymbol{\alpha})$ , the variational principle [16, 35] states that the expectation value of  $\hat{H}$

$$E[\psi_T] = \langle \hat{H} \rangle = \frac{\langle \psi_T | \hat{H} | \psi_T \rangle}{\langle \Psi_T | \Psi_T \rangle} \quad (2.38)$$

is an upper bound to the ground state energy

$$E_0 \leq \langle \hat{H} \rangle \quad (2.39)$$

Now we can define our PDF as (see section 2.9.9 for a more detailed reasoning)

$$P(\mathbf{R}) \equiv \frac{|\psi_T|^2}{\langle \Psi_T | \Psi_T \rangle} \quad (2.40)$$

and with a new quantity

$$E_L(\mathbf{R}; \boldsymbol{\alpha}) \equiv \frac{1}{\Psi_T(\mathbf{R}; \boldsymbol{\alpha})} \hat{H} \Psi_T(\mathbf{R}; \boldsymbol{\alpha}) \quad (2.41)$$

the so-called local energy, we can rewrite equation 2.38 as

$$E[\Psi_T(\mathbf{R}; \boldsymbol{\alpha})] = \langle E_L \rangle \quad (2.42)$$

The idea now is to find the lowest possible energy by varying a set of parameters  $\boldsymbol{\alpha}$ . This is done by numerical minimization (see chapter 5). We essentially minimize the expectation value of the energy were the expectation value itself is found with the Metropolis algorithm, see section 2.9.9.

An important property of the local energy is when we differentiate it with respect to one of the variational parameters  $\{\alpha\}$  within the context of an expectation value. The result in this case would be zero. This is easily seen by direct calculation

$$\begin{aligned}
 \left\langle \frac{\partial E_L}{\partial \alpha} \right\rangle &= \int \frac{|\psi|^2 \frac{\partial}{\partial \alpha} \left[ \frac{1}{\psi} H \psi \right]}{\int |\psi|^2 d\mathbf{r}} d\mathbf{r} \\
 &= \int \frac{|\psi|^2 \frac{\psi^* \frac{\partial}{\partial \alpha} (H \psi) - (H \psi^*) \frac{\partial \psi}{\partial \alpha}}{|\psi|^2}}{\int |\psi|^2 d\mathbf{r}} d\mathbf{r} \\
 &= \int \frac{\psi^* H \frac{\partial \psi}{\partial \alpha} - \psi^* H \frac{\partial \psi}{\partial \alpha}}{\int |\psi|^2 d\mathbf{r}} d\mathbf{r} \\
 &= 0
 \end{aligned} \tag{2.43}$$

We have used the fact that  $H$  is not dependant on any variational parameter and used the hermitian properties[16] of  $H$  to justify the movement of  $H$  within the integral.

This neat result presented in equation 2.43 will show its usefulness in the minimization when derivatives of the expectation value come into play since finding the derivative of the local energy would be much more of a hassle.<sup>14</sup>

We also write the derivative with respect to a variational parameters  $\alpha$  of the expectation value  $\langle E \rangle$  here for reference

$$\frac{\partial \langle E \rangle}{\partial \alpha} = 2 \left( \left\langle \frac{E_L}{\psi} \frac{\partial \psi}{\partial \alpha} \right\rangle - \langle E \rangle \left\langle \frac{1}{\psi} \frac{\partial \psi}{\partial \alpha} \right\rangle \right) \tag{2.44}$$

We have also applied equation 2.43 here.

### 2.9.9 Metropolis-Hastings Algorithm

The Metropolis algorithm bases itself on moves (also called transitions) as given in a Markov process[12, 35]. This process is given by

$$w_i(t + \varepsilon) = \sum_j w_{i \rightarrow j} w_j(t) \tag{2.45}$$

where  $w(j \rightarrow i)$  is just a transition from state  $j$  to state  $i$ . In order for the transition chain to reach a desired convergence while reversibility is kept, the well known condition for detailed balance must be fulfilled[43]. If detailed balance is true, then the following relation is true

$$w_i T_{i \rightarrow j} A_{i \rightarrow j} = w_j T_{j \rightarrow i} A_{j \rightarrow i} \Rightarrow \frac{w_i}{w_j} = \frac{T_{j \rightarrow i} A_{j \rightarrow i}}{T_{i \rightarrow j} A_{i \rightarrow j}} \tag{2.46}$$

---

<sup>14</sup>The differentiation of the wavefunction is enough to reduce the quality of life on its own!

We have here introduced two scenarios, the transition from configuration  $i$  to configuration  $j$  and the reverse process  $j$  to  $i$ . Solving the acceptance  $A$  for the two cases where the ratio in 2.46 is either 1 (in which case the proposed state  $j$  is accepted and transitions is made) and when the ratio is less then 1. The Metropolis algorithm would in this case not automatically reject the latter case, but rather reject it with a proposed uniform probability. Introducing now a probability distribution function(PDF)  $P$  the acceptance  $A$  can be expressed as

$$A_{i \rightarrow j} = \min \left( \frac{P_{i \rightarrow j}}{P_{j \rightarrow i}} \frac{T_{i \rightarrow j}}{T_{j \rightarrow i}}, 1 \right) \quad (2.47)$$

The so-called selection probability  $T$  is defined specifically for each problem. For our case the PDF in question is the absolute square of the wave function and the selection  $T$  is a Green's function derived in section 2.9.9. The algorithm itself would then be

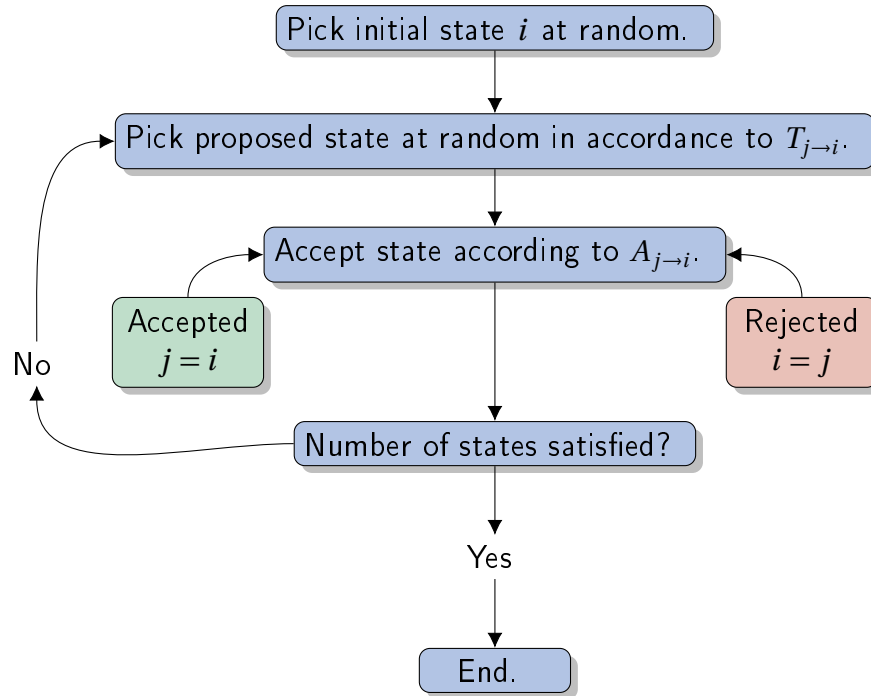


Figure 2.2: Metropolis algorithm.

### 2.9.9 Diffusion Theory and the PDF

The motivation for the use of diffusion theory is described very well in the Masters thesis of Jørgen Høgberget[24]. The essential results were a Green's function propagator arising from the *short time approximation* and the observation of interest here which has to do with the statistics describing the expectation value, it states that *any* distribution may be applied in calculation, however if we take a close look at the local energy (equation 2.41) we see that the local energy is not defined at the zeros of  $\Psi_T(\mathbf{R}; \boldsymbol{\alpha})$  for all distributions. This means that an arbitrary PDF does not guarantee

generation of points which makes  $\psi_T = 0$ . This can be overcome by introducing the square of the wave function to be defined as the distribution function as given in equation 2.40. This basically means that when using Quantum Monte-Carlo methods, the incorporation of the fact that when an energy is more undefined (meaning  $\psi_T \rightarrow 0$  the less probable that point is actually means the generation of states in which  $\psi_T$  is removed. The next chapter will derive the method that includes this observation into play, the so-called *importance sampling*.

### 2.9.9 Importance Sampling

Using the selection probability mentioned in section 2.9.9, the Metropolis-Hastings algorithm is called an *Importance sampling* because it essentially makes the sampling more concentrated around areas where the PDF has large values.

Because of the intrinsic statistical property of the wave function Quantum Mechanics can be modelled as a diffusion process, or more specifically, an *Isotropic Diffusion Process* which is essentially just a random walk model. Such a process is described by the Langevin equation with the corresponding Fokker-Planck equation describing the motion of the walkers (particles). See [23, 39, 47] for details. The full derivations presented here follows closely the descriptions in [23, 47]. Let us start off with the Langevin equation

$$\frac{\partial r}{\partial t} = D F(r(t)) + \eta \quad (2.48)$$

and apply Euler's method and obtain the new positions

$$r^{\text{new}} = r^{\text{old}} + D F^{\text{old}} \Delta t + \xi \quad (2.49)$$

with the  $r$ 's being the new and old positions in the Markov chain respectively and  $F^{\text{old}} = F(r^{\text{old}})$ . The quantity  $D$  is a diffusion therm equal to  $1/2$  due to the kinetic energy (remind of natural units) and  $\xi$  is a Gaussian distributed random number with 0 mean and  $\sqrt{\Delta t}$  variance.

As mentioned a particle is described by the Fokker-Planck equation

$$\frac{\partial P}{\partial t} = \sum_i D \frac{\partial}{\partial x_i} \left( \frac{\partial}{\partial x_i} - F_i \right) P \quad (2.50)$$

With  $P$  being the PDF (in current case the selection probability) and  $F$  being the drift therm. In order to achieve convergence, that is a stationary probability density, we need the left hand side to be zero in equation 2.50 giving the following equation

$$\frac{\partial^2 P}{\partial x_i^2} = P \frac{\partial F_i}{\partial x_i} + F_i \frac{\partial P}{\partial x_i} \quad (2.51)$$

with the drift-term being on the form  $\mathbf{F} = g(x)\partial P/\partial x$  we finally have that

$$\mathbf{F} = \frac{2}{\psi_T} \nabla \psi_T \quad (2.52)$$

This is the so-called *Quantum Force* which pushes the walkers towards regions where the wave function is large.

The missing part now is to model the selection probability in equation 2.47. Inserting the quantum force into the Focker-Planck equation (equation 2.50) the following diffusion equation appears

$$\frac{\partial P}{\partial t} = -D \nabla^2 P \quad (2.53)$$

Applying the *Fourier Transform* to spatial coordinate  $r$  in equation 2.53, the equation is transformed to

$$\frac{\partial P(\mathbf{s}, t)}{\partial t} = -D s^2 P(\mathbf{s}, t) \quad (2.54)$$

which has solution

$$P(\mathbf{s}, \Delta t) = P(\mathbf{s}, 0) e^{Ds^2 \Delta t} \quad (2.55)$$

Now we need to find the constant  $P(\mathbf{s}, 0)$ , and as is apparent with  $t = 0$ , we will make use of an initial condition. The initial positions are spread out from origin, that is  $D\Delta t \mathbf{F}_j$ . We can express this with a *Dirac-delta function* [3, 16] giving

$$P(\mathbf{s}, 0) = \delta(\mathbf{r}_i - D\Delta t \mathbf{F}_j) \quad (2.56)$$

Inserting this into equation 2.55 and making the inverse Fourier transform yields the following Green's function as solution

$$P(a, b, \Delta t) = \frac{1}{\sqrt{4\pi D \Delta t}} \exp\left(-\frac{(\mathbf{r}_a - \mathbf{r}_b - D\Delta t \mathbf{F}_b)^2}{4D \Delta t}\right) \quad (2.57)$$

This expression is precisely the selection probability  $T$ , Notice also that the indices  $a$  and  $b$  label a state transition  $a \rightarrow b$  and not particle indices. The full transition probability needs to be summed over for all particles since we only solved the Focker-Planck equation for 1 particle (since the other solutions are found in the exact same manner). For clarity the full selection probability ratio is

$$\frac{T(b, a, \Delta t)}{T(a, b, \Delta t)} = \sum_i \exp\left(-\frac{(\mathbf{r}_i^{(b)} - \mathbf{r}_i^{(a)} - D\Delta t \mathbf{F}_i^{(a)})^2}{4D \Delta t} + \frac{(\mathbf{r}_i^{(a)} - \mathbf{r}_i^{(b)} - D\Delta t \mathbf{F}_i^{(b)})^2}{4D \Delta t}\right) \quad (2.58)$$

### 2.9.9 The Trial Wavefunction: One-Body

The trial wave function is generally an arbitrary choice specific for the problem at hand, however it is in most cases favorable to expand the wave function in the eigenbasis (eigenstates) of the Hamiltonian since they form a complete set. This can be expressed as

$$\Psi_T(\mathbf{R}; \boldsymbol{\alpha}) = \sum_k C_k \psi_k(\mathbf{R}; \boldsymbol{\alpha}) \quad (2.59)$$

where the  $\psi_i$ 's are the eigenstates of the Hamiltonian. The coefficients can be found by any method preferable and the usual procedure is to use a set of basis functions and then minimize to find the coefficients  $\{C\}_{k=1}^L$ . We use the Hartree-Fock method to minimize in this thesis. The trial wavefunction is also generally expressed as a *Slater determinant* for the fermionic case and a general product for bosonic systems[10, 12, 16, 35] We will explain the fermionic case shortly since it is the main focus here and since the bosonic wavefunction is simple to express. The Slater is expressed as

$$\Phi_T(\mathbf{R}; \boldsymbol{\alpha}) = \det(\Phi(\mathbf{R}; \boldsymbol{\alpha}))\xi(s) \quad (2.60)$$

where the *Slater matrix*  $\Phi$  has elements

$$\Phi_{ij} = \phi_{n_j}(\mathbf{r}_i; \boldsymbol{\alpha}) \quad (2.61)$$

such that each row is evaluated for particle  $i$  and each column is for a quantum number  $n_j$  dependant on the basis used. The  $\xi(s)$  is the spin-dependant part. Notice also that we switched the labeling from  $\Psi_T$  to  $\Phi_T$ . This is to make a distinction between *one-body* and *correlation* terms. The latter will be introduced later in section 2.9.9. In this case the *single-particle* functions  $\phi_j(r)$  are expanded in some basis(i.e Hartree-Fock).

### 2.9.9 The Trial Wavefunction: Splitting the Slater Determinant

An important part of the trial-wavefunction presented here is that the one-body term is *independent* of spin, that is, the Hamiltonian is not explicitly dependant on the spin degrees of freedom. For the case of a Hamiltonian with an inherent spin part The following splitting of the Slater determinant is not valid! In that case the expectation value(presented in the variational principal in equation 2.12) would be a product of the expectation value over the spin-independent part of the Hamiltonian and the expectation value over the remaining spin-dependant parts[38]. The results presented here is however for systems of spin-independent systems, and in those cases the spin-part is essentially just another label which can be integrated out(similar to the procedure with the restricted Hartree-Fock method). For the splitting with a *spin-dependent* Hamiltonian see [34] and [22].

The procedure is simply to arrange the basis functions in such a way that we have  $N/2$  single-particle functions in spin-up and the same basis functions for spin-down. This means that the Slater is

$$\frac{1}{N!} \begin{pmatrix} \phi_1(\mathbf{r}_1)\xi_{\uparrow} & \dots & \phi_{N/2}(\mathbf{r}_1)\xi_{\uparrow} & \phi_1(\mathbf{r}_1)\xi_{\downarrow} & \dots & \phi_{N/2}(\mathbf{r}_1)\xi_{\downarrow} \\ \vdots & \vdots & \vdots & \vdots & \vdots & \vdots \\ \phi_1(\mathbf{r}_N)\xi_{\uparrow} & \dots & \phi_{N/2}(\mathbf{r}_N)\xi_{\uparrow} & \phi_1(\mathbf{r}_N)\xi_{\downarrow} & \dots & \phi_{N/2}(\mathbf{r}_N)\xi_{\downarrow} \end{pmatrix} \quad (2.62)$$

This restructuring of the single-particle states implies that

$$\det(\Phi) \propto \det(\Phi_{\uparrow}) \det(\Phi_{\downarrow}) \quad (2.63)$$

where we have defined

$$\begin{aligned} \Phi_{\uparrow} &= \begin{pmatrix} \phi_1(\mathbf{r}_1) & \dots & \phi_{N/2}(\mathbf{r}_1) \\ \vdots & \ddots & \vdots \\ \phi_1(\mathbf{r}_{N/2}) & \dots & \phi_{N/2}(\mathbf{r}_{N/2}) \end{pmatrix} \\ \Phi_{\downarrow} &= \begin{pmatrix} \phi_1(\mathbf{r}_{N/2+1}) & \dots & \phi_{N/2}(\mathbf{r}_{N/2+1}) \\ \vdots & \ddots & \vdots \\ \phi_1(\mathbf{r}_N) & \dots & \phi_{N/2}(\mathbf{r}_N) \end{pmatrix} \end{aligned} \quad (2.64)$$

Which in this sense means to put the first  $N/2$  particles in spin-up configuration and the remaining in spin-down and use the same single-particle functions. On a technical note, this rewriting is an approximation. However it can be shown (again see [34]) that the expectation value is still the same.

The one-body term is now rewritten to

$$\det(\Phi) = \det(\Phi_{\uparrow}) \det(\Phi_{\downarrow}) \quad (2.65)$$

### 2.9.9 The Trial Wavefunction: Jastrow Factor

As mentioned, we model the wavefunction as a product of the one-body Slater and a correlation part known as a *Jastrow factor*. The Jastrow can have many forms, but is build to exert some key features. It should [26].

- Be dependent on the inter-particle distances.
- Approach unity at large distances.
- Vanish when particles are close to one another.

In this thesis we explore two forms, the popular *Padé-function* and a more recent one build with a specific neural network known as a *Boltzmann Machine*.

#### Cusp Condition

The derivations for the cusp conditions is described well in the master thesis of Lars Eivind Lervåg [30]. We will here present the result of his for both two and three dimensions. Assuming the Jastrow factor  $J$  has the form

$$J = \prod_{i < j} e^{f(r_{ij})} \quad (2.66)$$

and considering the local energy as two particles  $i$  and  $j$  approach, the final results were the following conditions

$$\begin{aligned} \left. \frac{\partial f}{\partial r_{ij}} \right|_{r_{ij}=0} &= \frac{1}{D-1}, & \text{anti-parallel spin} \\ \left. \frac{\partial f}{\partial r_{ij}} \right|_{r_{ij}=0} &= \frac{1}{D+1}, & \text{parallel spin} \end{aligned} \quad (2.67)$$

which are known as the cusp conditions.

### Padé Function

A popular form is the *Padé-Jastrow* function. It is defined as[18, 22]

$$J_{\text{Padé}} = \exp \left( \sum_{i < j} \frac{\sum_l a_{ij}^{(l)} r_{ij}^l}{1 + \sum_l \beta_l r_{ij}^l} \right) \quad (2.68)$$

where the  $\beta_l$ 's are variational parameters. This function follows the key features mentioned for a correlation factor and the restrictions

$$a_{ij}^{2D} = \begin{cases} \frac{1}{3}, & \text{parallel spin} \\ 1, & \text{anti-parallel spin} \end{cases} \quad (2.69)$$

$$a_{ij}^{3D} = \begin{cases} \frac{1}{4}, & \text{parallel spin} \\ \frac{1}{2}, & \text{anti-parallel spin} \end{cases} \quad (2.70)$$

on the factor  $a$  along with the fact that  $a_{ij}^{(l)} = 0$  for  $l > 1$ , means we may relabel  $a_{ij}^{(l)} \rightarrow a_{ij}$  and  $\beta_l \rightarrow \beta$  and reduce the Padé-Jastrow factor to

$$J_{\text{Padé}} = \exp \left( \sum_{i < j} \frac{a_{ij} r_{ij}}{1 + \beta r_{ij}} \right) \quad (2.71)$$

For expressions concerning the gradient and Laplacian, see Appendix B.

### Simple Exponential

» REF THIS « With the desirable features for a correlation function in mind, one of the simplest forms for a correlation factor is a scaled exponential evaluated with the inter-particle distance, this is<sup>15</sup>

$$J = \exp \left( \sum_{i < j} a_{ij} r_{ij} \right) \quad (2.72)$$

---

<sup>15</sup>The  $a$ 's can also be variational parameters.



The  $a$  would be defined the same as with the Pad   function. In itself this function is fairly useless as it doesn't model correlations very well for different systems or even the same system with different parameters. However we will present a new type of function in the next section which does not give raise to any cusp conditions, but has a more flexible form and may in connection with this simple exponential give us all the necessary properties desired in a correlation function.

### The Trial Wavefunction: NQS Wavefunction

A more recent and completely different approach is to model the wavefunction with a *neural network* as presented by Carleo and Troyer[6]. The approach used here is based on the *Restricted Boltzmann Machine* as described by Hinton[21]. The form is

$$J_{\text{NQS}} = \exp\left(-\sum_{i=1}^N \frac{(\mathbf{r}_i - \mathbf{a}_i)^2}{2\sigma^2}\right) \prod_j^M \left(1 + \exp\left(b_j + \sum_{i=1}^N \sum_{d=1}^D \frac{x_i^{(d)} w_{i+d,j}}{\sigma^2}\right)\right) \quad (2.73)$$

The derivatives of this are given in Appendix B.

### 2.9.9 Connect the Jastrows

In the previous section we presented four functions that can be used to model correlations in quantum systems, however they all had some limitations as well as advantageous properties. The question then remains, can we create a function which exhibits all the nice properties mentioned and none of the limitations? The answer is a bit ambivalent. We don't really know for sure, but a good start is to multiply the functions having the cusp conditions in order (Pad   and exponential) with the NQS wavefunction and use this product as the new jastrow. The motivations for this is simple, we want the cusp conditions introduced by the old popular functions, but also want a more flexible type of function which can take care of other(possible) correlations in the system. How well this actually performed is presented in » REF RESULTS WHEN YOU HAVE SOME (GO GET THEM!) «. We will write out the exact form for clarity.

$$J = \exp\left(\sum_{i<j} a_{ij} r_{ij}\right) \exp\left(-\sum_{i=1}^N \frac{(\mathbf{r}_i - \mathbf{a}_i)^2}{2\sigma^2}\right) \prod_j^M \left(1 + \exp\left(b_j + \sum_{i=1}^N \sum_{d=1}^D \frac{x_i^{(d)} w_{i+d,j}}{\sigma^2}\right)\right) \quad (2.74)$$

$$J = \exp\left(\sum_{i<j} \frac{a_{ij} r_{ij}}{1 + \beta r_{ij}}\right) \exp\left(-\sum_{i=1}^N \frac{(\mathbf{r}_i - \mathbf{a}_i)^2}{2\sigma^2}\right) \prod_j^M \left(1 + \exp\left(b_j + \sum_{i=1}^N \sum_{d=1}^D \frac{x_i^{(d)} w_{i+d,j}}{\sigma^2}\right)\right) \quad (2.75)$$

It might not be completely clear as to why this function still makes it so that the total wavefunction satisfies the cusp conditions. The reason lies in the derivation of the conditions, the procedure in which the conditions presented in section 2.9.9 were found the only consideration was within the terms involving  $r_{ij}$  in the local energy, all other terms were canceled out or were otherwise non-divergent meaning the product between the jastrow would yield the same conditions.

## 2.10 Density Matrices

The Slater wavefunction presented throughout this chapter is quite complicated and the solution-space for the Schrödinger equation with said Slater is too large to extract any useful physical properties directly. Luckily we have one part of the physical system we may extract from a variational calculation, the so-called *one-body density*. From quantum mechanics the one-body density for a normalized wavefunction is defined as

$$\Lambda(\mathbf{r}, \mathbf{r}') = N \int \psi^*(\mathbf{r}, \mathbf{r}_2, \dots, \mathbf{r}_N) \psi(\mathbf{r}', \mathbf{r}_2, \dots, \mathbf{r}_N) d\mathbf{r}_2, \dots, d\mathbf{r}_N \quad (2.76)$$

which is just to integrate the wavefunction over all spacial coordinates except  $\mathbf{r}$  and  $\mathbf{r}'$ . The question now is what exactly does this mean, what information does this integral give us? The one-body density tells us that the element

$$N \int \psi^*(\mathbf{r}) \psi(\mathbf{r}) d\mathbf{r}_2, \dots, d\mathbf{r}_N = N \times P \text{ (Finding a particle within volume } d\mathbf{r} \text{ around point } \mathbf{r}) \quad (2.77)$$

with  $P$  denoting a probability. This might not give any tingles at first when it comes to extraction of physical properties of the system, however one has to keep in mind that the actual *configuration* of particles within the spacial solution-grid gives a direct insight into the actual physics of the system. A good example of this is the distribution

$$N \int \psi^*(\mathbf{r}_1) \psi(\mathbf{r}_1) d\mathbf{r}_1 = 0 \quad (2.78)$$

This integral is a *two-body density* and essentially what we have asked ourselves now is, what is the probability of finding two particles in the same exact state? The answer is apparently *zero* and we see that the all-time famous Pauli-exclusion principle practically appears straight out of the density definition.

With this result as motivation in mind, it is not unreasonable to question if density-matrices might possess more information about the physical nature of the system in question.

Before we tackle the procedure of calculating the densities with the Metropolis algorithm, let us express the full  $N$ -body density. The expressions are directly copied from this insightful article by Per-Olov Löwdin[32]. Density matrix of order  $p$  is defined to be

$$\Lambda^{(p)}(\mathbf{r}'_1, \dots, \mathbf{r}'_p | \mathbf{r}_1, \dots, \mathbf{r}_p) = \binom{N}{p} \int \psi^*(1', 2', \dots, p', \dots, N) \psi(1, 2, \dots, p, \dots, N) d\mathbf{r}'_{12}, \dots, d\mathbf{r}'_p \quad (2.79)$$

The integrals are over all permutations of  $\mathbf{r}'_{12}$ .

In order to actually find this density with the Metropolis algorithm we need to rewrite it in the

same manner as with the local energy, which is to introduce  $|\psi|^2$ . For the fermionic case this rewriting gives us the following matrix elements

$$\Lambda_{ij} = N \int \phi_i^*(\mathbf{r}_1) \phi_j(\mathbf{r}') \frac{\psi(\mathbf{r}', \mathbf{r}_2, \dots, \mathbf{r}_N)}{\psi(\mathbf{r}_1, \dots, \mathbf{r}_N)} |\psi(\mathbf{r}_1, \dots, \mathbf{r}_N)|^2 d\mathbf{r}' d\mathbf{r}_1 \dots d\mathbf{r}_N \quad (2.80)$$

where  $\phi$  are the single-particle basis functions within the Slater  $\psi$ .

The elements of the  $\Lambda$  matrix can then be calculated by simple counting. The basic premise is to essentially create a histogram of particle counts with the bins being various radial distances up to some cutoff  $r_{\max}$ . Then at every Metropolis step (after the test) we increment each value in the bins array with the number of particles currently within each respective bin. The array is then normalized by the usual total sum (sum of all values in the bins array), but also the radial distance to the power  $D$  to the right-most edge of each bin. The reason for this additional normalization is to account for the radial contributions to the configurations, a larger radial distance means the sparsity of the particle-density increases. We are however only interested in the non-dimensional count within each vicinity meaning we need to divide away the dimensional volume element of each bin. The element for a bin  $n$  is found to be<sup>16</sup>

$$\begin{aligned} V_n^{(D)} &= r_{n+1}^D - r_n^D \\ &= (r_n + \Delta r)^D - r_n^D \end{aligned} \quad (2.81)$$

In order to keep this stable we also notice that if the number of bins is satisfyingly large higher orders of  $\Delta r$  vanish and only the terms with linear factors of  $\Delta r$  give a significant contribution. Notice also that the highest order  $r_n^D$  gets canceled out. All this together gives

$$V_n^{(D)} = D r_n^{D-1} \Delta r \quad (2.82)$$

The factor  $D$  in front can be dropped as the histogram normalization cancels it anyways.

The resulting one-body densities are presented visually in » REF THESE FIGURES (GO GET EM!) «

---

<sup>16</sup>Constant proportional factors are dropped due to them being canceled in the histogram normalization (division of the sum of whole bin array).



## BASIS FUNCTIONS

Basis sets, the fundamental objects used in describing pretty much everything, anything from a coordinate system to an abstract vector-space or function-space are all part of the same set which we refer to as a basis. It is a set of objects applied to systems in order to essentially change our view of them, to extract desirable properties and to describe them in a rigidly fashion. In quantum mechanics the abstract vector-space models are used and the functions in mind are the wavefunctions thrown into the Schrödinger equation and the space at hand is the *Hilbert Space*. These functions are the central part of the particle-description in which quantum theory bases itself in, as such the choice of a basis is of monumental importance when solving quantum mechanical systems. Often<sup>1</sup> the choice of basis functions determine the efficiency and degree of usefulness that a specific method actually holds. This is usually to such degree that a poor choice of basis renders the method in question less useful or even completely unavailing.

The poor choice of basis sentiment is most definitely true for both the Hartree-Fock and the variational monte-carlo methods, and great care has to be taken when introducing such choices. For the variational method, the basis is taken directly from the Hartree-Fock method meaning most of the physical properties. In which case all except electron-electron correlations<sup>2</sup> are modeled quite well. For the basis in Hartree-Fock the choice needs to be in correspondence with the system of interest.

We will in this chapter mention some popular basis-sets used in atomic physics and deepen into a particular set of functions called *Gaussian Type orbitals* and use them with the well known *Hermite functions* and make a detailed calculation of the integral elements used in the Hartree-

---

<sup>1</sup>Read always

<sup>2</sup>Technically also nucleon-electron correlation as well, but quantum-dot systems do not have any atomic cores present.

Fock method. These integrals have been calculated in polar coordinates directly before[1], the motivation for calculating the integrals elements in Cartesian is due to the double-well potential, because of the higher order monomials in which they can be defined by the symmetry in polar coordinates is broken making the polar approach less desirable. The procedure in building the basis for the double-well system is also explained detail.

### 3.1 Hermite Functions

Hermite functions are functions of the following form

$$\phi_n^a(\mathbf{r}) \equiv \prod_d N_d H_{n_d}(\sqrt{a} x_d) \exp\left(-\frac{a}{2} x_d^2\right) \quad (3.1)$$

with  $\mathbf{r} = \sum_d \mathbf{e}_d x_d$  and the sum over  $d$  being the sum over the number of dimensions and the  $H_n$  is the Hermite polynomial of order  $n$ . The integer  $n_d$  is the order of the function<sup>3</sup> while the parameter  $a$  is a scaling factor and  $N_d$  is a normalization factor. These functions show up as eigenfunctions for the *quantum harmonic oscillator system*[16] with the scaling parameter  $a$  equal to the oscillator frequency ( $\omega$ ) of the system.

The Hermite functions are orthogonal and give a good ansatz for the VMC method, see section 2.9, with the scaling parameter transformed with an additional variational parameter. The problem with these are however that the matrix-elements introduced in the Hartree-Fock method (section 2.5) are not solvable directly with the Hermite functions as basis functions. However, we can write the Hermite functions in terms of *Hermite-Gaussians*. See section 3.2.2.

### 3.2 Gaussian Type Orbitals

*Gaussian Type Orbitals* or GTO's are functions of the following form[46]

$$G_n(\boldsymbol{\alpha}; \mathbf{r}, \mathbf{A}) \equiv \prod_d (x_d - A_d)^{n_d} e^{-\alpha_d (x_d - A_d)^2} \quad (3.2)$$

We call  $\alpha$  for the scaling parameter and  $i$  for the order of the GTO. The variable  $A$  is where the function is centered. These are in many literatures referred to as *primitive Gaussians* and they alone make a poor approximation to the true wave function.

In atomic physics these functions are used directly as a linear combination referred to as *contracted Gaussian functions*. These are written as

$$G_k(x, A) \equiv \sum_{a_k=0}^P C_{a_k} G_{a_k}(\alpha_{a_k}; x, A) \quad (3.3)$$

---

<sup>3</sup>In quantum mechanics the number  $n$  is referred to as the principal quantum number and is associated with the energy of a given orbital(energy-level) of the system.

and are fitted<sup>4</sup> to *Slater-type orbitals*, which are functions with decaying properties (present in atomic systems), or found by some variational method before-hand.

These functions are unfortunately not orthogonal, but they behave nicely in integrals and actually give an analytic expression for the interaction-elements mentioned in section 2.5. For this reason we will go forth and use the Gaussian contracted functions and actually fit them to Hermite functions.

### 3.2.2 Hermite-Gaussian Functions

The GTO's described can be explicitly expressed in terms of so-called *Hermite-Gaussian functions*<sup>5</sup> defined as

$$g_n(\mathbf{a}; \mathbf{r}, \mathbf{A}) = \prod_d \left( \frac{\partial}{\partial A_d} \right)^{n_d} e^{-\alpha_d (x_d - A_d)^2} \quad (3.4)$$

meaning

$$G_n(\mathbf{a}; \mathbf{r}, \mathbf{A}) = \prod_d (2\alpha_d)^{-n_d} \left( \frac{\partial}{\partial A_d} \right)^{n_d} e^{-\alpha_d (x_d - A_d)^2} \quad (3.5)$$

Some properties of the one-dimensional Hermite-Gaussians are as follows

$$\begin{aligned} \frac{\partial g_t}{\partial A_x} &= g_{t+1} \\ g_{t+1} &= \left( \frac{\partial}{\partial A_x} \right)^t \frac{\partial g_0}{\partial A_x} = 2\alpha(x - A_x) \left( \frac{\partial}{\partial A_x} \right)^t g_0 \\ g_{t+1} &= 2\alpha((x - A_x)g_t - t g_{t-1}) \\ (x - A_x)g_t &= \frac{1}{2\alpha} g_{t+1} + t g_{t-1} \end{aligned} \quad (3.6)$$

The mentioned rewriting of the Hermite functions in terms of the Hermite-Gaussians is

$$\phi_n^a(\mathbf{r}) = \prod_d N_d \sum_{l=0}^{n_d} C_{n_d l} g_l \left( \frac{\mathbf{a}}{2}, \mathbf{r}, \mathbf{A} \right) \quad (3.7)$$

with  $C_{n_d l}$  being the  $l'$ th Hermite-coefficient for the Hermite polynomial of order  $n_d$ . This means that the matrix-elements in Hartree-Fock is just a linear combination over integrals over Hermite-Gaussians. The following section will tackle this in detail for the two-dimensional case. The three-dimensional case is given by an excellent text by Trygve Helgaker and Peter R. Taylor[20], see also [19].

<sup>4</sup>Meaning we find the parameters  $C_{a_k}$  and  $\alpha_{a_k}$

<sup>5</sup>The reason for the name is that the polynomial factors generated by the differentiation are precisely the Hermite polynomials.

### 3.3 Integral Elements

In the Hartree-Fock scheme described in chapter 3 we need to calculate the integrals which define the different matrix elements. The integrals to be found are of the following form

$$\begin{aligned}
 \langle i | j \rangle &= \int_{-\infty}^{\infty} g_i(\alpha_i; r, A) g_j(\alpha_j; r, B) d\mathbf{r} \\
 \langle i | x_d^k | j \rangle &= \int_{-\infty}^{\infty} g_i(\alpha_i; r, A) r^k g_j(\alpha_j; r, B) d\mathbf{r} \\
 \langle i | \nabla^2 | j \rangle &= \int_{-\infty}^{\infty} g_i(\alpha_i; r, A) \nabla^2 g_j(\alpha_j; r, B) d\mathbf{r} \\
 \left\langle ij \left| \frac{1}{r} \right| kl \right\rangle &= \int_{-\infty}^{\infty} \int_{-\infty}^{\infty} g_i(\alpha_i; r_1, A) g_j(\alpha_j; r_2, B) \frac{1}{r_{12}} g_k(\alpha_k; r_1, C) g_l(\alpha_l; r_2, D) d\mathbf{r}_1 d\mathbf{r}_2
 \end{aligned} \tag{3.8}$$

where  $d\mathbf{r}$  means integration over all dimensions and with the  $g$ 's being the usual *Hermite-Gaussians* defined as

$$g_n(\alpha; \mathbf{r}, \mathbf{A}) = \prod_d (x_d - A_d)^{n_d} e^{-\alpha(x_d - A_d)^2} \tag{3.9}$$

We will in this chapter limit ourselves to work with isotropic Gaussians (meaning  $\alpha_d$  is the same for all dimensions) as this will yield a simpler closed-form solution to the integrals. For a calculation of integral elements using non-isotropic Gaussian functions see this wonderful article [7], this article takes gives a detailed calculations of integrals over s-type non-isotropic gaussians. The extension to general Gauss-Hermite can be done in the exact same manner as presented here, however the proportionality factors involved in the recursive relation is different.

Before we throw ourselves out into the integrals, let us first express the Hermite-Gaussians in a more convenient way (again see [20] and [19]). The Gaussians can be expressed as

$$g_n(\alpha; \mathbf{r}, \mathbf{A}) = \prod_d \left( \frac{\partial}{\partial A_{x_d}} \right)^{n_d} e^{-\alpha(x_d - A_d)^2} = \prod_d \left( \frac{\partial}{\partial A_{x_d}} \right)^{n_d} g_0(\alpha; \mathbf{r}, \mathbf{A}) \tag{3.10}$$

Since the derivatives are with respect to the center variables we may pull them out of the integration meaning the integrals will only be over s-type Gaussians, greatly simplifying the calculations. With the mentioned simplification in mind, the problem is to find a closed-form expression for the integrals over s-type Gaussians.

We also introduce the *Gaussian product rule*<sup>6</sup> which basically states that the product of two Gaussian functions is just a third Gaussian centered between the center of the two. The expressions

---

<sup>6</sup>Still in the isotropic case.



give

$$g_0(\alpha; \mathbf{r}, \mathbf{A})g_0(\beta; \mathbf{r}, \mathbf{B}) = K_{AB} \exp(-(\alpha + \beta)\mathbf{r}_s^2) \quad (3.11)$$

where

$$\begin{aligned} K_{AB} &\equiv \exp\left(-\frac{\alpha\beta}{\alpha+\beta}R_{AB}^2\right) \\ R_{AB} &= |\mathbf{A} - \mathbf{B}| \\ \mathbf{r}_s &= \mathbf{r} - \mathbf{P} \\ \mathbf{P} &= \frac{\alpha\mathbf{A} + \beta\mathbf{B}}{\alpha + \beta} \end{aligned} \quad (3.12)$$

the vector  $\mathbf{r}_s$  is just somewhere between  $\mathbf{A}$  and  $\mathbf{B}$  (We will see that  $r_s$  disappears when the integration is done). The Gaussian product rule greatly simplifies the integral over two Gaussian functions since we can just pull  $K_{AB}$  out of the integration since it is a constant.

### 3.3.3 Overlap Distribution

An *overlap distribution* is defined as the product between two Hermite-Gaussian functions, that is

$$\Omega_{ij} = \prod_d g_{i_d}(x_d, \alpha, A_d) g_{j_d}(x_d, \beta, B_d) = K_{A_d B_d} x_A^{i_d} x_B^{j_d} e^{-(\alpha+\beta)x_p^2} \quad (3.13)$$

with the Gaussian product rule, which is just another Gaussian function centered in  $P$ , but with the extra *monomial* factors in  $\mathbf{r} - \mathbf{A}$  and  $\mathbf{r} - \mathbf{B}$ . These factors are troublesome when integrating. With the motivation that Hermite-Gaussians make life simpler, we expand the overlap distribution in a Hermite-Gaussian basis. Following T. Helgaker[20] and working in one dimension (since Hermite-Gaussians can be split in each respective dimension) we have<sup>7</sup>

$$\Omega_{ij}(\alpha, \beta, \mathbf{r}, \mathbf{A}, \mathbf{B}) = \sum_{t=0}^{i+j} E_t^{ij} g_t(\alpha, \beta, \mathbf{r}, \mathbf{P}) \quad (3.14)$$

Again, we stress that the indices in equation 3.14 and the calculations further are in 1 dimension. Explicit expressions for the coefficients  $E_t^{ij}$  are difficult to derive, however a set of recurrence relations are possible to find using the properties of the Hermite-Gaussian functions. Consider

---

<sup>7</sup>The indices  $i$  and  $j$  are now in 1 dimension!

firstly the incremented distribution

$$\begin{aligned}
\Omega_{i+1,j} &= \sum_{t=0}^{i+1+j} E_t^{i+1,j} g_t \\
&= \left( x_P - \frac{\beta}{\alpha + \beta} (A_x - B_x) \right) \Omega_{ij} \\
&= \sum_{t=0}^{i+j} E_t^{ij} \left( x_P - \frac{\beta}{\alpha + \beta} (A_x - B_x) \right) g_t \\
&= \sum_{t=0}^{i+j} E_t^{ij} \left( \left( t g_{t-1} + \frac{1}{2(\alpha + \beta)} g_{t+1} \right) - \frac{\beta}{\alpha + \beta} (A_x - B_x) g_t \right) \\
&= \sum_{t=0}^{i+j} \left( (t+1) E_{t+1}^{ij} + \frac{1}{2(\alpha + \beta)} E_{j-1}^{ij} - \frac{\beta}{\alpha + \beta} (A_x - B_x) \right) g_t
\end{aligned} \tag{3.15}$$

Using the properties listed in equation 3.6 (mainly the recurrence) and the expansion equation 3.14. The incrementation of  $j$  follows the exact same derivation. The starting coefficient is thus

$$E_0^{00} = K_{AB} \tag{3.16}$$

This is found by inserting in  $i = j = 0$  into equation 3.15, realizing the exponential is the same for all  $i$  and  $j$  and using the orthogonality between the Hermite-Gaussians<sup>8</sup>. The recurrent coupled relations for the  $E$ 's are

$$\begin{aligned}
E_t^{i+1,j} &= \frac{1}{2(\alpha + \beta)} E_{t-1}^{ij} - \frac{\beta}{\alpha + \beta} (A_x - B_x) E_t^{ij} + (t+1) E_{t+1}^{ij} \\
E_t^{i,j+1} &= \frac{1}{2(\alpha + \beta)} E_{t-1}^{ij} - \frac{\alpha}{\alpha + \beta} (A_x - B_x) E_t^{ij} + (t+1) E_{t+1}^{ij}
\end{aligned} \tag{3.17}$$

The overlap distribution can with this be expanded in Hermite-Gaussian functions.

As mentioned, the whole point of using Hermite-Gaussian functions is because of the inherent definition with the derivative with respect to the centering (remember s-types). This means that for attaining the final expression we must in the end differentiate the expansion coefficients. We state here the coefficients differentiated with respect to the difference variable  $Q_x = A_x - B_x$

$$\begin{aligned}
E_0^{00;n+1} &= -\frac{2\alpha\beta}{\alpha + \beta} (Q_x E_0^{00;n} + n E_0^{00;n-1}) \\
E_t^{i+1,j;n} &= \frac{1}{2(\alpha + \beta)} E_{t-1}^{ij;n} - \frac{\beta}{\alpha + \beta} (Q_x E_t^{ij;n} + n E_t^{ij;n-1}) + (t+1) E_{t+1}^{ij;n} \\
E_t^{i,j+1;n} &= \frac{1}{2(\alpha + \beta)} E_{t-1}^{ij;n} - \frac{\alpha}{\alpha + \beta} (Q_x E_t^{ij;n} + n E_t^{ij;n-1}) + (t+1) E_{t+1}^{ij;n} \\
E_t^{ij;n} &\equiv \frac{\partial^n E_t^{ij}}{\partial Q_x^n}
\end{aligned} \tag{3.18}$$

---

<sup>8</sup>Another way of expressing this statement is to say that each index  $t$  in the sum corresponds to an equation for  $E_t^{ij}$ .

Notice that these expressions are just the same relations as for the coefficients, but with an extra factor in the middle.

### 3.3.3 Overlap Integral

With The simplification to s-types and the product rule, the integration may begin. Starting with the overlap  $\langle i | j \rangle$  and using equation 3.14<sup>9</sup>

$$\begin{aligned}
 \langle i | j \rangle &= \int_{-\infty}^{\infty} \Omega_{ij}(\alpha_p, \beta_p, \mathbf{r}, \mathbf{A}, \mathbf{B}) d\mathbf{r} \\
 &= \sum_p^{i+j} E_p^{ij} \int_{-\infty}^{\infty} g_p(\alpha, \beta, \mathbf{r}, \mathbf{P}) d\mathbf{r} \\
 &= \sum_p^{i+j} E_p^{ij} \int_{-\infty}^{\infty} (\mathbf{r} - \mathbf{P})^p e^{-(\alpha_p + \beta_p)(\mathbf{r} - \mathbf{P})^2} d\mathbf{r} \\
 &= \sum_p^{i+j} E_p^{ij} \left( \frac{((-1)^p - 1) \Gamma\left(\frac{p+1}{2}\right)}{2(\alpha_p + \beta_p)^{\frac{p+1}{2}}} \right)^d
 \end{aligned} \tag{3.19}$$

The power  $d$  comes from splitting the integral into the  $d$  dimensions. Also using the *multi-index notation*(section A.3)<sup>10</sup> and expanding

$$E_n^{ab} = \prod_d E_{n_d}^{a_d b_d} \tag{3.20}$$

Such that the coefficients are all just products over coefficients in each dimension. A substitution in each dimension(i.e  $u = x - P_x$ ) is also used. Notice in addition that the scaling factors  $\alpha$  and  $\beta$  are specific for each  $p$  because of the overlap expansion.

---

<sup>9</sup>Also using the following integral  $\int_{-\infty}^{\infty} e^{-\lambda x^2} = \sqrt{\frac{\pi}{\lambda}}$ ,  $\lambda > 0$ . See [27].

<sup>10</sup>The power  $d$  also means that with the multi-index notation the entire expression in the paranthesis are to be calculated for each dimension in  $p$  and then multiplied together.

### 3.3.3 Potential Integral

The second integral with the  $x_d^k$  part shows up in the external potential part of the Hamiltonian and again with the Gaussian product rule the expression gives

$$\begin{aligned}
\langle i | x_d^k | j \rangle &= \int_{-\infty}^{\infty} x_d^k \Omega_{ij}(\alpha_p, \beta_p, \mathbf{r}, \mathbf{A}, \mathbf{B}) d\mathbf{r} \\
&= \sum_p^{i+j} E_p^{ij} \int_{-\infty}^{\infty} x_d^k (\mathbf{r} - \mathbf{P})^p e^{-(\alpha_p + \beta_p)(\mathbf{r} - \mathbf{P})^2} d\mathbf{r} \\
&= \sum_p^{i+j} E_p^{ij} \left( \frac{((-1)^p - 1) \Gamma\left(\frac{p+1}{2}\right)}{2(\alpha_p + \beta_p)^{\frac{p+1}{2}}} \right)^{D-1} \int_{-\infty}^{\infty} (u + P_d)^k \exp(-(\alpha_p + \beta_p)u^2) du \\
&= \sum_p^{i+j} E_p^{ij} \left( \frac{((-1)^p - 1) \Gamma\left(\frac{p+1}{2}\right)}{2(\alpha_p + \beta_p)^{\frac{p+1}{2}}} \right)^{D-1} \sum_{l=0}^k \binom{k}{l} P_d^{k-l} \int_{-\infty}^{\infty} u^l \exp(-(\alpha_p + \beta_p)u^2) du \\
&= \sum_p^{i+j} E_p^{ij} \left( \frac{((-1)^p - 1) \Gamma\left(\frac{p+1}{2}\right)}{2(\alpha_p + \beta_p)^{\frac{p+1}{2}}} \right)^{D-1} \sum_{l=0}^k \binom{k}{l} \frac{P_d^{k-l}}{2(\alpha_p + \beta_p)^{\frac{l}{2}}} ((-1)^l + 1) \Gamma\left(\frac{l+1}{2}\right) \quad (3.21)
\end{aligned}$$

The integrals are split in each dimension and the dimensions not equal to  $d$  (in  $x_d^k$ ) are pulled out and the approach in equation 3.19 is applied. The integral over dimension  $d$  is then substituted with  $u = x_d + P_d$ . In line four  $(u + P_d)^k$  is rewritten with the *binomial expansion*<sup>11</sup>.

### 3.3.3 Laplacian Integral

The third integral with the Laplacian operator arises in the kinetic part of the Hamiltonian. This integral can be expressed in terms of equation 3.19, the overlap integral, however the Laplacian

---

<sup>11</sup>The integral  $\int_{-\infty}^{\infty} x^n e^{-ax^2} dx = \frac{1}{2} a^{-\frac{n}{2}} \Gamma\left(\frac{k+1}{2}\right)$ ,  $n > -1$ ,  $n$  even, see [27].

applied to a Hermite-Gaussian has to be calculated first

$$\begin{aligned}
\nabla^2 g_i(\alpha; \mathbf{r}, \mathbf{A}) &= \sum_d \frac{\partial^2}{\partial x_d^2} \left( \prod_{d'} (x - A_{d'})^{i_{d'}} \exp(-\alpha(x_{d'} - A_{d'})^2) \right) \\
&= \sum_d \prod_{d' \neq d} g_{i,d'} \frac{\partial^2}{\partial x_d^2} ((x_d - A_d)^{i_d} \exp(-\alpha(x_d - A_d)^2)) \\
&= \sum_d \prod_{d' \neq d} g_{i,d'} g_{i,d} \left( 4\alpha^2 (x_d - A_d)^{i_d+2} - 2\alpha(2i_d + 1)(x_d - A_d)^{i_d} \right. \\
&\quad \left. + i_d(i_d - 1)(x_d - A_d)^{i_d-2} \right) \\
&= g_i \sum_d \left( 4\alpha^2 (x_d - A_d)^{i_d+2} - 2\alpha(2i_d + 1)(x_d - A_d)^{i_d} \right. \\
&\quad \left. + i_d(i_d - 1)(x_d - A_d)^{i_d-2} \right)
\end{aligned} \tag{3.22}$$

Now for the integral we have

$$\begin{aligned}
\langle i | \nabla^2 | j \rangle &= \int_{-\infty}^{\infty} g_i(\alpha; \mathbf{r}, \mathbf{A}) \nabla^2 g_j(\beta; \mathbf{r}, \mathbf{B}) d\mathbf{r} \\
&= \sum_d \prod_{d' \neq d} \langle i_{d'} | \sigma_{d'}(S_d(\beta; \mathbf{x} - \mathbf{B}_d)) | j_{d'} \rangle
\end{aligned} \tag{3.23}$$

with

$$\begin{aligned}
S_d(\alpha; x_d - A_d) &\equiv (4\alpha^2 (x_d - A_d)^{i_d+2} - 2\alpha(2i_d + 1)(x_d - A_d)^{i_d} + i_d(i_d - 1)(x_d - A_d)^{i_d-2}) \\
\sigma_d(S_d) &\equiv \begin{cases} 1, & d' \neq d \\ S_d, & d' = d \end{cases}
\end{aligned} \tag{3.24}$$

meaning the Laplacian integral can be expressed in terms of the overlap integrals  $\langle i | j + 2 \rangle$ ,  $\langle i | j \rangle$  and  $\langle i | i - 2 \rangle$ <sup>12</sup>.

### 3.3.3 Coulomb Potential Integral

Lastly, the troublesome<sup>13</sup> Coulomb integral needs to be calculated. Due to the  $1/r$  term we cannot split the integral in each respective dimension as previously. Before we approach the full Coulomb integral, let's calculate a simpler integral over a so-called *Coulomb Potential distribution*

$$\int_{-\infty}^{\infty} e^{-\alpha(\mathbf{r}-\mathbf{A})^2} \frac{1}{|\mathbf{r}-\mathbf{B}|} d\mathbf{r} \tag{3.25}$$

<sup>12</sup>Since  $x g_i = g_{i+1}$  and  $\frac{g_i}{x} = g_{i-1}$ .

<sup>13</sup>Damn inverse term prevents dimensional decomposition.

The calculation of this integral will be beneficial for the calculation of the Coulomb integral as we can reuse most of the tricks used. With equation 3.11, the Gaussian product rule, in mind. We rewrite the inverse term with

$$\int_{-\infty}^{\infty} e^{r_B^2 t^2} dt = \frac{\sqrt{\pi}}{r_B} \Rightarrow \frac{1}{r_B} = \frac{1}{\sqrt{\pi}} \int_{-\infty}^{\infty} e^{r_B^2 t^2} dt \quad (3.26)$$

The Coulomb potential integral is thus, with equation 3.11 (again the product rule)

$$\begin{aligned} \int_{-\infty}^{\infty} \int_{-\infty}^{\infty} e^{-\alpha(r-A)^2} \frac{1}{|\mathbf{r}-\mathbf{B}|} d\mathbf{r} &= \frac{1}{\sqrt{\pi}} \int_{-\infty}^{\infty} e^{-\alpha(r-A)^2} e^{t^2(\mathbf{r}-\mathbf{B})^2} d\mathbf{r} dt \\ &= \frac{1}{\sqrt{\pi}} \int_{-\infty}^{\infty} \int_{-\infty}^{\infty} e^{-\frac{\alpha t^2}{\alpha+t^2}(\mathbf{A}-\mathbf{B})^2} e^{-(\alpha+t^2)r_S^2} d\mathbf{r} dt \\ &= \frac{1}{\sqrt{\pi}} \int_{-\infty}^{\infty} \left( \frac{\pi}{\alpha+t^2} \right)^{\frac{d}{2}} e^{-\frac{\alpha t^2}{\alpha+t^2}(\mathbf{A}-\mathbf{B})^2} dt \end{aligned} \quad (3.27)$$

The integral over  $t$  has to be addressed separately for two- and three dimensions. For the three-dimensional case the reader is referred to [20]. Here we will derive a closed-form form expression for the two-dimensional case. First let us use the following substitution

$$\begin{aligned} u &= \frac{t}{\sqrt{\alpha+t^2}} \\ t &= u \sqrt{\frac{\alpha}{1-u^2}} \\ \frac{du}{dt} &= \frac{\alpha}{(\alpha+t^2)^{\frac{3}{2}}} \end{aligned} \quad \begin{aligned} \lim_{t \rightarrow -\infty} u(t) &= -1 \\ \lim_{t \rightarrow \infty} u(t) &= 1 \end{aligned} \quad (3.28)$$

The integrand (ignoring the exponential part) is then

$$\begin{aligned} \frac{dt}{\alpha+t^2} &= \frac{1}{\alpha+t^2} \frac{(\alpha+t^2)^{\frac{3}{2}}}{\alpha} du \\ &= \frac{\sqrt{\alpha+t^2}}{\alpha} du \\ &= \frac{t}{\alpha u} du \\ &= \frac{1}{\alpha u} u \sqrt{\frac{\alpha}{1-u^2}} du \\ &= \frac{1}{\sqrt{\alpha}} \sqrt{\frac{1}{1-u^2}} du \end{aligned} \quad (3.29)$$

giving

$$I_{2D} = \sqrt{\frac{\pi}{\alpha}} \int_{-1}^1 \frac{1}{\sqrt{1-u^2}} e^{-\alpha u^2 |\mathbf{A}-\mathbf{B}|^2} du \quad (3.30)$$

and for the three-dimensional case we have a simpler form (easily seen with the same substitution)

$$I_{3D} = \pi \int_{-1}^1 e^{-au^2|A-B|^2} du \quad (3.31)$$

These integrals must be solved numerically using *Chebyshev-Gauss Quadrature*[49]. One can also rewrite the 2D-integral in terms of the *Modified Bessel function of first kind* by using  $u^2 = 1/2(1 - \cos(\theta))$ [50]. [20]. A take on this resulted nowhere as the closed form expanded itself in ever-increasing order of polynomial factors with the first and second order of the modified Bessel function of first kind. The 3D-integral can be rewritten with an *incomplete Gamma function*. From equation 3.10, the integrals have to be differentiated in order to get the final closed form expressions, see section 3.3.3.

### 3.3.3 Coulomb Interaction Integral

In the previous section an expression for integral over a Coulomb potential was derived. Before we embark into handling the full Coulomb interaction integral, another exercise with simpler interaction integral is worthwhile. The integral in question is

$$I' = \int_{-\infty}^{\infty} \int_{-\infty}^{\infty} e^{-\alpha(r'-A)^2} e^{-\beta(r-B)^2} \frac{1}{|r'-r|} dr dr' \quad (3.32)$$

This is an interaction between two distributions. Firstly, notice that we can rewrite the distribution centered in  $A$  and the Coulomb interaction with the previously calculated Coulomb potential integral given in equation 3.27. Using  $I$  as a general label for equation 3.30 and equation 3.31 we have

$$\begin{aligned} I' &= \int_{-\infty}^{\infty} \int_{-\infty}^{\infty} e^{-\alpha(r'-A)^2} e^{-\beta(r-B)^2} \frac{1}{|r'-r|} dr dr' \\ &= \int_{-\infty}^{\infty} I_D(\alpha; |r-A|) e^{-\beta(r-B)^2} dr \end{aligned} \quad (3.33)$$

Inserting in the definition for  $u$  (the substitution in equation 3.28) and using the extremely useful Gaussian product rule for the product between the distribution centered in  $B$  and the exponential factor in  $I$  (which is labelled the same for both the two- and three dimensional case) is

$$e^{-\alpha u^2(r-A)^2} e^{-\beta(r-B)^2} = e^{-(\alpha u^2 + \beta)r^2} e^{-\frac{\alpha u^2 \beta}{\alpha u^2 + \beta}(A-B)^2} \quad (3.34)$$

Inserting this into equation 3.33 with

$$v \equiv \begin{cases} \sqrt{\frac{\pi}{\alpha}} \sqrt{\frac{1}{1-u^2}}, & 2D \\ \pi, & 3D \end{cases} \quad (3.35)$$

we have

$$\begin{aligned}
 I' &= \int_{-\infty}^{\infty} \int_{-1}^1 v e^{-(\alpha u^2 + \beta) r s^2} e^{-\frac{\alpha u^2 \beta}{\alpha u^2 + \beta} (A-B)^2} d\mathbf{r} du \\
 &= \int_{-1}^1 v \left( \frac{\pi}{\alpha u^2 + \beta} \right)^{\frac{d}{2}} e^{-\frac{\alpha u^2 \beta}{\alpha u^2 + \beta} (A-B)^2} du
 \end{aligned} \tag{3.36}$$

Specializing to the two-dimensional case and substituting

$$\begin{aligned}
 v &= u \sqrt{\frac{\alpha + \beta}{\alpha u^2 + \beta}} \\
 \frac{dv}{du} &= \frac{\beta \sqrt{\alpha + \beta}}{(\alpha u^2 + \beta)^{3/2}} \\
 u &= v \sqrt{\frac{\beta}{\alpha + \beta - \alpha v^2}} \\
 v(-1) &= -1 \\
 v(1) &= 1
 \end{aligned} \tag{3.37}$$

The integrand is

$$\begin{aligned}
 \frac{1}{\sqrt{1-u^2}} \frac{1}{\alpha u^2 + \beta} du &= \frac{1}{\sqrt{1-u^2}} \frac{1}{\alpha u^2 + \beta} \frac{(\alpha u^2 + \beta)^{3/2}}{\beta \sqrt{\alpha + \beta}} dv \\
 &= \frac{1}{\sqrt{1-u^2}} \frac{u}{\beta v} dv \\
 &= \sqrt{\frac{\alpha + \beta - \alpha v^2}{(\alpha + \beta)(1-v^2)}} \frac{1}{\beta v} v \sqrt{\frac{\beta}{\alpha + \beta - \alpha v^2}} dv \\
 &= \frac{1}{\sqrt{\beta(\alpha + \beta)}} \frac{1}{\sqrt{1-v^2}} dv
 \end{aligned} \tag{3.38}$$

we have

$$I'_{2D} = \frac{\pi^{\frac{3}{2}}}{\sqrt{\alpha \beta (\alpha + \beta)}} \int_{-1}^1 \frac{1}{\sqrt{1-v^2}} e^{-\frac{\alpha \beta}{(\alpha + \beta)} v^2 (A-B)^2} dv \tag{3.39}$$

This expression will be of great use when calculating the final full interaction integral over the Coulomb distribution. The next section will derive the mentioned recurrence relation before the full Coulomb integral is calculated



### 3.3.3 Recurrence Relation

Following directly from [20], we proceed with finding a similar recurrence relation for the derivatives. We define a function containing the integral which needs to be solved numerically

$$\zeta_n(x) \equiv \int_{-1}^1 \frac{u^{2n}}{\sqrt{1-u^2}} e^{-u^2 x} du \quad (3.40)$$

$$\frac{\partial \zeta_n}{\partial x} = -\zeta_{n+1}$$

The Coulomb potential integral is then, in terms of  $\zeta_n(x)$

$$I_{2D} = \sqrt{\frac{\pi}{\alpha}} \zeta_0(\alpha R_{AB}^2) \quad (3.41)$$

and the first derivative with respect to  $A_x$  is

$$\begin{aligned} \frac{\partial I_{2D}}{\partial A_x} &= \sqrt{\frac{\pi}{\alpha}} \frac{\partial}{\partial A_x} \zeta_0(\alpha R_{AB}^2) \\ &= -2\sqrt{\alpha\pi} X_{AB} \zeta_1(\alpha R_{AB}^2) \end{aligned} \quad (3.42)$$

With this we define an auxiliary function

$$\begin{aligned} \zeta_{tu}^n &= \left( \frac{\partial}{\partial A_x} \right)^t \left( \frac{\partial}{\partial A_y} \right)^u \zeta_{00}^n \\ \zeta_{00}^n &= (-2)^n \alpha^{n-\frac{1}{2}} \zeta_n(\alpha R_{AB}^2) \end{aligned} \quad (3.43)$$

and take a look at the incrementation of  $t$

$$\begin{aligned} \zeta_{t+1,u}^n &= \left( \frac{\partial}{\partial A_x} \right)^t \left( \frac{\partial}{\partial A_y} \right)^u \frac{\partial \zeta_{00}^n}{\partial A_x} \\ &= \left( \frac{\partial}{\partial A_x} \right)^t X_{AB} \zeta_{0u}^{n+1} \end{aligned} \quad (3.44)$$

Using the commutator between  $\partial_{A_x}^t$ <sup>14</sup>

$$\begin{aligned} \frac{\partial^t}{\partial A_x^t} X_{AB} &= \left[ \frac{\partial^t}{\partial A_x^t}, X_{AB} \right] + X_{AB} \frac{\partial^t}{\partial A_x^t} \\ &= t \frac{\partial^{t-1}}{\partial A_x^{t-1}} + X_{AB} \frac{\partial^t}{\partial A_x^t} \end{aligned} \quad (3.45)$$

the final form of equation 3.44 is<sup>15</sup>

$$\begin{aligned} \zeta_{t+1,u}^n &= t \zeta_{t-1,u}^{n+1} + X_{AB} \zeta_{t,u}^{n+1} \\ \zeta_{t,u+1}^n &= u \zeta_{t,u-1}^{n+1} + Y_{AB} \zeta_{t,u}^{n+1} \end{aligned} \quad (3.46)$$

---

<sup>14</sup>  $\partial_x^t = \frac{\partial^t}{\partial x^t}$

<sup>15</sup> The incrementation of  $u$  is derived in the exact same manner as with  $t$ .

With this all Hermite integrals of order  $t + u \leq N$  can be calculated from  $\zeta$  of order  $n \leq N$ , the only difference being  $X_{AB}$  and  $Y_{AB}$ . The Coulomb interaction integral (equation 3.39) follows this exact recurrence, but with a different proportionality factor  $\alpha\beta/(\alpha + \beta)$ . We will write it out for the sake of clarity

$$\begin{aligned}\frac{\partial I'_{2D}}{\partial A_x} &= -\frac{2\alpha\beta}{\alpha + \beta} X_{AB} \zeta_1 \left( \frac{\alpha\beta}{\alpha + \beta} R_{AB}^2 \right) \\ \zeta_{00}^n &= \left( \frac{-2\alpha\beta}{\alpha + \beta} \right)^n \zeta_n \left( \frac{\alpha\beta}{\alpha + \beta} R_{AB}^2 \right)\end{aligned}\quad (3.47)$$

Notice that the only difference between the obtained recurrence relations and the ones obtained by Helgaker[19] is in equation 3.43 and equation 3.47. Other than this the incrementation of  $\zeta_n$  gives the exact same  $X_{AB}$  (and similar for the other directions) as with the incomplete gamma function.

### 3.3.3 Coulomb Distribution Integral

With the derived expressions for the Coulomb potential integral the full two-body distribution can be treated. The expression with the simplification in equation 3.10 gives

$$\begin{aligned}\left\langle ij \left| \frac{1}{r_{12}} \right| kl \right\rangle &= \int_{-\infty}^{\infty} \int_{-\infty}^{\infty} \Omega_{ik}(\boldsymbol{\alpha}, \boldsymbol{\gamma}, \mathbf{r}_1, \mathbf{A}, \mathbf{C}) \frac{1}{|\mathbf{r}_1 - \mathbf{r}_2|} \Omega_{jl}(\boldsymbol{\beta}, \boldsymbol{\delta}, \mathbf{r}_2, \mathbf{B}, \mathbf{D}) d\mathbf{r}_1 d\mathbf{r}_2 \\ &= \sum_{pq}^{i+k, j+l} E_p^{ik} E_q^{jl} \int_{-\infty}^{\infty} \int_{-\infty}^{\infty} \frac{g_p(\alpha + \gamma, \mathbf{r}_1, \mathbf{P}) g_q(\beta + \delta, \mathbf{r}_2, \mathbf{Q})}{|\mathbf{r}_1 - \mathbf{r}_2|} d\mathbf{r}_1 d\mathbf{r}_2 \\ &= \frac{a}{\sqrt{(\alpha + \gamma + \beta + \delta)}} \sum_{pq}^{i+k, j+l} E_p^{ik} E_q^{jl} (-1)^q \zeta_{p+q} \left( \frac{(\alpha + \gamma)(\beta + \delta)}{\alpha + \gamma + \beta + \delta}, \mathbf{R}_{s_1 s_2} \right)\end{aligned}\quad (3.48)$$

Where we have used the multi-index<sup>16</sup> notation for  $p, q, i, k, j$ , and  $l$  equation 3.20 and used equation 3.39 to arrive at the final step. An additional simplification due to the fact that  $\zeta_n$  is only dependant on the relative distance of the centers is also used, for the x-coordinate it is stated as

$$\left( \frac{\partial}{\partial P_x} \right)^{p_x} \left( \frac{\partial}{\partial Q_x} \right)^{q_x} = (-1)^{p_x + q_x} \left( \frac{\partial}{\partial P_x} \right)^{p_x + q_x} \quad (3.49)$$

and the same for the other directions. The factor  $a$  is

$$a \equiv \begin{cases} \frac{\pi^{\frac{3}{2}}}{\sqrt{(\alpha + \gamma)(\beta + \delta)}}, & 2D \\ \frac{\pi^{\frac{5}{2}}}{(\alpha + \gamma)(\beta + \delta)}, & 3D \end{cases} \quad (3.50)$$

<sup>16</sup>Essentially just expanding an index in each dimension, for instance  $i = (i_x, i_y, i_z)$  with corresponding  $p = (p_x, p_y, p_z)$  with each index inside the tuple running to each respective index, meaning for instance  $p_x = 0$  to  $i_x$  and so on.

## 3.4 Double-Well Functions

This section will explain the building of a basis for the *double-well potential*. We will expand them in a linear combination of harmonic oscillator functions and find the coefficients of this expansion by solving the arising eigenvalue-problem. Let us first express the potential

$$U^{\text{DW}}(r) = V^{\text{HO}}(r) + V_n^{\text{DW}}(r) \quad (3.51)$$

A double well potential is essentially just a perturbation of the usual Harmonic oscillator potential (which is a single-well). The  $V_n^{\text{DW}}$  part is assumed to be a polynomial of degree  $n$ . This means that the integral over such a potential can be calculated using equation 3.21.

### 3.4.4 The Eigenvalue problem

The mentioned eigenvalue problem comes from the basis expansion of the spacial part and from the trick of projecting with a single function from left. We will explain briefly. First let us express the expansion,

$$|\psi_p^{\text{DW}}\rangle = \sum_l C_{lp} |\psi_l^{\text{HO}}\rangle \quad (3.52)$$

and then project from left the bra  $\langle\psi_k^{\text{HO}}|$  in the inner-product space of  $h^{\text{DW}}$

$$\langle\psi_k^{\text{HO}}| h^{\text{DW}} |\psi_p^{\text{DW}}\rangle = \sum_l C_{lp} \langle\psi_k^{\text{HO}}| h^{\text{DW}} |\psi_l^{\text{HO}}\rangle = \sum_l C_{lp} \epsilon_l^{\text{DW}} \quad (3.53)$$

This gives us an eigenvalue equation

$$\mathbf{H} \mathbf{C} = \epsilon^{\text{DW}} \mathbf{C} \quad (3.54)$$

with

$$H_{ij} = \langle\psi_i^{\text{HO}}| h^{\text{DW}} |\psi_j^{\text{HO}}\rangle \quad (3.55)$$

Using equation 3.51 we can write  $H_{ij}$  as

$$H_{ij} = \epsilon_i^{\text{HO}} \delta_{ij} + \langle\psi_i^{\text{HO}}| V_n^{\text{DW}} |\psi_j^{\text{HO}}\rangle \quad (3.56)$$

by using the solution to Schrödinger's equation for the harmonic oscillator system.

We are now in a position to build a basis for the double-well system by reusing all the results and expressions concerning the single-well system. The only difference is the extra integral over  $V_n^{\text{DW}}$  where  $n$  would be larger than 2 (as is the case with the harmonic oscillator potential).

For clarity let us also write out the expression for the resulting Hartree-Fock basis to be used with the Variational Monte-Carlo method.

$$\psi_p^{\text{HF}} = \sum_{kl} C_{pk}^{\text{HF}} C_{kl} \psi_l^{\text{HO}} \quad (3.57)$$

The procedure of diagonalizing  $H_{ij}$  also gives an additional set of energies we can use. The full form of the integral-elements involved in Hartree-Fock is thus

$$\begin{aligned} \langle \psi_p^{\text{DW}} | \psi_q^{\text{DW}} \rangle &= \delta_{pq} \epsilon_p^{\text{DW}} \delta_{pq} \\ \langle \psi_p^{\text{DW}} | h^{\text{DW}} | \psi_q^{\text{DW}} \rangle &= \epsilon_p^{\text{DW}} \delta_{pq} \\ \langle \psi_p^{\text{DW}} \psi_q^{\text{DW}} | \frac{1}{r_{12}} | \psi_r^{\text{DW}} \psi_s^{\text{DW}} \rangle &= \sum_{ijkl} C_{tp} C_{uq} C_{vr} C_{ws} \langle \psi_t^{\text{HO}} \psi_u^{\text{HO}} | \frac{1}{r_{12}} | \psi_v^{\text{HO}} \psi_w^{\text{HO}} \rangle \end{aligned} \quad (3.58)$$

Where the two-body elements over the harmonic oscillator functions can be calculated by expansion in s-type Gaussian constituents and then using equation 3.48.

With this eigenvalue problem in mind, one might ask why go through the trouble? The reason lies in the form of the double-well potential. Since it is a simple shift of the single-well(harmonic oscillator) it is reasonable to assume that the energies(the eigenvalues  $\epsilon^{\text{DW}}$ ) are only shifted slightly off from the single-well energies. It is then also reasonable to believe that a basis set expansion in the single-well functions(harmonic oscillator functions) give a nice basis for building the double-well basis.

### 3.4.4 Choosing the Basis Functions

In order to actually solve the eigenvalue equation we use Python and the NumPy package, however we still need to choose the  $\psi^{\text{HO}}$ 's first. This will be experimented with and we will choose enough to reach to *Hartree-Fock limit*. The choice will also follow the Harmonicoscillator levels in terms of degeneracy(see figure 5.3b and figure 5.3a). This means for instance that if we choose to only use 1 spacial function we only need the ground-state function, but there is no reason to believe that the electron-configuration would prefer any two(or 3 in 3D) of the functions in the second level over one another. This means that we choose the basisfunctions according to the *magic numbers* of the Harmonicoscillator system basis.

### 3.4.4 Degeneracy

When we tackled the single-well problem the energy-levels were degenerate and followed the magic numbers. For the double-well only the degeneracy due to spin is present. This means that

we can(still with two-spin fermions) run the simulations with  $N = 2, 4, 6, \dots$  instead of the original  $N = 2, 6, 12, 20, \dots$  in two dimensions and  $N = 2, 8, 20, 30, \dots$  in three.

### 3.5 Summary

This chapter tackled the one- and two-body integrals over s-type Gaussian functions in two dimensions by using the results and approach of Trygve Helgaker. We will here rewrite the expressions found and write out the full expression for integrals over harmonic oscillator functions.

Firstly the integrals over Hermite-Gaussians (monomials multiplied by exponential). The Hermite-Gaussian was expressed as

$$g_n(\boldsymbol{\alpha}; \mathbf{r}, \mathbf{A}) = \prod_d \left( \frac{\partial}{\partial A_d} \right)^{n_d} e^{-\alpha_d (x_d - A_d)^2} \quad (3.59)$$

An expansion of these in terms of Hermite-polynomials was then made to arrive at an overlap distribution, with the Gaussian product rule for the product of two Hermite-Gaussians, with a recursive relation for the expansion coefficients

$$\begin{aligned} \Omega_{ij}(\alpha, \beta, \mathbf{r}, \mathbf{A}, \mathbf{B}) &= \sum_{t=0}^{i+j} E_t^{ij} g_t(\alpha, \beta, \mathbf{r}, \mathbf{P}) \\ E_t^{i+1,j} &= \frac{1}{2(\alpha + \beta)} E_{t-1}^{ij} - \frac{\beta}{\alpha + \beta} (A_x - B_x) E_t^{ij} + (t+1) E_{t+1}^{ij} \\ E_t^{i,j+1} &= \frac{1}{2(\alpha + \beta)} E_{t-1}^{ij} - \frac{\alpha}{\alpha + \beta} (A_x - B_x) E_t^{ij} + (t+1) E_{t+1}^{ij} \\ E_0^{00} &= K_{AB} \end{aligned} \quad (3.60)$$

The overlap integral was then found to be

$$\langle g_i(\boldsymbol{\alpha}; \mathbf{r}, \mathbf{A}) | g_j(\boldsymbol{\beta}; \mathbf{r}, \mathbf{B}) \rangle = \sum_p^{i+j} E_p^{ij} \left( \frac{((-1)^p - 1) \Gamma\left(\frac{p+1}{2}\right)}{2(\alpha_p + \beta_p)^{\frac{p+1}{2}}} \right)^d \quad (3.61)$$

The integral over a potential  $x_d^k$  was found with the binomial expansion to be

$$\begin{aligned} \langle g_i(\boldsymbol{\alpha}; \mathbf{r}, \mathbf{A}) | x_d^k | g_j(\boldsymbol{\beta}; \mathbf{r}, \mathbf{B}) \rangle &= \sum_{p=\text{even}}^{i+j} E_p^{i+j} \left( \frac{\Gamma\left(\frac{p+1}{2}\right)}{2(\alpha_p + \beta_p)^{\frac{p+1}{2}}} \right)^{D-1} \times \\ &\quad \sum_{\substack{l=0 \\ \text{even}}}^k \binom{k}{l} \frac{P_d^{k-l}}{2(\alpha_p + \beta_p)^{\frac{l}{2}}} \Gamma\left(\frac{l+1}{2}\right) \end{aligned} \quad (3.62)$$

and the integral with the Laplacian was

$$\begin{aligned} \langle g_i(\boldsymbol{\alpha}; \mathbf{r}, \mathbf{A}) | \nabla^2 | g_j(\boldsymbol{\beta}; \mathbf{r}, \mathbf{B}) \rangle &= \\ &\quad \sum_d \prod_{d' \neq d} \langle g_{i_{d'}}(\alpha_{d'}; x_{d'}, A_{d'}) | \sigma_{d'}(S_d(\boldsymbol{\beta}; x_d - B_d)) | g_{j_{d'}}(\beta_{d'}; x_{d'}, B_{d'}) \rangle \end{aligned} \quad (3.63)$$

with

$$S_d(\alpha; x_d - A_d) \equiv (4\alpha^2(x_d - A_d)^{i_d+2} - 2\alpha(2i_d + 1)(x_d - A_d)^{i_d} + i_d(i_d - 1)(x_d - A_d)^{i_d-2})$$

$$\sigma_d(S_d) \equiv \begin{cases} 1, & d' \neq d \\ S_d, & d' = d \end{cases} \quad (3.64)$$

Finally the integral over the Coulomb interactions was calculated using a recursive relation for the one-dimensional integral it was defined by. The expressions are

$$\left\langle g_{iA}^a g_{jB}^\beta \left| \frac{1}{r_{12}} \right| g_{kC}^\delta g_{lD}^\gamma \right\rangle = \frac{a}{\sqrt{(\alpha + \gamma + \beta + \delta)}} \sum_{pq}^{i+k, j+l} E_p^{ik} E_q^{jl} (-1)^q \xi_{p+q} \left( \frac{(\alpha + \gamma)(\beta + \delta)}{\alpha + \gamma + \beta + \delta}, \mathbf{R}_{s_1 s_2} \right) \quad (3.65)$$

with

$$a \equiv \begin{cases} \frac{\pi^{\frac{3}{2}}}{\sqrt{(\alpha + \gamma)(\beta + \delta)}}, & 2D \\ \frac{\pi^{\frac{5}{2}}}{(\alpha + \gamma)(\beta + \delta)}, & 3D \end{cases} \quad (3.66)$$

And the recursive relation in two dimensions(left) and three dimensions (right)

$$\begin{aligned} \xi_{t+1,u}^n &= t \xi_{t-1,u}^{n+1} + X_{AB} \xi_{t,u}^{n+1} & \xi_{t+1,u,v}^n &= t \xi_{t-1,u,v}^{n+1} + X_{AB} \xi_{t,u,v}^{n+1} \\ \xi_{t,u+1}^n &= u \xi_{t,u-1}^{n+1} + Y_{AB} \xi_{t,u}^{n+1} & \xi_{t,u+1,v}^n &= u \xi_{t,u-1,v}^{n+1} + Y_{AB} \xi_{t,u,v}^{n+1} \\ \xi_{t,u,v+1}^n &= u \xi_{t,u,v-1}^{n+1} + Y_{AB} \xi_{t,u,v}^{n+1} & \xi_{t,u,v+1}^n &= u \xi_{t,u,v-1}^{n+1} + Y_{AB} \xi_{t,u,v}^{n+1} \\ \xi_{00}^n &= \left( \frac{-2\alpha\beta}{\alpha + \beta} \right)^n \zeta_n \left( \frac{\alpha\beta}{\alpha + \beta} R_{AB}^2 \right) & \xi_{000}^n &= (-2\alpha\beta)^n \zeta_n \left( \frac{\alpha\beta}{\alpha + \beta} R_{AB}^2 \right) \\ \zeta_n(x) &= \int_{-1}^1 \frac{u^{2n}}{\sqrt{1-u^2}} e^{-u^2 x} du & \zeta_n(x) &= \int_{-1}^1 u^{2n} e^{-u^2 x} du \end{aligned} \quad (3.67)$$

We also give a reminder again that these expressions are only valid for *isotropic* Gaussian functions, Gaussians whose scaling factor(i.e  $\alpha$ ) is the same in all dimensions. For the non-isotropic case the see [7].

And as promised, here are the full expressions for the integral elements with harmonic oscillator functions using equation 3.65 and the orthogonality of the harmonic oscillator functions

$$\langle \psi_i^{\text{HO}} | \psi_j^{\text{HO}} \rangle = N_i \delta_{ij} \quad (3.68)$$

$$\langle \psi_i^{\text{HO}} | h^{\text{HO}} | \psi_j^{\text{HO}} \rangle = N_i \varepsilon_i^{\text{HO}} \delta_{ij} \quad (3.69)$$

$$\left\langle \psi_i^{\text{HO}} \psi_j^{\text{HO}} \left| \frac{1}{r_{12}} \right| \psi_k^{\text{HO}} \psi_l^{\text{HO}} \right\rangle = N_{ijkl} \frac{a}{\sqrt{2\omega}} \sum_{tuvw}^{ijkl} H_{tuvw}^{ijkl} \sum_{pq}^{t+v, u+w} E_p^{tv} E_q^{uw} (-1)^q \xi_{p+q} \left( \frac{\omega}{2}, \mathbf{0} \right) \quad (3.70)$$

$$a \equiv \begin{cases} \frac{\pi^{\frac{3}{2}}}{\sqrt{\omega}}, & 2\text{D} \\ \frac{\pi^{\frac{5}{2}}}{\omega}, & 3\text{D} \end{cases} \quad (3.71)$$

with the notations

$$\begin{aligned} N_{ijkl} &= X_i X_j X_k X_l \\ \sum_{tuvw}^{ijkl} &= \sum_p^t \sum_q^u \sum_r^v \sum_s^w \\ \sum_{pq}^{t+v, u+w} &= \sum_p^{t+v} \sum_q^{u+w} \\ H_{tuvw}^{ijkl} &= H_{i,t} H_{j,u} H_{k,v} H_{l,w} \\ E_p^{tv} &= E_{p,t+v} \end{aligned} \quad (3.72)$$

And using the multi-index notation for the dimensions in  $p$  and  $q$  indices. The  $H$  are the Hermite coefficients.

## 3.6 Further Work

This concludes this chapter on basis functions. We have found an expression for the integral elements involving Hermite-Gaussians and used these to express the integral over harmonic oscillator functions which in turn gave an expression for the integrals over double-well functions as they were just expanded in harmonic oscillator functions. The next chapter will present optimizations methods used in the variational method and the implementations of these integrals are presented in chapter 6.

As a note for further work the expressions found here are for isotropic gaussians only. For certain systems, like the one presented in article[7], more flexibility in the Gaussian functions can be desired, such that finding expression for the integrals of Gaussian functions with higher order monomial factors and extending the existing code to calculate those can be of desire.





## NUMERICAL OPTIMIZATION

Numerical optimizations, the one field that can be applied to virtually anything. All the big problems in the world, from cancer research to financial modeling, from finding variational energies to modeling large scale atomic systems. You can be pretty sure that any field of research one can name has some scheme which can be reformulated into a problem in which numerical optimization methods can be applied. As such, the field of numerical optimization has not been viewed more useful than now -especially with the computing power at hand and machine learning having become quite of a popular.

In the Variational Monte Carlo method in section 2.9 the essential point was to vary a set of *variational parameters* in order to reach an eigenbasis which gives the ground-state energy of the Hamiltonian in question. There are many ways one could approach this. One way could be to wildly guess random parameters and hope for the best, obviously this is a poor approach. The more sound approach would be to optimize (minimization in the VMC case) the wavefunction using methods from (as the title suggests) *numerical optimization*. The methods used in this thesis was the *Conjugate Gradient method*, a version of the *Adaptive Stochastic Gradient Descent*, the well known *BFGS* method and a more recent *Stochastic-Adaptive-BFGS* and also *Simulated Annealing*. The explaining of the approaches for numerical optimization is only made briefly. For a better mathematical explanation see the various references in the text.

### 4.1 The Optimization Problem

We will explain the general approach for minimizing a multi-variate function and set the terminology in this section.

The problem in question is the following. Given a continuously differentiable function  $f : \mathbb{R}^n \rightarrow \mathbb{R}$ , for what set of parameters  $\{x\}_{k=1}^n$  is

$$\nabla_x f = \mathbf{0} \quad (4.1)$$

fulfilled<sup>1</sup>. This means we seek a point  $\mathbf{x}_m$  in real space where the variation of the value of  $f$  is zero. In reality the condition in equation 4.1 is only approximate, that is we terminate the search for a minimum if we reached a point where the absolute value of  $f$  is within a threshold  $\epsilon$

$$|\nabla_x f| \leq \epsilon \quad (4.2)$$

One might at this point have the question, wouldn't the condition presented in equation 4.2 (and equation 4.1) be valid for a maximum as well? The answer is yes, it would. The simple fix to this is to define the *search direction*, more precisely the sign of the search direction. The next section explains this in better detail.

## 4.2 Gradient Descent

We defined the optimization problem and defined a simple condition for the extremal and mentioned a search direction in the previous section. A search direction in our context is a direction  $\mathbf{p} \in \mathbb{R}^n$  which points towards  $\mathbf{x}_m$ . To find  $\mathbf{p}$  we use the well known *second derivative test* to determine the curvature of  $f$ . This, mentioned qualitatively, means that the gradient of  $f$  at any point  $\mathbf{x}_i$  points towards an extremal and that the negative gradient (negative sign) points towards the minimum and the positive gradient points towards the maximum. This observation gives a simple rule for finding  $\mathbf{x}_m$ . Start out with blindly guessing a point  $\mathbf{x}_0$  and keep updating the parameters according to the following recursive rule

$$\mathbf{x}_n = \mathbf{x}_{n-1} - \gamma \nabla_x f \quad (4.3)$$

and terminate the search when equation 4.2 is fulfilled<sup>2</sup> [36]. Here is an algorithmic view

---

<sup>1</sup> $\nabla_x = \sum_k \mathbf{e}_k \frac{\partial}{\partial x_k}$  with  $\mathbf{e}_k \in \mathbb{R}^n$  a unit vector along direction  $k$ .

<sup>2</sup>Change the negative sign in front of the gradient if a maximum is desired.

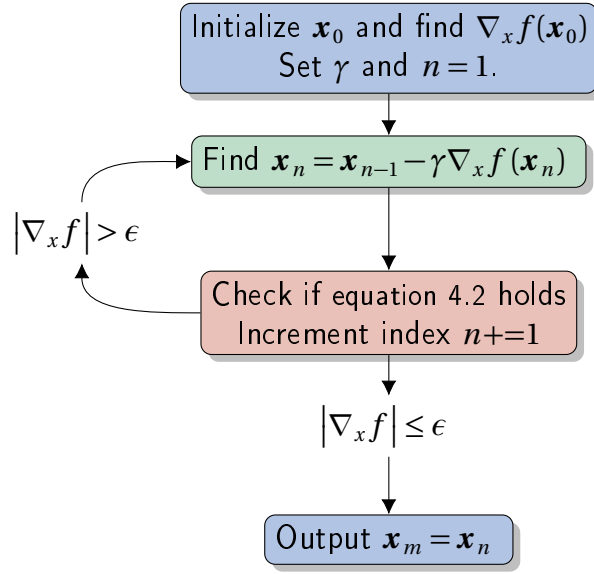


Figure 4.1: Gradient Descent algorithm.

This method of finding the minimum is known as the method of *Gradient Descent* and its power lies in its simplicity. The problem however is stability, the termination condition is firstly not optimal and the step-size  $\gamma$  is a constant which can give a lot of oscillations around minimum as the algorithm might get close to the minimum and then *over-shoot* and go past the minimum point, turn around (because the sign changes) and over-shoot again and then keep going. Many (seriously many) methods have been devised to account for these problems and others. We will confine ourselves with the methods mentioned in the introduction of this chapter.

As an illustration of the method here are a couple of figures of the method applied to two test-functions. One simple sphere-function

$$f(\mathbf{x}) = \sum_{d=1}^D x_d^2 \quad (4.4)$$

and the Rosenbrock function

$$f(\mathbf{x}) = \sum_{d=1}^{D-1} 100(x_{d+1} - x_d^2)^2 + (x_d - 1)^2. \quad (4.5)$$

Here are two figures of the functions

### Sphere Function

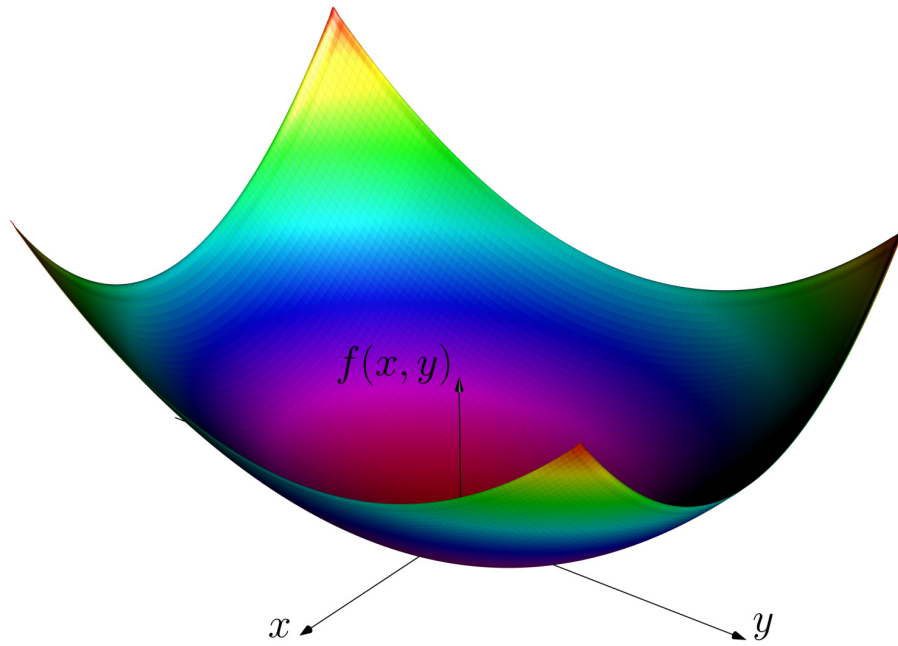


Figure 4.2: Illustration of sphere function[45] with minimum  $\mathbf{x}_m = (0, 0)$  with value  $f(\mathbf{x}_m) = 0$ .

### Rosenbrock Function

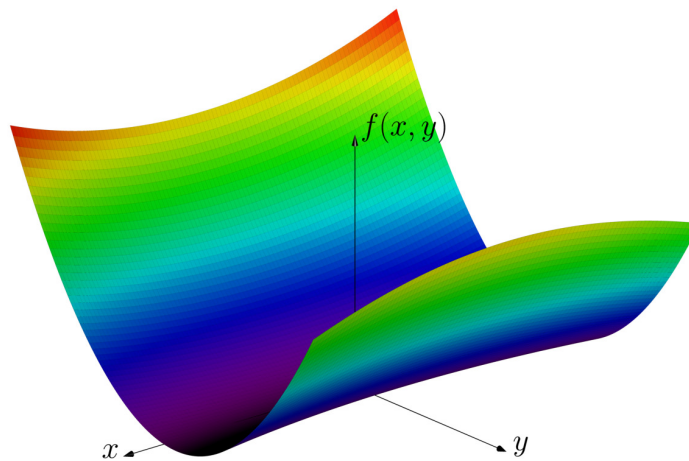


Figure 4.3: Illustration of Rosenbrock function[45] with minimum  $\mathbf{x}_m = (1, 1)$  with value  $f(\mathbf{x}_m) = 0$ .

As for the convergence we give a table with number of iterations.

Table 4.1: Table showing convergence of the gradient descent method with the spherical function.  $\mathbf{x}_0$  is the initial starting point,  $\gamma$  is the step-size,  $\mathbf{x}_m$  is the minimum after the given iterations and  $f(\mathbf{x}_m)$  is the function value at said minimum point.

| $\mathbf{x}_0$ | $\gamma$ | Iterations | $\mathbf{x}_m$                                   | $f(\mathbf{x}_m)$       |
|----------------|----------|------------|--|-------------------------|
| (5,5)          | 0.9      | 20         | (-0.072, -0.072)                                 | 0.010                   |
| (5,5)          | 0.9      | 50         | $(-8.920 \times 10^{-5}, -8.920 \times 10^{-5})$ | $1.591 \times 10^{-8}$  |
| (5,5)          | 0.9      | 100        | $(-1.273 \times 10^{-9}, -1.273 \times 10^{-9})$ | $3.242 \times 10^{-18}$ |
| (5,5)          | 0.5      | 20         | (0.0, 0.0)                                       | 0.0                     |
| (5,5)          | 0.5      | 50         | (0.0, 0.0)                                       | 0.0                     |
| (5,5)          | 0.5      | 100        | (0.0, 0.0)                                       | 0.0                     |
| (5,5)          | 0.1      | 20         | (0.072, 0.072)                                   | 0.010                   |
| (5,5)          | 0.1      | 50         | $(8.920 \times 10^{-5}, 8.920 \times 10^{-5})$   | $1.591 \times 10^{-8}$  |
| (5,5)          | 0.1      | 100        | $(1.273 \times 10^{-9}, 1.273 \times 10^{-9})$   | $3.242 \times 10^{-18}$ |

Table 4.2: Table showing convergence of the gradient descent method with the Rosenbrock function.  $\mathbf{x}_0$  is the initial starting point,  $\gamma$  is the step-size,  $\mathbf{x}_m$  is the minimum after the given iterations and  $f(\mathbf{x}_m)$  is the function value at said minimum point.

| $\mathbf{x}_0$ | $\gamma$ | Iterations | $\mathbf{x}_m$ | $f(\mathbf{x}_m)$      |
|----------------|----------|------------|----------------|------------------------|
| (0,0.5)        | 0.001    | 100        | (0.181, 0.030) | 0.034                  |
| (0,0.5)        | 0.001    | 500        | (0.512, 0.258) | 0.327                  |
| (0,0.5)        | 0.001    | 1000       | (0.675, 0.454) | 0.106                  |
| (0,0.5)        | 0.001    | 100000     | (1.000, 1.000) | 0.0                    |
| (0,0.5)        | 0.0001   | 100        | (0.027, 0.068) | 1.399                  |
| (0,0.5)        | 0.0001   | 500        | (0.105, 0.009) | 0.801                  |
| (0,0.5)        | 0.0001   | 1000       | (0.184, 0.031) | 0.666                  |
| (0,0.5)        | 0.0001   | 100000     | (0.994, 0.989) | $3.131 \times 10^{-5}$ |

From tables 4.1 and 4.2 it is apparent that with the gradient descent method the step-size is of great importance. With the spherical function one needs a sweet-spot value to reach the minimum while for the more complex Rosenbrock function the number of iterations needed is very high and with a lower step-size the minimum was actually not even reached with 100000 iterations. In conclusion, the gradient descent method is great for its simplicity, but it does not incorporate the curvature of the function when minimizing meaning the choice for the step-size and greatly determines the outcome of the minimization, and for functions where the minimum lies in a fairly flat valley, as with the Rosenbrock function, the computational cost increases since the number of iterations needed for convergence is high.

### 4.3 Adaptive Stochastic Gradient Descent

Along with the limitations of the method of gradient descent, the *Adaptive Stochastic Gradient Descent* tries to account for those, but also takes into account the variance introduced by the stochastic nature of the probability distribution. As such many variations of the method have been proven to be popular among problems in which the function to be minimized is an expectation value. The method used in this thesis is the one described in [48]. We will give a summary of the method here, for a more detailed outline and description see [48].

Like the gradient descent method the adaptive stochastic gradient descent method updates the parameters in the same manner as in equation 4.3, the difference however is that the step  $\gamma$  is changed for each iteration in accordance to the following

$$\begin{aligned}\gamma_{n+1} &= \frac{a}{t_{n+1} + A} \\ t_{n+1} &= \max(t_n + g(X_n), 0) \\ X_n &= -\nabla f_n \cdot \nabla f_{n+1} \\ g(x) &= g_{\min} + \frac{g_{\max} - g_{\min}}{1 - \frac{g_{\max}}{g_{\min}} e^{-\frac{x}{\omega}}}\end{aligned}\tag{4.6}$$

The whole idea of the method is that the form of  $g$  and the accumulative combination of gradient estimations for each step the total error would tend quickly to zero, meaning the central element (namely the gradient) in the minimization is well behaving.

The main concern with the method is the convergence, although the error in the gradient estimations tend towards zero, the step-sizes themselves will also be quite small after some iterations. For this reason we use the adaptive method with a quasi-Newton method. This means that we start with a random guess at the parameters and keep iterating with the quasi-Newton method until the norm of the gradient is below some threshold, at which the adaptive method is applied from that point and onward till convergence is reached.

### 4.4 Newtons-Method and Quasi-Newton Methods

We will here explain briefly *Newton's method* and *Quasi-Newton* methods as the ideas presented will be used in the next section.

Newton's method [28] (or Newton-Raphson method) is originally a method for finding the zeros of a function. The rule states that given a real-valued function  $f : \mathbb{R} \rightarrow \mathbb{R}$  and an initial guess  $x \in \mathbb{R}$

for the zero-point, recursively find better approximations for the zero by

$$x_{n+1} = x_n - \frac{f(x_n)}{f'(x_n)} \quad (4.7)$$

This method would then within a number iterations find the zero that is closest to  $x_0$ .

For the optimization problem the condition for a point to be an extremal is equation 4.1 meaning, again, that one needs to find the zero of the derivative. Newton's method in this case would be

$$x_{n+1} = x_n - \frac{f'(x_n)}{f''(x_n)}, \quad n \geq 0 \quad (4.8)$$

Of course in the real world one might work with multi-variate function, not to worry as Newton's method for optimization problems in the multi-variate case with  $f : \mathbb{R}^n \rightarrow \mathbb{R}$  (still real-valued) is

$$\mathbf{x}_{n+1} = \mathbf{x}_n - [\mathbf{H}f(\mathbf{x}_n)]^{-1} \dot{\nabla} f(\mathbf{x}_n), \quad n \geq 0 \quad (4.9)$$

where  $\mathbf{H}$  is the Hessian matrix. One might also introduce a step-length multiplied to the Hessian part in order to induce conditions[36] which ensure some stability of the method.

Newton's method, in most cases, converges faster(less iterations) towards the minimum than gradient descent making it favorable, however the full Hessian has to be known. This matrix(or its inverse) is in many cases too expensive to compute or difficult to express in closed-form. In these cases the class of methods known as Quasi-Newton methods can be utilized.

Quasi-Newton methods give an estimate of the inverse Hessian by using the first derivatives. Introduce the Taylor approximation of  $f$  around an iteration point  $\mathbf{x}_n$

$$f(\mathbf{x}_k + \mathbf{s}) \approx f(\mathbf{x}_k) + (\nabla f(\mathbf{x}_k))^T \mathbf{s} + \frac{1}{2} \mathbf{s}^T \mathbf{H} \mathbf{s} \quad (4.10)$$

differentiate with respect to the change  $\mathbf{s}$

$$\nabla_s f(\mathbf{x}_k + \mathbf{s}) \approx \nabla f(\mathbf{x}_k) + \mathbf{H} \mathbf{s} \quad (4.11)$$

and introduce the condition in equation 4.1 and set this gradient to zero to find the change  $\mathbf{s}$

$$\mathbf{s} = -\mathbf{H}^{-1} \nabla f(\mathbf{x}_k) \quad (4.12)$$

Another way to determine this particular form for  $\mathbf{s}$  is to say that the approximation to the Hessian must satisfy the *secant equation* which is equation 4.11. The updating rule for  $\mathbf{x}_n$  is then given by

$$\mathbf{x}_{n+1} = \mathbf{x}_n - \gamma_k \mathbf{H}_n^{-1} \nabla f(\mathbf{x}_n) \quad (4.13)$$

where  $\gamma_k$  is again introduced to give some stability conditions. The important part of this equation is the index on the inverse Hessian. This is essentially just a relabeling at the change  $\mathbf{s}$  is

technically applied for each iterate  $\mathbf{x}_n$ . Note also that  $\mathbf{s}$  takes the role of the search direction in this case. The algorithm is then to make an initial guess on the Hessian(usually just the identity matrix) and then use a type of updating formula that finds a new approximation for the Hessian at each step  $n$ . There are a number of these updating formulas, just to mention some we have DFP, SR1, McCormick, Broyden, BFGS and more. The one we will mention in more detail is the BFGS method, but a main formula that shows up in all of the updating methods is the *Sherman-Morrison formula* for the inverse. This basically means that the need for calculation of the inverse matrix is completely removed.

With the mentioned expression we can devise an algorithm similar to Newton's method for finding the minimum  $\mathbf{x}_m$ . Starting with an initial guess for the inverse Hessian  $\mathbf{H}_0^{-1}$  and minimum  $\mathbf{x}_0$  with the condition that  $\mathbf{H}_0^{-1}$  is positive-definite (identity matrix is a nice start if nothing else is known) proceed with

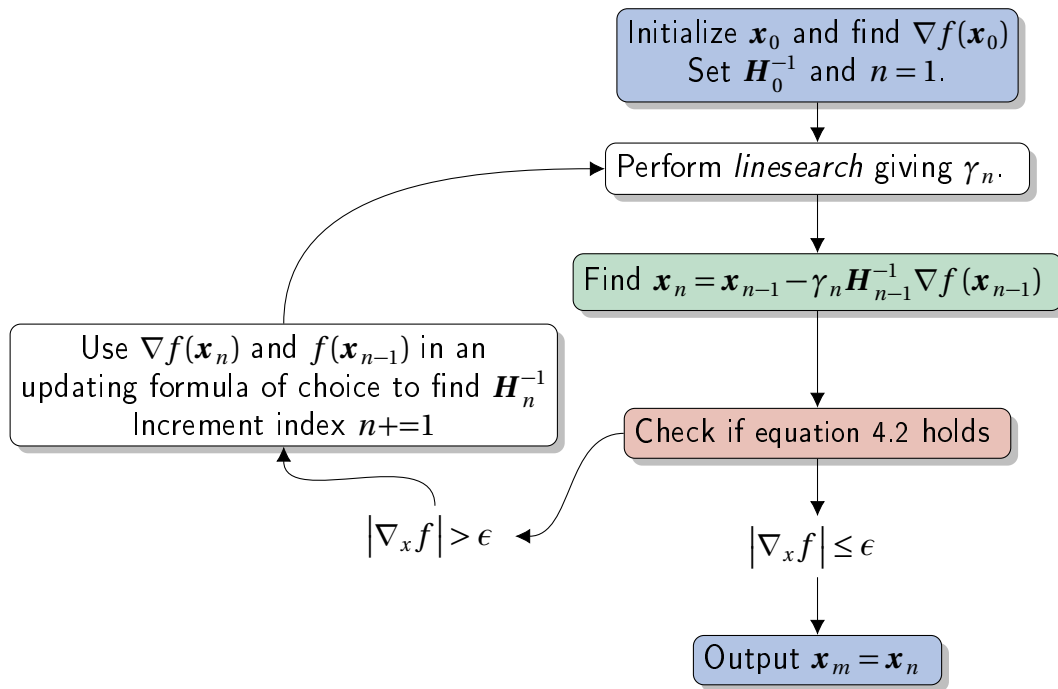


Figure 4.4: Quasi-Newton algorithm.

To illustrate the power of the method we again apply it to the sphere function and the Rosenbrock function using the BFGS scheme as the updating method and the Moré-Thuente linesearch method to find the step-size. The table of convergence is as follows



Table 4.3: Table showing convergence of a Quasi-Newton method with BFGS method with the spherical function.  $\mathbf{x}_0$  is the initial starting point,  $\mathbf{x}_m$  is the minimum after the given iterations and  $f(\mathbf{x}_m)$  is the function value at said minimum point.

| $\mathbf{x}_0$ | Iterations | $\mathbf{x}_m$   | $f(\mathbf{x}_m)$ |
|----------------|------------|------------------|-------------------|
| (1, 1)         | 1          | (−0.071, −0.071) | 1.000             |
| (−1, 2)        | 1          | (0.447, −0.894)  | 1.000             |
| (1, 1)         | 2          | (0.000, 0.000)   | 0.000             |
| (−1, 2)        | 2          | (0.000, 0.000)   | 0.000             |
| (10, 10)       | 1          | (−0.071, −0.071) | 1.000             |
| (10, 10)       | 2          | (0.000, 0.000)   | 0.000             |
| (100, 100)     | 1          | (−0.071, −0.071) | 1.000             |
| (100, 100)     | 2          | (0.000, 0.000)   | 0.000             |

Table 4.4: Table showing convergence of a Quasi-Newton method with BFGS method with the Rosenbrock function.  $\mathbf{x}_0$  is the initial starting point,  $\mathbf{x}_m$  is the minimum after the given iterations and  $f(\mathbf{x}_m)$  is the function value at said minimum point.

| $\mathbf{x}_0$ | Iterations | $\mathbf{x}_m$  | $f(\mathbf{x}_m)$ |
|----------------|------------|-----------------|-------------------|
| (−0.5, 2.0)    | 1          | (−0.706, 0.708) | 7.280             |
| (−0.5, 2.0)    | 2          | (−0.780, 0.649) | 3.342             |
| (−0.5, 2.0)    | 10         | (0.238, 0.051)  | 0.584             |
| (−0.5, 2.0)    | 30         | (1.000, 1.000)  | 0.000             |
| (5.5, −10.0)   | 1          | (−0.996, 0.091) | 85.214            |
| (5.5, −10.0)   | 2          | (−0.908, 1.087) | 10.549            |
| (5.5, −10.0)   | 10         | (0.027, 0.012)  | 0.9613            |
| (5.5, −10.0)   | 30         | (1.000, 1.000)  | 0.000             |

Comparing tables 4.3 and 4.4 with tables 4.1 and 4.3 we can see that the BFGS scheme outperforms the gradient descent method by a stupendous and almost comical amount with the number of iterations in mind. However one still has to keep in mind that each iterations of the BFGS method is far more computationally extensive meaning the gradient descent method can be more favorable in the case where the function to be minimized is expensive to compute.

For our case, the latter sentiment is true. The expectation value to the energy still has a large complexity, however with the optimizations mentioned in sections 5.3.3 and 5.3.3 the time it takes to calculate the expectation value is not too large and the BFGS scheme can still be used.

## 4.5 BFGS Method

In the previous section(also mentioned in figure 4.4) we gave an outline for Newton's method and the class known as Quasi-Newton methods. The latter used an approximation for the inverse of

the Hessian matrix, which was updated at each step in the algorithm. For the sake of brevity only conditions employed to arrive at the expression for the updating formula and the formula itself is given here, for more see [4, 13, 14, 36, 44]. The conditions enforced is

- Secant condition:  $\mathbf{H}_{n+1}\mathbf{s}_n = \nabla f(\mathbf{x}_{n+1}) - \nabla f(\mathbf{x}_n)$
- Strong curvature:  $\mathbf{s}_k^T \cdot (f(\mathbf{x}_{n+1}) - \nabla f(\mathbf{x}_n)) > 0$

and the resulting formula states with  $\mathbf{y}_k = f(\mathbf{x}_{n+1}) - \nabla f(\mathbf{x}_n)$

$$\mathbf{H}_{n+1} = \mathbf{H}_n + \frac{\mathbf{y}_n \mathbf{y}_n^T}{\mathbf{y}_n^T \mathbf{s}_n} - \frac{\mathbf{H}_n \mathbf{s}_n \mathbf{s}_n^T \mathbf{H}_n}{\mathbf{s}_n^T \mathbf{H}_n \mathbf{s}_n} \quad (4.14)$$

With the Sherman-Morrison formula[42] the inverse is updated with

$$\mathbf{H}_{n+1}^{-1} = \mathbf{H}_n^{-1} + \frac{(\mathbf{s}_n^T \mathbf{y}_n + \mathbf{y}_n^T \mathbf{H}_n^{-1} \mathbf{y}_n)(\mathbf{s}_n \mathbf{s}_n^T)}{(\mathbf{s}_n^T \mathbf{y}_n)^2} - \frac{\mathbf{H}_n^{-1} \mathbf{y}_n \mathbf{s}_n^T + \mathbf{s}_n \mathbf{y}_n^T \mathbf{H}_n^{-1}}{\mathbf{s}_n^T \mathbf{y}_n} \quad (4.15)$$

## 4.6 Linesearch methods

In the optimization methods described in section 4.4 there was one important part neglected, namely how to find the step-length  $\gamma_n$  introduced in the updating formula. As it is, one can choose it in any manner desired, however a class of one-dimensional minimization methods known as *linesearch methods* are often used to get an (usually rough) estimate for the step length at each iteration in the optimization. These methods all have some conditions for stability and convergence as an innate property, meaning the validity of the step length is better<sup>3</sup>. Some popular linesearch methods are backtracking linesearch, Hager-Zhang method, Strong Wolfe conditions and the More-Thuente linesearch method. The one used here is the latter. For an exact derivation and explanation of linesearch methods in general see [36]. See also the fantastic article by Jorge J. Moré and David J. Thuente[33].

The basic idea of linesearch methods is to solve a one-dimensional problem of minimizing

$$\phi(\alpha) = f(\alpha \mathbf{p}_k + \mathbf{x}_k) \quad (4.16)$$

with  $f : \mathbb{R}^n \rightarrow \mathbb{R}$  and  $\mathbf{p}_k$  is a search direction as described with the quasi-Newton methods and  $\mathbf{x}_k$  is the current iterate(point) in the minimization. Notice also that

$$\frac{\partial \phi}{\partial \alpha} = \mathbf{p}_k \cdot \nabla f(\alpha \mathbf{p}_k + \mathbf{x}_k) \quad (4.17)$$

by the chain-rule and the gradient on the right hand side is over the parameters  $\mathbf{x}_k$ . One usually perform this linesearch loosely since the search direction is not necessarily directly pointing

---

<sup>3</sup>It's actually present...

towards the minimum, meaning we only search for a step length that gives a *sufficient decrease* in the function value  $f$ . The basic procedure is then to use one of these linesearch methods to find  $\gamma_n$  at each iteration in the minimization and then use the step-length outputted by the linesearch algorithm to update the parameters.

## 4.7 Stochastic-Adaptive-BFGS

In section 4.5 we mentioned the popular BFGS method for updating the Hessian matrix and its inverse. A more recent method which uses that method with the stochastic nature of a functional expectation value is a method called SABFGS[15] described by Zhou C., Gao W. and Goldfarb D. This method uses the BFGS update for the Hessian, but uses an adaptive step instead of the deterministic linesearch for the step-size.

There one problem however, the method itself is only valid for *self-concordant* functions. The energy-functional is by-far not within this criteria. This problem can be accounted for by using the Wolfe-conditions. That is to check that the step-size satisfies the Wolfe-conditions at each iteration before actually making an update. The algorithm presented takes this into account aswell.

---

### Algorithm 1 SA-BFGS

---

```

Input:  $\mathbf{x}_0, \mathbf{H}_0, \mathbf{G}_0, \beta < 1$ 
for  $k = 0$  to  $M_{\max}$  do
     $\mathbf{g}_k = \nabla F_k(\mathbf{x}_k)$                                  $\triangleright$  Gradient in current step
     $\mathbf{d}_k = -\mathbf{H}_k \mathbf{g}_k$                                  $\triangleright$  Search direction
     $\delta_k = \sqrt{\mathbf{d}_k^T \mathbf{G}_k(\mathbf{x}_k) \mathbf{d}_k}$ 
     $\alpha_k = \frac{\mathbf{g}_k^T \mathbf{H}_k \mathbf{g}_k}{\delta_k^2}$ 
     $t_k = \frac{\alpha_k}{1 + \alpha_k \delta_k}$                                  $\triangleright$  Step size
     $\mathbf{g}_{k+1} = \nabla F_k(\mathbf{x}_k + t_k \mathbf{d}_k)$                  $\triangleright$  Propose new set of parameters
    if  $\mathbf{g}_{k+1}^T \mathbf{d}_k < \beta \mathbf{g}_k^T \mathbf{d}_k$  then             $\triangleright$  Wolfe-Conditions
        Set  $\mathbf{d}_k = -\mathbf{g}_k$ 
        Recompute  $\delta_k, \alpha_k$  and  $t_k$ 
        Set  $\mathbf{H}_{k+1} = \mathbf{H}_k$  and  $\mathbf{G}_{k+1} = \mathbf{G}_k$ 
    else
        Set  $\mathbf{H}_{k+1}$  with BFGS inverse update             $\triangleright$  equation 4.15
        Set  $\mathbf{G}_{k+1}$  with BFGS update                     $\triangleright$  equation 4.14
    end if
     $\mathbf{x}_{k+1} = \mathbf{x}_k + t_k \mathbf{d}_k$                          $\triangleright$  Update parameters
end for

```

---

## 4.8 Simulated Annealing

A huge problem with the mentioned methods is the fact that they only converge towards a *local minimum* which is not necessarily the *global minimum* which of desire. Many methods already exists to account for this, the one used in this thesis and to be described in this section is the method known as *simulated annealing*. Simulated annealing follows a simple algorithm, namely

---

### Algorithm 2 Simulated Annealing

---

```

Initialize a solution  $s = s_0$ . ▷ I.e a set of parameters  $\{\alpha\}_{k=1}^N$ 
for  $j = 1$  to  $M_{\max}$  do
    Set temperature  $T$  with specific function for  $\frac{j}{M_{\max}}$ 
    Pick a new state  $s_{\text{new}}$  within some neighbour of  $s$ 
    if  $P(f(s), f(s_{\text{new}}), T) \geq \xi$  then ▷ Metropolis-Test.
         $s = s_{\text{new}}$ 
    end if
end for

```

---

The idea is to start with searching a large part of the solution space, since a high temperature increases the search-range, and hope that as  $j$  reaches  $M_{\max}$  the probability function  $P$  is such that the solution is trapped within the down-hill of the global minimum.

The specific form of  $P$ ,  $T$  and how to choose a neighbour is specific from problem to problem however an effective and simple way to define these is by using the Metropolis-algorithm with

$$P = \exp\left(-\frac{f(s_{\text{new}}) - f(s)}{T}\right), \quad (4.18)$$

define the temperature as

$$T_j = \frac{T_{\max}}{j}, \quad (4.19)$$

with  $T_{\max}$  being the initial temperature, and choose new neighbours within some min/max range from the current  $s$ [25]. After the annealing is done a Quasi-Newton method is used and then the adaptive method is used to converge to the minimum. In order to test this scheme we apply it to more complex functions with many local minima. Two such functions are the *Ackley function*[45] defined as

$$f(\mathbf{x}) = -a \exp\left(-b \sqrt{\frac{1}{D} \sum_{d=1}^D x_d^2}\right) - \exp\left(-\frac{1}{D} \sum_{d=1}^D \cos(c x_d)\right) + a + \exp(1) \quad (4.20)$$

and the *Rastrigin function*[45]

$$f(\mathbf{x}) = 10D + \sum_{d=1}^D (x_d^2 - 10 \cos(2\pi x_d)) \quad (4.21)$$

with  $D$  being the number of parameters and  $a$ ,  $b$  and  $c$  being parameters to be tweaked. Figures are shown below

### Ackley Function

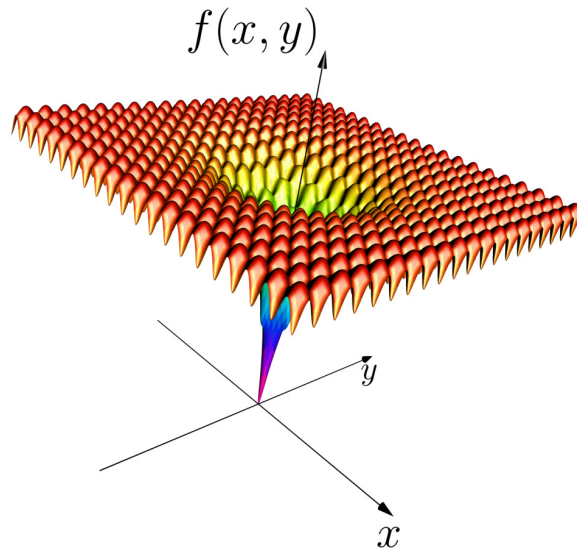


Figure 4.5: Illustration of Ackley function[45] with global minimum  $\mathbf{x}_m = (0, 0)$  of value  $f(\mathbf{x}_m) = 0$ .

### Rastrigin Function

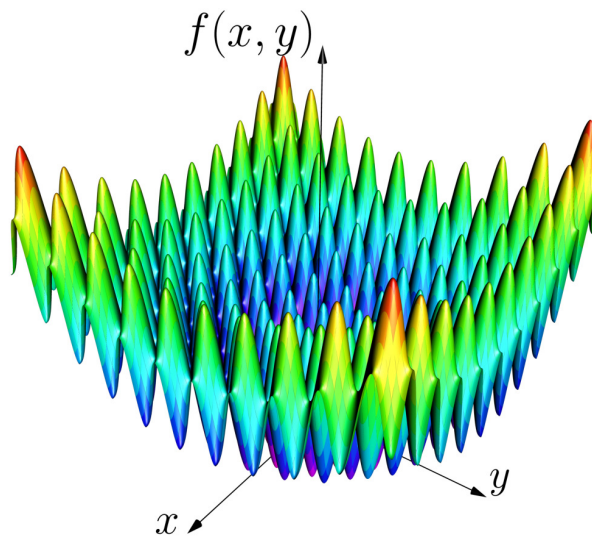


Figure 4.6: Illustration of Rastrigin function[45] with global minimum  $\mathbf{x}_m = (0, 0)$  of value  $f(\mathbf{x}_m) = 0$ .

As for convergence, we again employ the same procedure as with the spherical and Rosenbrock functions as previously, but with the Ackelyn and Rastrigin functions and present the tables here.

Table 4.5: Table showing convergence of the simulated annealing method with the Ackelyn function.  $\mathbf{x}_0$  is the initial starting point,  $T_{\max}$  is the initial temperature,  $\mathbf{x}_m$  is the minimum after the given iterations and  $f(\mathbf{x}_m)$  is the function value at said minimum point. The neighbouring function used is a simple gaussian applied to all parameters with mean being the current value of the parameter and variance 1.0.

| $\mathbf{x}_0$ | $T_{\max}$ | Iterations | $\mathbf{x}_m$   | $f(\mathbf{x}_m)$ |
|----------------|------------|------------|------------------|-------------------|
| (-10.0, 0.40)  | 100.0      | $10^2$     | (0.130, 0.096)   | 1.046             |
| (-10.0, 0.40)  | 100.0      | $10^3$     | (0.007, -0.026)  | 0.097             |
| (-10.0, 0.40)  | 100.0      | $10^4$     | (0.002, -0.004)  | 0.011             |
| (-10.0, 0.40)  | 100.0      | $10^5$     | (-0.003, -0.003) | 0.013             |
| (-0.01, 0.01)  | 100.0      | $10^2$     | (-0.101, 0.036)  | 0.584             |
| (-0.01, 0.01)  | 100.0      | $10^3$     | (-0.012, -0.006) | 0.044             |
| (-0.01, 0.01)  | 100.0      | $10^4$     | (-0.004, 0.001)  | 0.013             |
| (-0.01, 0.01)  | 100.0      | $10^5$     | (-0.001, -0.001) | 0.003             |
| (-10.0, 0.40)  | 50.0       | $10^2$     | (0.012, -0.122)  | 0.702             |
| (-10.0, 0.40)  | 50.0       | $10^3$     | (-0.021, 0.023)  | 0.113             |
| (-10.0, 0.40)  | 50.0       | $10^4$     | (0.008, -0.016)  | 0.061             |
| (-10.0, 0.40)  | 50.0       | $10^5$     | (0.002, -0.003)  | 0.009             |
| (-0.01, 0.01)  | 50.0       | $10^2$     | (0.141, 0.059)   | 0.959             |
| (-0.01, 0.01)  | 50.0       | $10^3$     | (-0.007, -0.041) | 0.162             |
| (-0.01, 0.01)  | 50.0       | $10^4$     | (-0.013, 0.003)  | 0.043             |
| (-0.01, 0.01)  | 50.0       | $10^5$     | (0.001, 0.002)   | 0.005             |

Table 4.6: Table showing convergence of the simulated annealing method with the Rastrigin function.  $\mathbf{x}_0$  is the initial starting point,  $T_{\max}$  is the initial temperature,  $\mathbf{x}_m$  is the minimum after the given iterations and  $f(\mathbf{x}_m)$  is the function value at said minimum point. The neighbouring function used is a simple gaussian applied to all parameters with mean being the current value of the parameter and variance 1.0.

| $\mathbf{x}_0$ | $T_{\max}$ | Iterations | $\mathbf{x}_m$   | $f(\mathbf{x}_m)$ |
|----------------|------------|------------|------------------|-------------------|
| (-5.0, 1.0)    | 100.0      | $10^2$     | (-0.988, 0.967)  | 2.152             |
| (-5.0, 1.0)    | 100.0      | $10^3$     | (0.045, -0.038)  | 0.684             |
| (-5.0, 1.0)    | 100.0      | $10^4$     | (0.007, -0.002)  | 0.009             |
| (-5.0, 1.0)    | 100.0      | $10^5$     | (0.001, -0.002)  | 0.001             |
| (-0.01, 0.001) | 100.0      | $10^2$     | (-0.873, 0.016)  | 3.844             |
| (-0.01, 0.001) | 100.0      | $10^3$     | (-0.011, -0.010) | 0.043             |
| (-0.01, 0.001) | 100.0      | $10^4$     | (0.001, 0.010)   | 0.021             |
| (-0.01, 0.001) | 100.0      | $10^5$     | (-0.002, -0.002) | 0.001             |
| (-5.0, 1.0)    | 50.0       | $10^2$     | (-0.936, -0.016) | 1.731             |
| (-5.0, 1.0)    | 50.0       | $10^3$     | (0.063, 0.020)   | 0.864             |
| (-5.0, 1.0)    | 50.0       | $10^4$     | (0.014, -0.004)  | 0.045             |
| (-5.0, 1.0)    | 50.0       | $10^5$     | (0.002, 0.000)   | 0.001             |
| (-0.01, 0.001) | 50.0       | $10^2$     | (0.977, -0.024)  | 1.168             |
| (-0.01, 0.001) | 50.0       | $10^3$     | (-0.012, -0.017) | 0.085             |
| (-0.01, 0.001) | 50.0       | $10^4$     | (0.002, 0.004)   | 0.004             |
| (-0.01, 0.001) | 50.0       | $10^5$     | (-0.001, -0.003) | 0.001             |

We can see from tables 4.5 and 4.6 that the simulated annealing method does get close to the actual minimum, however a great number of iterations is needed and even as we reach  $10^5$  iterations the method still doesn't converge towards the minimum. This seems quite dissappointing, but one has to remember that the method is to be used as a way to reach an area were deterministic methods such as gradient descent method or the BFGS scheme is guaranteed to converge towards the minimum. As long as we control the temperature properly such a point can be found with simulated annealing.





## IMPLEMENTATION

With almost every expression given in chapter 3 being some kind of sum it is not hard to imagine that solving them by hand would be quite the challenge and most like<sup>1</sup> impossible, but with the modern computer at our disposal they can be tackled numerically. However in order to get the data from the numerical simulations the actual implementation, the raw code, has to be made, tested, verified and run.

This chapter will explain the code used in the thesis in detail. The code itself is given in » REF GITHUB REPO «. General information of the usage of packages are given in appendix » REF APPENDIX « while the structure and workflow of the code is given here. We will first present a workflow-chart of the two main code-bases used, namely the Hartree-Fock implementation and the Variational Monte-Carlo implementation.

---

<sup>1</sup>Read definitely.

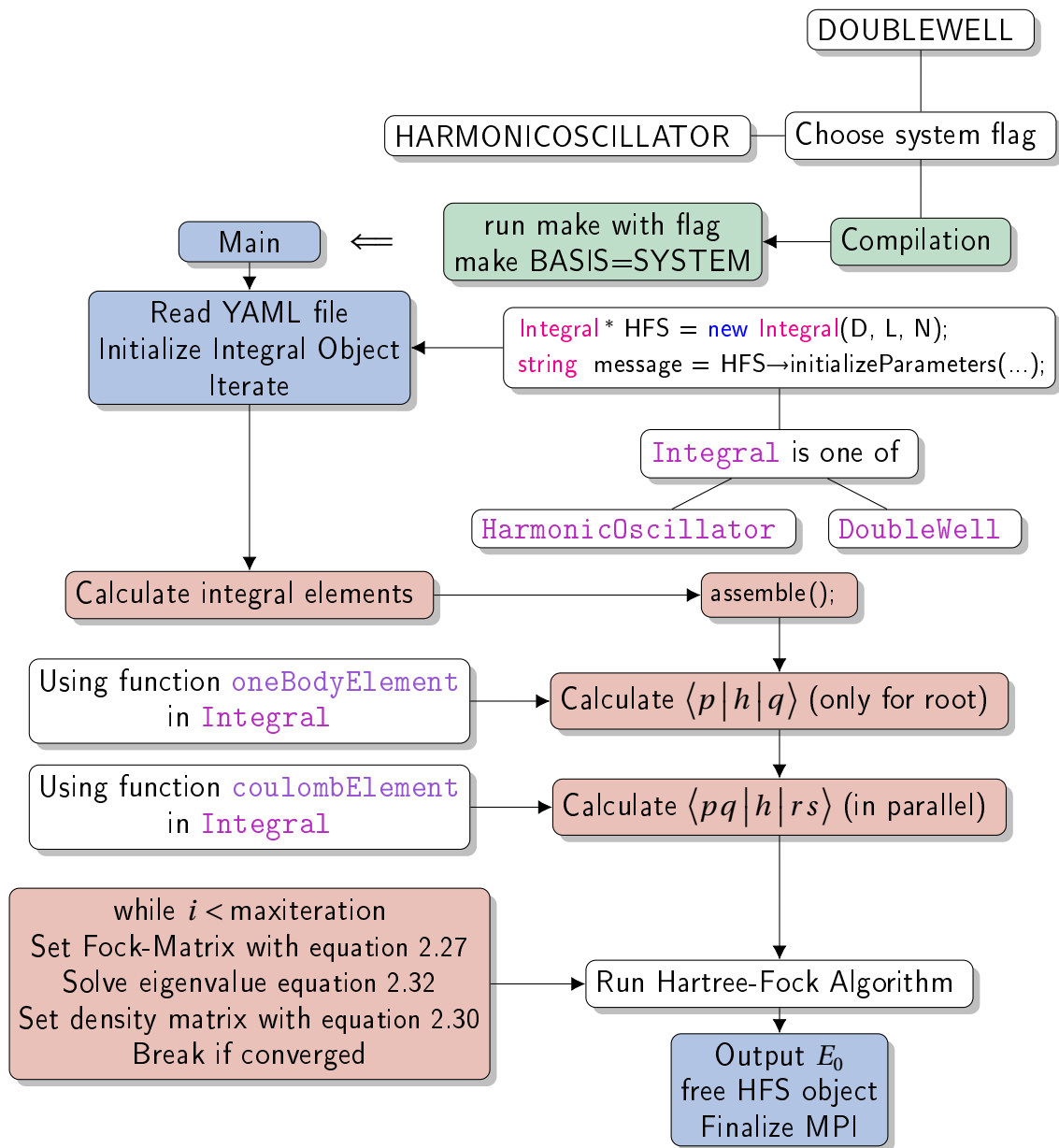


Figure 5.1: Flow chart of Hartree-Fock implementation.

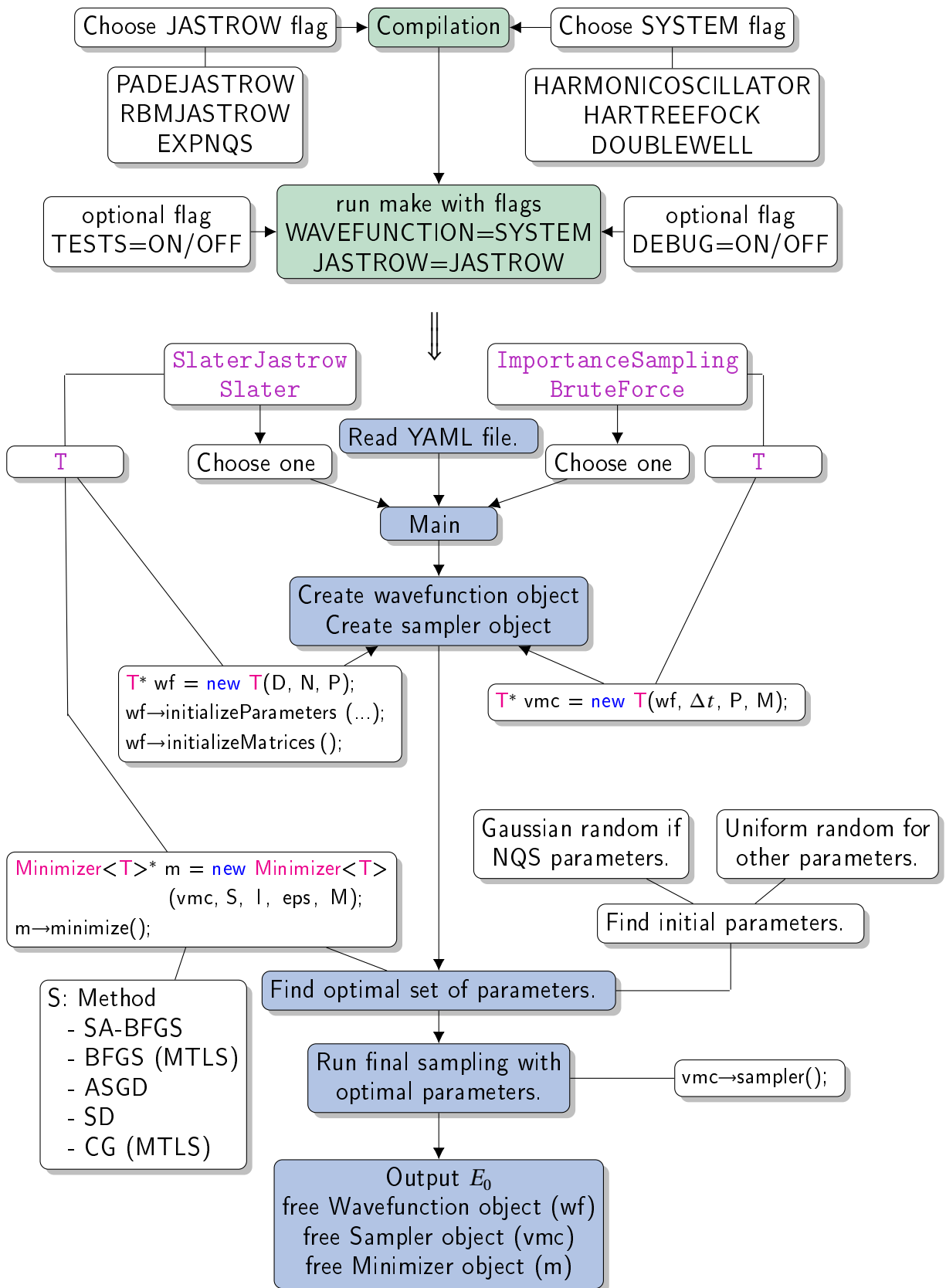


Figure 5.2: Flow chart of Variational Monte-Carlo implementation.

## 5.1 Cartesian Basis

In chapter 4 we mentioned the use of basis functions the different Many-Body methods. These can be pre-built using nifty intuition. One such observation is in the way harmonic oscillator functions station themselves on energy-levels(in the full-shell case). The following image<sup>2</sup> describes this for the first few levels

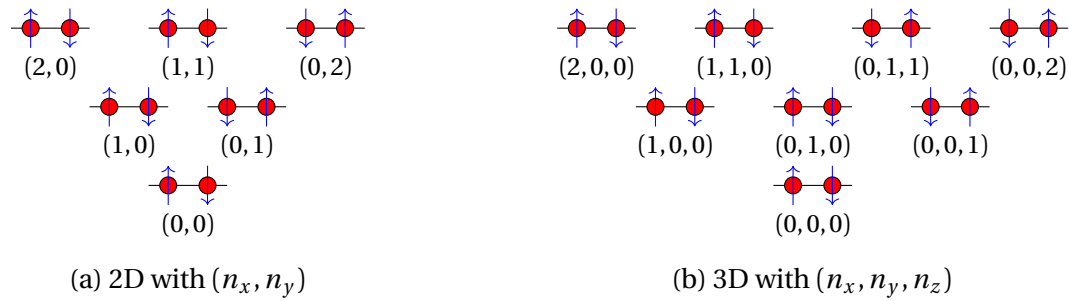


Figure 5.3: Harmonic Oscillator Levels

This specific arrangement of basis-functions is implemented in class `Cartesian` and is used in both the Hartree-Fock and VMC implementations. It essentially builds a matrix of states with the rows being the specific state and the columns containing the quantum numbers(in cartesian), the spin-value(as an integer), magic number and energy(in natural units proportional to the oscillator frequency). The essential form is

$$\begin{pmatrix} n_x & n_y & s & m_s & E & M \end{pmatrix} \quad \begin{pmatrix} n_x & n_y & n_z & s & m_s & E & M \end{pmatrix} \quad (5.1)$$

with the  $n$ 's being the principal numbers,  $s$  the spin value  $m_s$  the spin projection(up or down in our case),  $E$  the energy and  $M$  the magic number. All the numbers above are integers, meaning the actual energy  $E$  need to be converted if the actual energy of the state is desired, the same is applied to the spin projection(which is to multiply by 1/2). The `Cartesian` class builds the states with alternating spin (the spacial parts are doubled with spin), but also has a function for restructuring by setting the states with spin down in acending order first and the same states with spin up after.

## 5.2 Hartree-Fock

The Hartree-Fock method described in section 2.5 is implemented in » REF GITHUB «. Only the restricted case is implemented and is present as the class `HartreeFockSolver`. The matrix-

<sup>2</sup>As the old idiom goes; "A picture is worth a thousand words"

elements(integrals) are implemented in `HermiteIntegrals` class. This class also uses an auto-generated header for the Hermite-coefficients, see section 5.5 below. The `HartreeFockSolver` is implemented in a general way such that an abstract class for the integral elements is all that is needed. The `HartreeFockSolver` can then be inherited and used. An example of how to create a solver object with the Double-Well system called HFS with number of dimensions  $D$ , number of basis functions  $L$  and number of particles  $N$ .

```
DoubleWell* HFS = new DoubleWell(D, L, N);
string message = HFS->initializeParameters (...);
```

With the (...) meaning one initializes it with however manner the function was made. The initialization function must also return a message determined by the success of the initialization. If it succeeds it returns an empty message while if not it returns a pre-defined message.

Here is a simple example code-snippet which initializes and runs the Hartree-Fock algorithm

```
DoubleWell* HFS = new DoubleWell(D, L, N);

string message = HFS->initializeParameters (...);
if (message.compare("")) {
    if (myRank == 0) {
        std::cout << message << std::endl;
    }
    delete HFS;
    finalize ();
}

double E = HFS->iterate (M, 1e-8, true);
```

The `iterate` function takes in  $M$  as the maximum number of iterations, the convergence tolerance (when to break the iteration) and a boolean for showing progress or not. It calculates the integral-elements and runs the Hartree-Fock algorithm and returns the estimation of the ground-state energy.

### 5.2.2 Parallelization of Two-Body Matrix

The most time-consuming part of the Hartree-Fock procedure is the calculation of the two-body matrix-elements giving the interaction terms. This is parallelized in the `assemble` function in `HartreeFockSolver`. The basic premise is to represent the  $N^4$  elements in  $\langle pq | r^{-1} | rs \rangle$  as a one-dimensional array with the mapping

$$(p, q, r, s) \rightarrow p + N(q + N(r + Ns)) \quad (5.2)$$

that is the element  $(p, q, r, s)$  is stored in position  $(p + N(q + N(r + Ns)))$  in the one-dimensional array. The symmetry

$$(p, q, r, s) = (q, p, r, s) \quad (5.3)$$

reduces the number of elements down to  $N(N+1)/2$ . Notice also that the number of  $(r, s)$  elements each process needs to calculate is also this same size meaning the total size is actually

$$\text{totalsize} = \frac{N^2(N+1)^2}{4} \quad (5.4)$$

and all the symmetries imply that the following elements are the same

$$\begin{aligned} &(p, q, r, s) \\ &(r, q, p, s) \\ &(r, s, p, q) \\ &(p, s, r, q) \\ &(q, p, s, r) \\ &(s, p, q, r) \\ &(s, r, q, p) \\ &(q, r, s, p) \end{aligned} \quad (5.5)$$

A matrix  $\text{pqMap}$  of size  $N(N+1)/2 \times 2$  is then created with elements

$$\text{pqMap}_{pq} = (p, q) \quad (5.6)$$

This is essentially just a matrix with each row being a tuple with  $p$  and  $q$  value.

The rows are then distributed evenly among  $P$  processes according to

$$\text{rows}_p = \begin{cases} \left\lfloor \frac{\frac{N}{2}(N+1)}{P} \right\rfloor & \text{rank} < \left( \frac{N}{2}(N+1) \bmod P \right) \\ \left\lfloor \frac{\frac{N}{2}(N+1)}{P} \right\rfloor & \text{else} \end{cases} \quad (5.7)$$

The problem now however is that processes of higher and higher ranks may end up with calculating more since larger indices involve computationally more heavy functions to be evaluated. We can account for this by weighting the number of rows each process gets by the product<sup>3</sup> of the principal quantum numbers for the state which the indices represent, that is

$$S_i = \sum_{j=0}^{P_i} \prod_d (n_{jd} + 1) \quad (5.8)$$

---

<sup>3</sup>The product is used since the loops are nested and run up to the given quantum number.

The sum with index  $j$  runs over the sub-chunk for process  $i$  where the size of each chunk is defined by equation 5.7. The algorithm is as follows

---

**Algorithm 3** Even Weighting

---

```

Make an array sizes of size  $P$  with the number of elements for each process.
Make an array displ of size  $P$  with the displacement (index).
Make array  $S$  of size  $P$  with elements as specified in equation 5.8.
Set elements of sizes array to zero.
 $O = \text{Floor}(\text{Mean}(S))$ 
 $p = 0$  ▷ Index for process
 $j_s = 0$  ▷ Total sum for each  $p$ 
 $k = 0$  ▷ Index for displacement in sizes array
 $V_{\max} = O + 3n_{\max}^2$  ▷  $n_{\max}$  is the largest  $n$ -quantum number in the system.
for  $l = 0$  to  $l < \frac{N(N+1)}{2}$  do ▷ Iterate over rows in pqMap
     $j_s = j_s + \prod_d (n_{p_d}^{(l)} + 1)(n_{q_d}^{(l)} + 1)$ 
     $k += 1$ 
    if  $j_s \geq V_{\max}$  then ▷ Make sure not to overshoot
         $\text{sizes}[p] = k - 1$  ▷ Discard the last element
         $l = l - 1$  ▷ Re-evaluate for next  $p$ 
         $k = 0$ 
         $j_s = 0$ 
         $p += 1$ 
    else if  $j_s > O$  then ▷ Chunk for process  $p$  is good.
         $\text{sizes}[p] = k$  ▷ update sizes
         $k = 0$ 
         $j_s = 0$ 
         $p += 1$ 
    else if  $l = \frac{N(N+1)}{2} - 1$  and  $j_s \leq O$  then ▷ Throw remaining rows at last
         $\text{sizes}[p] = k$ 
    end if
end for

```

---

Each process then gets its respective chunk of `pqMap` array such that the each process calculates its own chunk according to the size set. Each process then calculates the two-body elements with the  $(p, q)$  elements received. The total size for each process also needs to take the  $(r, s)$  elements into account as they are also of size  $N(N + 1)/2$ . Each sub-chunk is then sent to root process and concatenated to a large one-dimensional array and the actual two-body matrix of size  $N^4$  is assembled and antisymmetrized. The Hartree-Fock algorithm is then run only on one process.

### 5.2.2 Tabulation of Two-Body Matrix

The `HartreeFockSolver` class uses an input file for the two-body matrix if given and calculates and writes one out if not given. As of now this is done in a brute-force fashion, that is the entire

matrix, including all zero-values, are written to file. This entire structure can be improved upon by introducing a *Sparse-Matrix* structure, which is a matrix in which only the non-zero elements are stored and a displacement array for the given indices of the non-zero elements is created. This would decrease the every-increasing memory usage and reduce the calculation time as look-up time in the array.

The most promising road for implementing a Sparse structure is to use the SparseMatrix module in Eigen since the entire code-base already builds heavily upon Eigen from before.

## 5.3 Variational Monte Carlo

The Variational Monte-Carlo implementation is mainly in three classes, namely `VMC`, `BruteForce` and `ImportanceSampling`. The structure is set with `BruteForce` and `ImportanceSampling` both inheriting from `VMC`. This structure essentially gives room for splitting specific parts of the Brute-Force algorithm from the Metropolis-Hastings algorithm, but still using the same code for minimization. We will explain the minimization parts in the next section.

The main input which `VMC` needs is a wavefunction. An abstract class-template is implemented and can be generated using a python script, also given in the same GitHub repository »REF GITHUB«. The template is built in such a way that one only needs to fill in specific analytic expressions for the gradient, Laplacian and gradient for the variational parameters. The latter part is optional.

The wavefunction itself is built using the `Slater` or `SlaterJastrow` class. However, in order to use the `SlaterJastrow` one has to specify which Jastrow function to use at compile time. A simple example illustrates this better

```
SlaterJastrow* wf = new SlaterJastrow(dim, numParticles, parameters);
wf->initializeParameters(omega);
wf->initializeMatrices();

ImportanceSampling<SlaterJastrow>* vmc = new
    ImportanceSampling<SlaterJastrow>(wf, stepmc, parameters,
                                     maxIterations, rank, numProcs);

double E = vmc->sampler();

delete vmc;
delete wf;
```

The first chunk initializes the SlaterJastrow class with the pre-specified system which needs to be given at compile time as a flag i.e `WAVEFUNCTION=HARMONICOSCILLATOR`. The second part sets the sampling to use Metropolis-Hastings algorithm. The parameters variable must be



an Eigen[17] vector or array and contain the variational parameters. The representation of each element in this vector(or array) is specific to each system. For a more detailed explanation see » REF GITHUB «.

This is just an example of how to build a simple run, however we have also built a run file which uses YAML[9]. The basic template is as follows

```
omega: 1.0
numparticles: 6
maxitermc: 100000
stepmc: 0.01
parameters: [0.99, 0.47] #optional
numparameters: 2
jastrow: true #optional
importance: true #optional
```

This is a template used for the `HarmonicOscillator` with the Padé-function as Jastrow factor. If the NQS-function is used an additional parameter 'numhiddenbias' giving the number of hidden biases used, is needed. Again, for more detail see » REF GITHUB «

This form of input makes it fairly simple to actually run the code for different systems with ease. One needs to compile with the specific flag for the system(wavefunction and Jastrow) and then supply an YAML input file at runtime.

### 5.3.3 Slater Optimizations

In the Metropolis sampling we need access to the ratio of two determinants, namely the Slater wavefunction at the current state and the one at previous state. These are quite expensive to calculate<sup>4</sup>. This can be overcome by using the fact that moving only *one* particle at each iteration also constitutes to a state-transition. Following [23] and given row  $i$  as the index for the row that is changed, the following expressions are valid

$$\begin{aligned}\frac{\Psi}{\Psi'} &= \sum_j \psi_{ij} \psi_{ji}'^{-1} \\ \frac{\nabla_i \Psi}{\Psi} &= \sum_j \psi_{ij} \nabla_i \psi_{ji}^{-1} \\ \frac{\nabla_i^2 \Psi}{\Psi} &= \sum_j \psi_{ij} \nabla_i^2 \psi_{ji}^{-1}\end{aligned}\tag{5.9}$$

with  $\Psi'$  being the wavefunction at previous state. One might ask now, but isn't this just worse? We have gone from needing two determinants to needing two inverses!? Fret not, the Sherman-Morrison formula[42] for updating an inverse matrix if only one row has changed in the original

---

<sup>4</sup>Actual complexity of a determinant is  $n \times n$ , with  $n$  being the size of the Slater matrix.

matrix comes to the rescue. The elements of the inverse can by this be expressed as (with  $i$  being the row that changed)

$$\psi_{kj}^{-1} = \begin{cases} \psi_{kj}'^{-1} - \frac{\Psi}{\Psi'} \psi_{ki}'^{-1} \sum_{l=1}^N \psi_{il}' \psi_{lj}'^{-1}, & j \neq i \\ \frac{\Psi}{\Psi'} \psi_{ki}'^{-1} \sum_{l=1}^N \psi_{il}' \psi_{lj}'^{-1}, & j = i \end{cases} \quad (5.10)$$

This means that the inverses and the determinant ratios can be calculated fully once before the sampling and then updated using the above formulas. This procedure is implemented in the `Slater` class.

### 5.3.3 Jastrow Optimizations

The Jastrow factors presented in section 2.9.9, section 2.9.9 and section 2.9.9 also give rise to optimizations in the case of moving only one particle at a time. In particular, the Padé function and the simple exponential can both be represented by a matrix of size  $N \times D$  like this

$$\mathbf{J} = \left( \mathbf{J}(\mathbf{r}_1) \dots \mathbf{J}(\mathbf{r}_N) \right) \quad (5.11)$$

Moving one particle at a time means only one column in  $\mathbf{J}$  is changed meaning only that column needs to be updated. Additionally, the  $\mathbf{J}$  matrix doesn't actually need to be present in the code since we are only interested in ratios  $J/J'$ . If only one index  $i$  changes we have

$$\begin{aligned} \frac{J}{J'} &= \exp \left( \sum_{i < j} (f_{ij} - f'_{ij}) \right) \\ &= \exp \left( \sum_{i \neq j} f_{ij} \right) \end{aligned} \quad (5.12)$$

Notice that  $i$  is fixed in the last step.

The gradient of  $J$  can be represented as an  $N \times N \times D$  matrix

$$\nabla \mathbf{J} = \begin{pmatrix} 0 & \nabla \mathbf{J}(\mathbf{r}_{1,2}) & \dots & \nabla \mathbf{J}(\mathbf{r}_{1,N-1}) \\ \nabla \mathbf{J}(\mathbf{r}_{2,1}) & 0 & \dots & \nabla \mathbf{J}(\mathbf{r}_{2,N-1}) \\ \vdots & \vdots & \ddots & \vdots \\ \nabla \mathbf{J}(\mathbf{r}_{N,1}) & \dots & \dots & 0 \end{pmatrix} \quad (5.13)$$

When only one particle is moved at a time only one row and column changes in this matrix. In addition the matrix is symmetric with the expect a negative sign,

$$\nabla \mathbf{J}(\mathbf{r}_{ij}) = -\nabla \mathbf{J}(\mathbf{r}_{ji}) \quad (5.14)$$

Both of these optimizations are implemented in the `PadeJastrow` and `ExpNQS` classes.

For the NQS-Jastrow we notice that the sum in the exponential involving the weights can be represented as a matrix  $\mathbf{W}$  of size  $N \times H$  with  $H$  being the number of hidden biases with elements

$$W_{i,j} = \sum_d \frac{x_i^{(d)} w_{i+d,j}}{\sigma^2} \quad (5.15)$$

and the entire exponential with the hidden biases is represented as a vector  $\mathbf{B}$  of size  $H$  with elements

$$B_j = \exp\left(b_j + \sum_i W_{i,j}\right) \quad (5.16)$$

So for each iteration only one row in  $\mathbf{W}$  is updated and then the entire  $\mathbf{B}$  vector is recalculated and reused.

The part involving only the visible biases can be optimized in the same manner as with the Padé function and simple exponential, meaning one only needs to calculate

$$\frac{J_a}{J'_a} = \exp\left(\frac{(r_i - a_i)^2}{\sigma^2}\right) \quad (5.17)$$

Again with  $i$  being the index of the moved particle. These optimizations are implemented in the `RBMJastrow` class.

### 5.3.3 Optimization For Tabulation

The `Slater` class checks on compile time the specific wavefunction class for the functions

- `set`: Called during initialization (before each sampling)
- `reSetAll`: Sets all matrices to zero (used in testing)
- `initializeMatrices`: Allocate memory
- `update`: Update positions and wavefunction
- `reset`: Revert to previous positions and wavefunction
- `resetGradient`: Revert to previous gradient
- `acceptState`: Update previous positions and wavefunction to current
- `acceptGradient`: Update previous gradient to current one

If these functions are implemented in the wavefunction class they will be called in by the `VMC` class during the Metropolis sampling. The whole purpose for this is so that calculations can be tabulated and then only the parts which are changed be updated. Detailed explanation of what the functions can, and need to, do is given in the GitHub repository.

### 5.3.3 Tabulating Hermite Polynomials

In the `HarmonicOscillator` and `HartreeFock` classes used by `VMC` we calculate the Hermite polynomials

$$\begin{aligned} H_n(\sqrt{\omega}r) &= \prod_d H_{n_d}(\sqrt{\omega}x_d) \\ H_n(\sqrt{\omega}r) &= \prod_d H_{n_d-1}(\sqrt{\omega}x_d) \\ H_n(\sqrt{\omega}r) &= \prod_d H_{n_d-2}(\sqrt{\omega}x_d) \end{aligned} \tag{5.18}$$

for  $n = 0, \dots, L$  where  $L$  is the number of basis functions in the Hartree-Fock basis for `HartreeFock` and highest order of single-particle function for `HarmonicOscillator`. These are tabulated in a matrix of size  $N \times D \times L$  with  $N$  being the number of particles and  $D$ . The mapping goes by

$$H_{ijk} = H_{n_j^{(d)}}(\sqrt{\omega}x_i^{(d)}) \tag{5.19}$$

For each iteration in the Metropolis sampling, if we only move one particle at a time, only one row changes in  $H_{ijk}$ . This update is reflected in the functions mentioned in section 5.3.3. `initializeMatrices` firstly allocates space for two matrices which represent the current and old versions of  $H_{ijk}$ , the `set` function set calculates  $H_{ijk}$  using the auto-generated header explained in section 5.5, `update` then updates the row which has changed and then `acceptState` or `reset` is called depending on the Metropolis-Test.

## 5.4 Minimization

The central part of the Variational Monte-Carlo method is the actual *variation* of parameters. This is, as explained in chapter 3, a minimization problem. We will in this chapter explain the implementation of the methods presented in chapter 5 and also show some examples of how to use `Minimizer` class, in which the mentioned methods are implemented.

The main class for minimizations is the `Minimizer` and is built as a *friend class*. This is a C++ declaration<sup>5</sup> which goes into the header of the class who is to befriend (in our case `VMC`) with the class who is to be the friend (`Minimizer`). In this way `Minimizer` has full access to all

---

<sup>5</sup>A C++ declaration is a phrase which goes in front of variables, functions and other objects and is a pure compiler specific rule.

the variables and functions defined inside **VMC** even if said variables and functions are declared as *private*<sup>6</sup>. The reason for this choice is just to split the whole minimization part of the variational method from the actual sampling.

The means to make a **Minimizer** object is to initialize it as

```
Minimizer<T>* m = new Minimizer<T>(vmc, "method", numIterations, eps);
m->minimize();
```

where **T** is a sampler type (either **BruteForce** or **ImportanceSampling**) and **vmc** is the object with said type initializes. The **minimize** function is the function which actually does the minimization and follows the procedure given in figure 5.4.

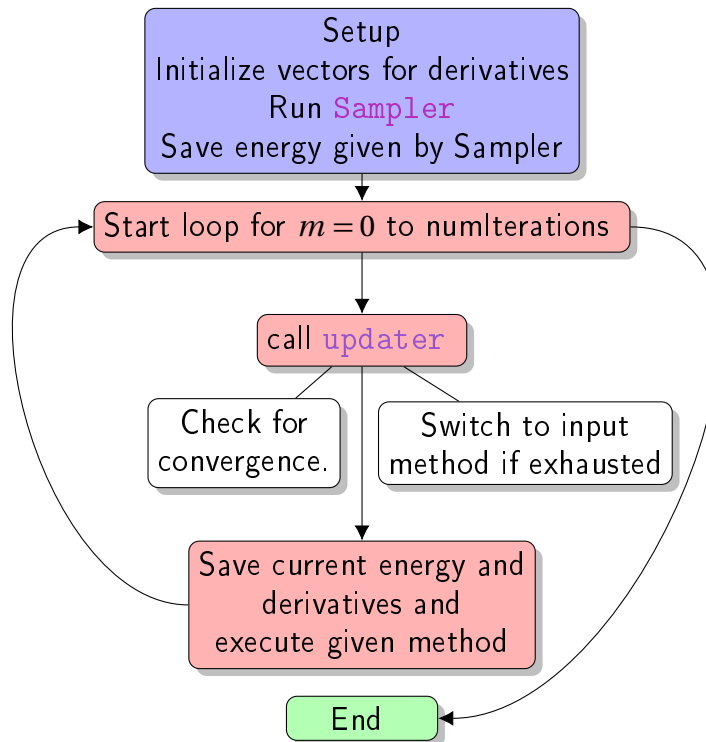


Figure 5.4: Flow chart of procedure done by **minimize** function.

The energy after the last cycle (or after threshold is met) is the energy currently saved within the **VMC** object.

## 5.5 Auto-Generation

### 5.5.5 Hermites

The analytic expressions involved in the quantum-dot systems are dependent on Hermite polynomials and their coefficients. These are calculated symbolically using the recurrence relation

<sup>6</sup>On an equal note, this is really not a good idea in general

for Hermite functions with the SymPy package in python. These expressions are then written to C++ code and written to a C++ -header file. The script can be found in <https://github.com/Oo1nsane1oO/Hermite>. The generated header file is then included in the integral class in `HartreeFockSolver` and in the wavefunction classes (namely `HartreeFock` and `HarmonicOscillator`) in `VMC`.

### 5.5.5 Double-Well Basis

The basis built by the procedure described in section 3.4 is done in python using the eigenvalue solver in the SciPy package. The script itself can be found in <https://github.com/Oo1nsane1oO/doubleWellFit>, but is also included in the Hartree-Fock repository.

The script itself basically just builds (calculates the elements of) the  $H$  matrix from equation 3.56 and then finding its eigenvalues and eigenvectors which are then written to a C++ header file as a class with a static function to get coefficients and eigenvalues. This file is then included in the `DoubleWell` integral class as a base class of inheritance.

## 5.6 Verification

In order to be confident in the results presented for the double-well potential we, along with unit-tests, benchmarked our results with the harmonic oscillator potential. The tests are set-up with the UnitTest++ [8] and one only needs to pass a flag `TESTS = ON` at compile time to enable them.

### 5.6.6 Hartree-Fock

The first of the tests for the Hartree-Fock method was to see if it reproduced the exact energies in the case of no interaction (neglect Coulomb-term in Hamiltonian). These tests are given in the tests directory in the GitHub repository.

The benchmarks using the Hartree-Fock method with harmonic oscillator potential is given in table 6.2. These results are directly compared with the master's thesis [31] and article [37].

For the double-well system the only benchmark was the result from master's thesis of Høgger [24] with 2 particles. However it is expected that the energies lie somewhere between the single-well results and the non-interaction case due to the potential itself being a perturbation of the single-well system. The results are given in » REF(AND MAKE) TABLE «

### 5.6.6 Variational Monte-Carlo

The first tests here were also to find the exact energies, which are also given as tests in a similar fashion as with the Hartree-Fock. The second benchmark was to check if the energies were

comparable with the results of [24] using basis functions of form

$$\phi_j(\mathbf{r}) = \psi_{n_j}^{\text{HO}}(\sqrt{\alpha\omega}r) \quad (5.20)$$

with the Padé function given in equation 2.71.

For the real deal with the Hartree-Fock basis we checked that the VMC method could reproduce the Hartree-Fock energies when no Jastrow factor was used, that is only a single-particle Slater-determinant *with no variational parameters* as the wavefunction ansatz

$$\phi_{ij}^{\text{HF}} = \sum_l C_{jl} \psi_{n_l}^{\text{HO}}(\sqrt{\omega}r_i) \quad (5.21)$$

These results are also implemented as a bunch of tests.

For the benchmarks, we compared our energies again with the thesis of Høgberget[24]. The results are given in » REF (AND MAKE) TABLE «

For the double-well system we only used a Hartree-Fock basis and checked that the Hartree-Fock energies were reproduced (in case with no Jastrow). The only benchmark was again the system with two particles.





## RESULTS

No amount of physics theory will ever be interesting if it was not backed up by some proof or atleast some results.

In this chapter we present the results from the simulations of the quantum dot system in the harmonic oscillator system and the double-well system. We also present some results regarding the minimization scheme in the VMC method.

### 6.1 Tweaks and Experimentation

With the minimization methods clarified and the function to be minimized outlined the actual minimization could start<sup>1</sup>.

Within the minimization methods presented there are quite the number of constant parameters which needed to be set pre-hand. Often one finds these some-what heuristically with a close eye on the function to be minimized. This approach is the one we used in the VMC method, with the most memorable one being the parameters set in the simulated annealing method.

#### 6.1.1 Simulated Annealing

With the simulated annealing the idea was to use it as a sort of "thermalization", that is to run it initially in hope that it finds the valley within the function-mesh in which the global minima lies. We tried anything from

---

<sup>1</sup>With the methods at disposal the *real challenge* was yet to come...

## 6.2 Hartree-Fock

Here we present the results from the quantum-dot simulations using the Hartree-Fock method. The two systems of interest were the harmonic oscillator and the double-well system.

Table 6.1: RHF with the 2D HO-system.  $L$  is the number of spacial orbitals used and  $N$  is the number of particles. The "—" indicates that the system cannot be run with such few basis functions.

|          |     | $N$      |           |           |            |            |            |             |
|----------|-----|----------|-----------|-----------|------------|------------|------------|-------------|
| $\omega$ | $L$ | 2        | 6         | 12        | 20         | 30         | 42         | 56          |
| 0.10     | 1   | 0.596333 | —         | —         | —          | —          | —          | —           |
|          | 3   | 0.709635 | 4.864244  | —         | —          | —          | —          | —           |
|          | 6   | 0.526903 | 4.435740  | 17.272337 | —          | —          | —          | —           |
|          | 10  | 0.679018 | 4.019787  | 15.358377 | 43.303270  | —          | —          | —           |
|          | 15  | 0.525666 | 3.963148  | 14.098239 | 38.031297  | 89.280189  | —          | —           |
|          | 21  | 0.525666 | 3.870617  | 13.700447 | 35.572157  | 78.990503  | 162.260603 | —           |
|          | 28  | 0.525635 | 3.863135  | 13.270861 | 34.076983  | 71.159148  | 144.850714 | 269.962677  |
|          | 36  | 0.525635 | 3.852880  | 13.151070 | 32.907610  | 70.171143  | 135.399113 | 242.763519  |
|          | 45  | 0.525635 | 3.852591  | 13.000151 | 32.379047  | 67.961359  | 128.642142 | 227.093062  |
|          | 55  | 0.525635 | 3.852393  | 11.683965 | 31.823087  | 66.272349  | 124.116636 | 216.406591  |
|          | 66  | 0.525635 | 3.852391  | 12.933578 | 31.606556  | 65.024272  | 120.477371 | 207.859610  |
|          | 78  | 0.525635 | 3.852382  | 12.929215 | 31.359747  | 51.369240  | 92.494105  | 162.039924  |
| 0.28     | 91  | 0.525635 | 3.852381  | 12.924947 | 31.280274  | 63.531909  | 90.361587  | 153.361100  |
|          | 105 | 0.525635 | 3.852381  | 12.924756 | 31.190173  | 50.801070  | 89.034638  | 148.084050  |
|          | 120 | 0.525635 | 3.852381  | 12.924659 | 26.316806  | 62.778269  | 88.267263  | 144.999311  |
|          | 1   | 1.223192 | —         | —         | —          | —          | —          | —           |
|          | 3   | 1.223192 | 9.266117  | —         | —          | —          | —          | —           |
|          | 6   | 1.141775 | 8.725018  | 32.056852 | —          | —          | —          | —           |
|          | 10  | 1.141775 | 8.139719  | 29.582103 | 79.220310  | —          | —          | —           |
|          | 15  | 1.141741 | 8.095876  | 27.596111 | 72.011644  | 161.787811 | —          | —           |
|          | 21  | 1.141741 | 8.021956  | 27.194900 | 67.907357  | 146.711579 | 292.019496 | —           |
|          | 28  | 1.141717 | 8.020571  | 26.722532 | 66.336613  | 139.073038 | 265.763686 | 483.281000  |
|          | 36  | 1.141717 | 8.019625  | 26.651149 | 64.754792  | 134.380347 | 252.164864 | 441.883026  |
|          | 45  | 1.141713 | 8.019611  | 26.559697 | 64.309088  | 131.153627 | 242.160894 | 418.703743  |
| 0.50     | 55  | 1.141713 | 8.019571  | 26.554432 | 63.805612  | 129.589656 | 236.417148 | 402.296590  |
|          | 66  | 1.141712 | 8.019571  | 26.550045 | 63.695333  | 128.063933 | 231.961536 | 391.319694  |
|          | 78  | 1.141712 | 8.019570  | 26.550035 | 63.567267  | 127.516181 | 229.033490 | 383.057251  |
|          | 91  | 1.141712 | 8.019570  | 26.550031 | 63.552773  | 126.918914 | 191.095832 | 377.466395  |
|          | 105 | 1.141712 | 8.019569  | 26.550027 | 63.539438  | 126.748572 | 225.641452 | 373.080210  |
|          | 120 | 1.141712 | 8.019569  | 26.550025 | 63.539007  | 126.559672 | 188.304714 | 303.460780  |
|          | 1   | 1.886227 | —         | —         | —          | —          | —          | —           |
|          | 3   | 1.886227 | 13.640713 | —         | —          | —          | —          | —           |
|          | 6   | 1.799856 | 13.051620 | 46.361130 | —          | —          | —          | —           |
|          | 10  | 1.799856 | 12.357471 | 43.663267 | 113.412648 | —          | —          | —           |
|          | 15  | 1.799748 | 12.325128 | 41.108851 | 105.288766 | 230.039825 | —          | —           |
|          | 21  | 1.799748 | 12.271499 | 40.750512 | 99.754600  | 211.984502 | 413.129302 | —           |
|          | 28  | 1.799745 | 12.271375 | 40.302719 | 98.193478  | 202.100349 | 380.824889 | 681.044994  |
| 1.00     | 36  | 1.799745 | 12.271361 | 40.263752 | 96.553216  | 197.568022 | 363.766695 | 629.293351  |
|          | 45  | 1.799743 | 12.271337 | 40.216688 | 96.223206  | 193.554142 | 352.630536 | 601.088912  |
|          | 55  | 1.799743 | 12.271326 | 40.216252 | 95.833317  | 192.225626 | 345.721160 | 581.182893  |
|          | 66  | 1.799742 | 12.271324 | 40.216195 | 95.785792  | 190.810227 | 341.838273 | 568.944986  |
|          | 78  | 1.799742 | 12.271320 | 40.216165 | 95.734582  | 190.462448 | 338.512355 | 559.966285  |
|          | 91  | 1.799742 | 12.271320 | 40.216144 | 95.733305  | 190.069482 | 337.206237 | 554.039857  |
|          | 105 | 1.799742 | 12.271320 | 40.216143 | 95.732781  | 190.007169 | 335.822963 | 550.259738  |
|          | 120 | 1.799742 | 12.271320 | 40.216139 | 95.732764  | 189.942874 | 335.425547 | 547.163579  |
|          | 1   | 3.253314 | —         | —         | —          | —          | —          | —           |
|          | 3   | 3.253314 | 22.219813 | —         | —          | —          | —          | —           |
|          | 6   | 3.162691 | 21.593198 | 73.765549 | —          | —          | —          | —           |
|          | 10  | 3.162691 | 20.766919 | 70.673849 | 177.963297 | —          | —          | —           |
|          | 15  | 3.161921 | 20.748402 | 67.569930 | 168.939788 | 357.543694 | —          | —           |
|          | 21  | 3.161921 | 20.720257 | 67.296869 | 161.339721 | 336.270048 | 637.559628 | —           |
|          | 28  | 3.161909 | 20.720132 | 66.934745 | 159.958722 | 322.684662 | 597.572501 | 1045.153168 |
|          | 36  | 3.161909 | 20.719248 | 66.923094 | 158.400172 | 318.435444 | 574.794727 | 979.581293  |
|          | 45  | 3.161909 | 20.719248 | 66.912244 | 158.226030 | 314.080027 | 563.971458 | 943.145991  |
|          | 55  | 3.161909 | 20.719217 | 66.912035 | 158.017667 | 313.170733 | 555.393205 | 920.685095  |
|          | 66  | 3.161909 | 20.719215 | 66.911365 | 158.010276 | 312.139011 | 552.472493 | 906.165846  |
|          | 78  | 3.161909 | 20.719215 | 66.911364 | 158.004951 | 312.010418 | 549.388384 | 898.709307  |
|          | 91  | 3.161908 | 20.719215 | 66.911323 | 158.004757 | 311.869364 | 548.688114 | 892.082465  |
|          | 105 | 3.161908 | 20.719215 | 66.911322 | 158.004317 | 311.863887 | 547.907494 | 889.765470  |
|          | 120 | 3.161908 | 20.719215 | 66.911321 | 158.004315 | 311.860399 | 547.801022 | 887.301998  |

Table 6.2: RHF with the 3D HO-system.  $L$  is the number of spacial orbitals used and  $N$  is the number of particles. The "—" indicates that the system cannot be run with such few basis functions.

|          |     | $N$      |           |            |            |
|----------|-----|----------|-----------|------------|------------|
| $\omega$ | $L$ | 2        | 8         | 20         | 40         |
| 0.10     | 1   | 0.552355 | —         | —          | —          |
|          | 4   | 0.706087 | 7.035821  | —          | —          |
|          | 10  | 0.529067 | 6.630816  | 37.165887  | —          |
|          | 20  | 0.694713 | 6.005329  | 33.059287  | 130.747321 |
|          | 35  | 0.529066 | 5.960234  | 30.287665  | 112.917323 |
|          | 56  | 0.529066 | 5.872465  | 27.977530  | 104.463835 |
|          | 84  | 0.529065 | 5.868615  | 28.424272  | 92.416262  |
|          | 120 | 0.529065 | 5.862549  | 28.165123  | 85.209104  |
| 0.28     | 1   | 1.262270 | —         | —          | —          |
|          | 4   | 1.744849 | 13.801205 | —          | —          |
|          | 10  | 1.237384 | 13.307332 | 68.950504  | —          |
|          | 20  | 1.237384 | 12.483549 | 63.643967  | 235.682314 |
|          | 35  | 1.237229 | 12.455162 | 59.237015  | 210.630043 |
|          | 56  | 1.237229 | 12.399375 | 58.417453  | 197.754907 |
|          | 84  | 1.237225 | 12.398982 | 57.328784  | 190.564893 |
|          | 120 | 1.237225 | 12.398687 | 57.201823  | 186.064771 |
| 0.50     | 1   | 2.064282 | —         | —          | —          |
|          | 4   | 2.064282 | 20.707652 | —          | —          |
|          | 10  | 2.038858 | 20.174413 | 99.689043  | —          |
|          | 20  | 2.038858 | 19.243279 | 93.747893  | 333.818879 |
|          | 35  | 2.038523 | 19.225643 | 88.237201  | 304.701805 |
|          | 56  | 2.038523 | 19.191660 | 87.541531  | 287.355799 |
|          | 84  | 2.038509 | 19.191654 | 86.506890  | 280.356812 |
|          | 120 | 2.038509 | 19.191626 | 86.439181  | 274.994258 |
| 1.00     | 1   | 3.798016 | —         | —          | —          |
|          | 4   | 3.798016 | 34.557120 | —          | —          |
|          | 10  | 3.772173 | 33.996867 | 158.555190 | —          |
|          | 20  | 3.772173 | 32.945301 | 152.252978 | 516.025169 |
|          | 35  | 3.771606 | 32.937947 | 145.038663 | 481.710199 |
|          | 56  | 3.771606 | 32.925002 | 144.518526 | 458.308755 |
|          | 84  | 3.771574 | 32.924935 | 143.704615 | 452.880282 |
|          | 120 | 3.771574 | 32.924628 | 143.684577 | 446.315149 |

## 6.3 VMC

Here are the results for the quantum-dot simulations with the variational method both with and without a Hartre-Fock basis. We only used a basis as large as the one needed to reach the Hartree-Fock limit » REF THIS « or up to the largest one run in case the limit was not reached. The exact numbers are seen in table 6.2.





## A.1 Lagrange Multiplier Method

See [2, 5]. The optimization method of Lagrange multipliers maximizes(or minimizes) a function  $f : \mathbb{R}^N \rightarrow \mathbb{R}$  with a constraint  $g : \mathbb{R}^N \rightarrow \mathbb{R}$ . We assume that  $f$  and  $g$  have continuous first derivatives in all variables(continuous first partial derivatives).

Given the above we can define a so-called Lagrangian  $\mathcal{L}$

$$\mathcal{L}[x_1, \dots, x_N, \lambda_1, \dots, \lambda_M] = f(x_1, \dots, x_N) - \lambda g(x_1, \dots, x_N) \quad (\text{A.1})$$

where the  $\lambda$  is called a Lagrange-multiplier. We now state that if  $f(x_1^0, \dots, x_N^0)$  is a maxima of  $f(x_1, \dots, x_N)$  then there exists a Lagrange-multiplier  $\lambda_0$  such that  $(x_1^0, \dots, x_N^0, \lambda_0)$  is a stationary point for the Lagrangian. This then yields the  $N + 1$  Lagrange-equations

$$\sum_{i=1}^N \frac{\partial \mathcal{L}}{\partial x_i} + \frac{\partial \mathcal{L}}{\partial \lambda} = 0 \quad (\text{A.2})$$

to be solved for  $x_1, \dots, x_N$  and  $\lambda$ .

## A.2 Interaction-Term in Fock-Operator

Introducing the so-called permutation operator  $P$  which interchanges the labels of particles meaning we can define

$$A \equiv \frac{1}{N!} \sum_p (-1)^p P \quad (\text{A.3})$$

the so-called *antisymmetrization* operator. This operator has the following traits

- The Hamiltonian  $H$  and  $A$  commute since the Hamiltonian is invariant under permutation.

- $A$  applied on itself (that is  $A^2$ ) is equal to itself since permuting a permuted state reproduces the state.

We can now express our Slater  $\Psi_T$  in terms of  $A$  as

$$\Psi_T = \sqrt{N!} A \prod_{i,j} \psi_{ij} \quad (\text{A.4})$$

where  $\psi_{ij} = \psi_j(\mathbf{r}_i)$  is element  $i, j$  of the Slater matrix (the matrix associated with the Slater determinant  $\Psi_T$ ).

The interaction part of  $H$  is then

$$\langle \Psi_T | H_I | \Psi_T \rangle = N! \prod_{i,j} \langle \psi_{ij} | A H_I A | \psi_{ij} \rangle \quad (\text{A.5})$$

The interaction  $H_I$  and  $A$  commute since  $A$  commutes with  $H$  giving

$$A H_I A | \psi_{ij} \rangle = \frac{1}{N!^2} \sum_{i < j} \sum_p (-1)^{2p} f_{ij} P | \psi_{ij} \rangle \quad (\text{A.6})$$

$$= \frac{1}{N!^2} \sum_{i < j} f_{ij} (1 - P_{ij}) | \psi_{ij} \rangle \quad (\text{A.7})$$

The factor  $1 - P_{ij}$  comes from the fact that contributions with  $i \neq j$  vanishes due to orthogonality when  $P$  is applied. The final expression for the interaction term is thus

$$\langle \Psi_T | H_I | \Psi_T \rangle = \sum_{i < j} \prod_{k,l} [\langle \psi_{kl} | f_{ij} | \psi_{kl} \rangle - \langle \psi_{kl} | f_{ij} | \psi_{lk} \rangle] \quad (\text{A.8})$$

Writing out the product and realizing the double summation over pairs of states we end up with

$$\langle \Psi_T | H_I | \Psi_T \rangle = \frac{1}{2} \sum_{i,j} [\langle \psi_{ij} \psi_{ji} | f_{ij} | \psi_{ij} \psi_{ji} \rangle - \langle \psi_{ij} \psi_{ji} | f_{ij} | \psi_{ji} \psi_{ij} \rangle] \quad (\text{A.9})$$

More comprehensive details and derivations are given in [22, 47].

### A.3 Multi-Index Notation

» REF THIS « This section will give a brief overlook of a notation which compresses indices running in similar fashion, the so-called *multi-index notation*. We will make use of this to reduce indices in each dimension down to one.

The rules are states as, given a n-tuple  $(x_1, \dots, x_n)$  over any field  $\mathbb{F}$  (real, complex, etc.), a multi index is defined to be

$$i = (n_1, \dots, n_n) \in \mathbb{Z}_+^n \quad (\text{A.10})$$

with expansions

$$\begin{aligned}
 |i| &= i_1 + \dots + i_n \\
 i! &= i_1! \dots i_n! \\
 x^i &= x_1^{i_1} \dots x_n^{i_n} \in \mathbb{F}[x] \\
 i \pm j &= (i_1 \pm j_1, \dots, i_n \pm j_n) \in \mathbb{Z}
 \end{aligned}
 \tag{A.11}$$

In essence the notation just wraps the notion of element-wise operations into one index variable.







## B.1 Derivatives of Hermite Functions

The gradient of Hermite functions on the form

$$\psi_n(r) = \prod_d \psi_{n_d}(x_d) = \prod_d H_{n_d}(\sqrt{\omega} x_d) e^{-\frac{\omega}{2} x_d^2} \quad (\text{B.1})$$

is

$$\begin{aligned} \nabla \psi_n(r) &= \sum_d \hat{e} \prod_{d' \neq d} \psi_{n_{d'}} \frac{\partial \psi_{n_d}}{\partial x_d} \\ &= \sum_d \hat{e} \prod_{d' \neq d} \psi_{n_{d'}} \psi_{n_d} \sqrt{\omega} \left( \frac{\partial H_{n_d}}{\partial u} \frac{1}{H_{n_d}} - x_d \right) \\ &= \psi_n \sqrt{\omega} \sum_d \hat{e} \left( 2n_d \frac{H_{n_d-1}(\sqrt{\omega} x_d)}{H_{n_d}(\sqrt{\omega} x_d)} - x_d \right) \end{aligned} \quad (\text{B.2})$$

and the Laplacian follows

$$\begin{aligned} \nabla^2 \psi_n(r) &= \sum_d \prod_{d' \neq d} \psi_{n_{d'}} \frac{\partial^2 \psi_{n_d}}{\partial x_d^2} \\ &= \psi_n \omega \sum_d \left( \frac{(4n_d(n_d-1)H_{n_d-2}(\sqrt{\omega} x_d) - \sqrt{\omega} x_d H_{n_d-1}(\sqrt{\omega} x_d))}{H_{n_d}(\sqrt{\omega} x_d)} + \omega x_d^2 - 1 \right) \end{aligned} \quad (\text{B.3})$$

The derivative with respect to the variational parameter  $\alpha$  is

$$\begin{aligned}
\frac{\partial \psi_n}{\partial \alpha} &= \frac{\partial}{\partial \alpha} \prod_d H_{n_d}(\sqrt{\omega} x_d) e^{-\frac{\omega}{2} x_d^2} \\
&= \sum_d \prod_{d' \neq d} \psi_{n_{d'}}(x_{d'}) \frac{\partial \psi_{n_d}(x_d)}{\partial \alpha} \\
&= \psi_n(r) \sum_d \omega x_d \left( \frac{n_d}{\sqrt{\alpha \omega}} \frac{H_{n_d-1}(\sqrt{\alpha \omega} x_d)}{H_{n_d}(\sqrt{\alpha \omega} x_d)} - \frac{\omega x_d^2}{2} \right) \\
&= \psi_n(r) \left( \sqrt{\frac{\omega}{\alpha}} \sum_d x_d n_d \frac{H_{n_d-1}(\sqrt{\alpha \omega} x_d)}{H_{n_d}(\sqrt{\alpha \omega} x_d)} - \frac{\omega}{2} r^2 \right)
\end{aligned} \tag{B.4}$$

## B.2 Derivatives of Padé-Jastrow Function

Given the Padé-Jastrow function

$$J = \exp \left( \sum_{i < j} f_{ij} \right), \quad f_{ij} = \frac{a_{ij} r_{ij}}{1 + \beta r_{ij}} \tag{B.5}$$

The general expression for the gradient and Laplacian with respect to particle position  $k$  is

$$\begin{aligned}
\nabla_k J &= J \sum_{j \neq k} \frac{\mathbf{r}_{kj}}{r_{kj}} \frac{\partial f_{kj}}{\partial r_{kj}} \\
\nabla_k^2 J &= \frac{(\nabla_k J)^2}{J} + J \sum_{j \neq k} \left( \frac{\partial f_{kj}}{\partial r_{kj}} \frac{D-1}{r_{kj}} + \frac{\partial^2 f_{kj}}{\partial r_{kj}^2} \right)
\end{aligned} \tag{B.6}$$

Notice that the sum with  $j \neq k$  is only a sum over  $j$  with  $k$  fixed. The derivatives of  $f$  are

$$\begin{aligned}
\frac{\partial f_{kj}}{\partial r_{kj}} &= \frac{a_{kj} r_{kj}^2}{(1 + \beta r_{kj})^2} \\
\frac{\partial^2 f_{kj}}{\partial r_{kj}^2} &= -\frac{2a_{kj}\beta}{(1 + \beta r_{kj})^3}
\end{aligned} \tag{B.7}$$

And the derivative with respect to the variational parameter  $\beta$

$$\frac{\partial f_{kj}}{\partial \beta} = -\frac{a_{kj} r_{kj}^2}{(1 + \beta r_{kj})^2} \tag{B.8}$$

## B.3 Derivatives of NQS-Wavefunction

Given the NQS-Wavefunction

$$J = \exp \left( -\sum_{i=1}^N \frac{(\mathbf{r}_i - \mathbf{a}_i)^2}{2\sigma^2} \right) \prod_j^M (1 + E_j) \tag{B.9}$$

The gradient is

$$\begin{aligned}\frac{\nabla_k J}{J} &= \nabla_k \ln(J) \\ &= -\frac{\mathbf{r}_k - \mathbf{a}_k}{\sigma^2} + \sum_{j=0}^M \sum_{d=1}^D \hat{\mathbf{e}}_d \frac{w_{k+d,j}}{\sigma^2 \left(1 + \frac{1}{E_j}\right)}\end{aligned}\quad (\text{B.10})$$

and the Laplacian

$$\begin{aligned}\frac{\nabla_k^2 J}{J} &= \nabla_k^2 \ln(J) \\ &= \left(\frac{\nabla_k J}{J}\right)^2 - \frac{D}{\sigma^2} + \sum_{j=1, d=1}^{M,D} \frac{w_{k+d,j}^2 E_j}{\sigma^4 \left(1 + E_j\right)^2}\end{aligned}\quad (\text{B.11})$$

with

$$\begin{aligned}W_j &\equiv \sum_{i=1}^N \sum_{d=1}^D \frac{x_i^{(d)} w_{i+d,j}}{\sigma^2} \\ E_j &\equiv \exp(b_j + W_j)\end{aligned}\quad (\text{B.12})$$

The derivative with respect to the visible bias is

$$\frac{1}{J} \frac{\partial J}{\partial a_l} = \frac{x_l - a_l}{\sigma^2} \quad (\text{B.13})$$

and the hidden bias

$$\begin{aligned}\frac{1}{J} \frac{\partial J}{\partial b_l} &= \frac{\partial}{\partial b_l} \ln(J) \\ &= \frac{1}{1 + \frac{1}{E_j}}\end{aligned}\quad (\text{B.14})$$

and the weights

$$\begin{aligned}\frac{1}{J} \frac{\partial J}{\partial w_{kl}} &= \frac{\partial}{\partial w_{kl}} \ln(J) \\ &= \frac{x_k}{\sigma^2 \left(1 + \frac{1}{E_j}\right)}\end{aligned}\quad (\text{B.15})$$

Notice that the indices  $k$  and  $l$  are here indiscriminate towards the dimensional component in relation to  $x$ . This means that  $x_l$  or  $x_k$  represents just a particle position in a dimension.



## BIBLIOGRAPHY

- [1] E. Anisimovas and A. Matulis. “Energy spectra of few-electron quantum dots”. In: *Journal of Physics: Condensed Matter* (1998), p. 601.
- [2] Dacorogna B. *Introduction to the calculus of variations*. Imperial College Press; World Scientific, 2004. ISBN: 9781860945083.
- [3] M. L. Boas. *Mathematical Methods in the Physical Sciences, 3rd Edition*. Wiley, 2005. ISBN: 978-0-471-19826-0.
- [4] C. G. Broyden. “The Convergence of a Class of Double-rank Minimization Algorithms 1. General Considerations”. In: *IMA Journal of Applied Mathematics* (1970). DOI: [10.1093/imamat/6.1.76](https://doi.org/10.1093/imamat/6.1.76).
- [5] van Brunt B. *The Calculus of Variations*. Springer, 2004. ISBN: 9780387402475.
- [6] G. Carleo and M. Troyer. “Solving the Quantum Many-Body Problem with Artificial Neural Networks”. In: *Science* 355.6325 (2017), pp. 602–606. ISSN: 0036-8075. DOI: [10.1126/science.aag2302](https://doi.org/10.1126/science.aag2302).
- [7] M. S. Carroll. “Implications Of Simultaneous Requirements For Low-Noise Exchange Gates In Double Quantum Dots”. In: *Phys. Rev. B* (2010). DOI: [10.1103/PhysRevB.82.075319](https://doi.org/10.1103/PhysRevB.82.075319).
- [8] UnitTest++ developers. *UnitTest++*. <https://github.com/unittest-cpp/unittest-cpp/wiki>.
- [9] YAML developers. *YAML*. <http://yaml.org/>.
- [10] W. H. Dickhoff and D. Van Neck. *Many-body theory exposed!: Propagator Description of Quantum Mechanics in Many-Body Systems*. World Scientific, 2005. ISBN: 981256294X.
- [11] N. D. Drummond, M. D. Towler, and R. J. Needs. “Jastrow Correlation Factor for Atoms, Molecules, and Solids”. In: *Phys. Rev. B* 70 (2004), p. 235119. DOI: [10.1103/PhysRevB.70.235119](https://doi.org/10.1103/PhysRevB.70.235119).
- [12] A. L. Fetter and J. D. Walecka. *Quantum Theory of Many-particle Systems*. McGraw-Hill College, 1971. ISBN: 9780070206533.
- [13] R. Fletcher. “A New Approach To Variable Metric Algorithms”. In: *The Computer Journal* (1970). DOI: [10.1093/comjnl/13.3.317](https://doi.org/10.1093/comjnl/13.3.317).

- [14] D. Goldfarb. “A Family of Variable-Metric Methods Derived by Variational Means”. In: *Math. Comp.* 24 (1970). DOI: <https://doi.org/10.1090/S0025-5718-1970-0258249-6>.
- [15] D. Goldfarb. “Stochastic Adaptive Quasi-Newton Methods for Minimizing Expected Values”. In: *Proceedings of the 34th International Conference on Machine Learning*. Proceedings of Machine Learning Research. PMLR, 2017.
- [16] D.J. Griffiths. *Introduction to quantum mechanics*. 2nd Edition. Pearson PH, 2005. ISBN: 0131911759.
- [17] Gaël Guennebaud, Benoît Jacob, et al. *Eigen v3*. <http://eigen.tuxfamily.org>. 2010.
- [18] W. A. Hammond B. L. Lester Jr. and P.J. Reynolds. *Monte Carlo Methods in Ab Initio Quantum Chemistry*. World Scientific, 1994. ISBN: 9810203225.
- [19] T. Helgaker. *Molecular Integral Evaluation*. 2006.
- [20] T. Helgaker and P. R. Taylor. *Gaussian Basis Sets and Molecular Integrals*. 1995.
- [21] G. Hinton. *A Practical Guide to Training Restricted Boltzmann Machines*. <https://www.cs.toronto.edu/~hinton/absps/guideTR.pdf>.
- [22] M. Hjort-Jensen. *Computational Physics: Hartree-Fock methods and introduction to Many-Body Theory*. <https://www.github.com/CompPhysics/ComputationalPhysics2/blob/gh-pages/doc/pub/basicMB/pdf>. 2017.
- [23] M. Hjort-Jensen. *Computational Physics: Variational Monte Carlo methods*. <https://www.github.com/CompPhysics/ComputationalPhysics2/blob/gh-pages/doc/pub/vmc/pdf>. 2017.
- [24] Høgberget J. *Quantum Monte-Carlo Studies of Generalized Many-body Systems*. MA Thesis. University of Oslo, 2013.
- [25] Rogers J. “Global Optimization of Statistical Functions With Simulated Annealing”. In: *Journal of Econometrics* (1994), pp. 65–99. ISSN: 0304-4076. DOI: [https://doi.org/10.1016/0304-4076\(94\)90038-8](https://doi.org/10.1016/0304-4076(94)90038-8).
- [26] R. Jastrow. “Many-Body Problem with Strong Forces”. In: *Phys. Rev.* (1955). DOI: [10.1103/PhysRev.98.1479](https://doi.org/10.1103/PhysRev.98.1479).
- [27] A. Jeffrey, ed. *Handbook of Mathematical Formulas and Integrals (Third Edition)*. Academic Press, 2004. ISBN: 978-0-12-382256-7. DOI: <https://doi.org/10.1016/B978-012382256-7/50034-8>.
- [28] D. C. Lay. *Linear Algebra and Its Applications (4th Edition)*. Addison Wesley / Pearson, 2011. ISBN: 9780321385178.

- [29] D. S. Lemons and A. Gythiel. “Paul Langevin’s 1908 paper “On the Theory of Brownian Motion” [“Sur la théorie du mouvement brownien,” C. R. Acad. Sci. (Paris) 146, 530–533 (1908)]”. In: *American Journal of Physics* 65 (1997), pp. 1079–1081. DOI: [10.1119/1.18725](https://doi.org/10.1119/1.18725).
- [30] L. E. Lervåg. *VMC Calculations of Two-Dimensional Quantum Dots*. MA Thesis. University of Oslo, 2010.
- [31] Magnus Pedersen Lohne. *Coupled-Cluster Studies of Quantum Dots*. MA Thesis. University of Oslo, 2010.
- [32] P Löwdin. “Quantum Theory of Many-Particle Systems. I. Physical Interpretations by Means of Density Matrices, Natural Spin-Orbitals, and Convergence Problems in the Method of Configurational Interaction”. In: *Phys. Rev.* 97 (6 1955), pp. 1474–1489. DOI: [10.1103/PhysRev.97.1474](https://doi.org/10.1103/PhysRev.97.1474).
- [33] J. J. Moré and D. J. Thuente. “Line Search Algorithms with Guaranteed Sufficient Decrease”. In: *ACM Trans. Math. Softw.* (1994). DOI: [10.1145/192115.192132](https://doi.org/10.1145/192115.192132).
- [34] J. W. Moskowitz and M. H. Kalos. “A New Look At Correlations In Atomic And Molecular Systems. I. Application Of Fermion Monte Carlo Variational Method”. In: *International Journal of Quantum Chemistry* (). DOI: [10.1002/qua.560200508](https://doi.org/10.1002/qua.560200508).
- [35] J. W. Negele and Orland H. *Quantum Many-Particle Systems*. Perseus BOOKs, 1998. ISBN: 9780738200521.
- [36] J. Nocedal and S. J. Wright. *Numerical Optimization*. Springer-Verlag New York, 2006. ISBN: 978-1-4939-3711-0. DOI: [10.1007/978-0-387-40065-5](https://doi.org/10.1007/978-0-387-40065-5).
- [37] F. Pederiva. “Ab Initio Computation of the Energies of Circular Quantum Dots”. In: *Phys. Rev. B* 84 (11 2011), p. 115302. DOI: [10.1103/PhysRevB.84.115302](https://doi.org/10.1103/PhysRevB.84.115302).
- [38] F. Pederiva. “Variational Monte Carlo for Spin-orbit Interacting Systems”. In: *Phys. Rev. B* (2012). DOI: [10.1103/PhysRevB.85.045115](https://doi.org/10.1103/PhysRevB.85.045115).
- [39] E. Platen and N. Bruti-Liberati. *Numerical Solution of Stochastic Differential Equations with Jumps in Finance*. Springer-Verlag Berlin Heidelberg, 2010. ISBN: 9783642120572.
- [40] P. Pulay. “Convergence Acceleration of Iterative Sequences. The Case of SCF Iteration”. In: *Chemical Physics Letters* 73.2 (1980), pp. 393–398. ISSN: 0009-2614. DOI: [https://doi.org/10.1016/0009-2614\(80\)80396-4](https://doi.org/10.1016/0009-2614(80)80396-4).
- [41] P. Pulay. “Improved SCF convergence acceleration”. In: *Journal of Computational Chemistry* 3.4 (), pp. 556–560. DOI: [10.1002/jcc.540030413](https://doi.org/10.1002/jcc.540030413).
- [42] Jack S. and M. Winifred. “Adjustment of an Inverse Matrix Corresponding to a Change in One Element of a Given Matrix”. In: *The Annals of Mathematical Statistics* 21 (1950). DOI: [10.1214/aoms/1177729893](https://doi.org/10.1214/aoms/1177729893).

- [43] J. P. Sethna. *Statistical Mechanics: Entropy, Order parameters and complexity*. Oxford University Press, USA, 2006. ISBN: 9780198566779.
- [44] D. F. Shanno. “Conditioning of quasi-Newton methods for function minimization”. In: *Math. Comp.* 0274029 (1970). DOI: [10.2307/2004840](https://doi.org/10.2307/2004840).
- [45] S. Surjanovic and D. Bingham. *Virtual Library of Simulation Experiments: Test Functions and Datasets*. <http://www.sfu.ca/~ssurjano>. 2018.
- [46] J. Olsen T. Helgaker P. Jørgensen. *Molecular Electronic-Structure Theory*. Wiley, 2014. ISBN: 978-0-47-196755-2. DOI: [10.1002/9781119019572](https://doi.org/10.1002/9781119019572).
- [47] J. M. Thijssen. *Computational Physics*. 2nd Edition. Cambridge University Press, 2013. ISBN: 9781107677135.
- [48] M. A. Viergever. “Adaptive Stochastic Gradient Descent Optimisation for Image Registration”. In: *Int J Comput. Vision* (2009). DOI: [10.1007/s11263-008-0168-y](https://doi.org/10.1007/s11263-008-0168-y).
- [49] Wolfram|Alpha. *Chebyshev-Gauss Quadrature*. <http://mathworld.wolfram.com/Chebyshev-GaussQuadrature.html>. 2018.
- [50] Wolfram|Alpha. *Modified Bessel Function of the First Kind*. <http://mathworld.wolfram.com/ModifiedBesselFunctionoftheFirstKind.html>. 2018.